

**HETEROGENEOUS PROTEIN DISTRIBUTION DURING RAPID AND
EQUILIBRIUM FREEZING**

A THESIS
SUBMITTED TO THE FACULTY OF
UNIVERSITY OF MINNESOTA
BY

Alan Michael Twomey

IN PARTIAL FULFILLMENT OF THE REQUIREMENTS
FOR THE DEGREE OF
MASTER OF SCIENCE

Adviser: Alptekin Aksan

April 2013

© Copyright by Alan Twomey 2013

All Rights Reserved

Acknowledgements

I would like to thank my adviser, Professor Alptekin Aksan, for his support and guidance throughout the duration of my graduate studies. I have learned a great deal and I have benefited from his dedication to research, his attention to detail, and his flexibility.

I would also like to express my gratitude to Professor Hiroshi Takamatsu and Professor Kosaku Kurata, of Kyushu University. They were exceptional hosts during my summer-long stay in Professor Takamatsu's laboratory and have given useful direction to this research project. Likewise, I would like to thank Yutaka Nagare, a graduate student in the laboratory, who helped set up confocal Raman microspectroscopy experiments and acquired temperature profile data for directional solidification experiments.

Professor Raj Suryanarayanan carefully reviewed the manuscript for Chapter 2 and provided detailed feedback, for which I am grateful. I would also like to thank Mehak Mehta for her assistance in performing X-ray diffraction.

I am grateful to the members of my master's committee, Professor Chris Hogan and Professor Raj Suryanarayanan.

Lastly, I would like to extend my thanks to my fellow Biostabilization Laboratory members Jonathan Frost, Lisa Kasinkas, Molly Lefebvre, Baris Mutlu, and Jonathan Sakkos, for stimulating discussions and feedback. I would like to express my particular thanks to Rebekah Less and Marcus Kramer, who offered their expertise and suggestions, as well assisted in performing FTIR and gel electrophoresis experiments.

Dedication

To my grandmother, Margaret Helen Ryan Ek, for her guidance and encouragement
throughout my education.

Abstract

Interactions between proteins and ice were studied *in situ* using FTIR and confocal Raman microspectroscopy under equilibrium and non-equilibrium conditions over a range of temperatures. During quasi-equilibrium freezing of aqueous solutions of dimethyl sulfoxide (DMSO) and bovine serum albumin, preferential exclusion of albumin and/or DMSO was observed. It was hypothesized that the albumin may be adsorbed onto the ice interface or entrapped in the ice phase.

To investigate protein-ice interactions during freezing under non-equilibrium conditions, confocal Raman microspectroscopy was used to map the distribution of albumin and the cryoprotective agent trehalose. Microheterogeneity was found in the composition of the freeze-concentrated liquid phase that indicated that albumin was preferentially distributed near or at the boundary of the ice phase. The observed microheterogeneity did not occur under all freezing protocols, which suggests that the technique developed here could be used to develop freezing protocols that would reduce harmful protein-ice interactions.

Table of Contents

Acknowledgments	i
Dedication	ii
Abstract	iii
Table of Contents	iv
List of Tables	vi
List of Figures	vii
Chapter 1: Introduction	1
1.1) Motivation	1
1.2) Freezing Basics	1
1.2.1) Supercooling	2
1.2.2) Ice Nucleation	2
1.2.3) Freeze Concentration	3
1.2.4) Ice Morphology	3
1.3) Spectroscopy as a Method for Studying Freezing Phenomena	4
Chapter 2: <i>In situ</i> Spectroscopic Quantification of Protein-Ice Interactions*	5
2.1) Introduction	5
2.2) The Approach	7
2.3) Materials and Methods	11
2.3.1) FTIR Spectroscopy	11
2.3.1.1) Equilibrium Freezing Experiments	12
2.3.1.2) Bulk Freezing Experiments at -20°C	13
2.3.2) Confocal Raman Microspectroscopy	14
2.3.3) IR Spectral Analysis	15
2.3.4) Raman Spectral Analysis	16
2.4) Results	17
2.4.1) FTIR Experiments at -4°C and -6°C	18

2.4.2)	FTIR Experiments at -8.5°C, -13°C, -17.5°C, and -20°C.....	19
2.4.3)	Confocal Raman Experiments at -17.5°C.....	21
2.4.4)	Additional FTIR Experiments between -20°C and -35°C.....	21
2.4.5)	Bulk Freezing Experiments at -20°C.....	22
2.5)	Discussion.....	23
2.6)	Summary.....	24
Chapter 3:	Mapping of Protein and Cryoprotectant Distribution in Directional Solidification using Confocal Raman Microspectroscopy.....	27
3.1)	Introduction.....	27
3.2)	Materials and Methods.....	29
3.2.1)	Calibration Experiments.....	31
3.2.2)	Directional Solidification Experiments.....	31
3.2.3)	Raman Spectral Calibration and Analysis.....	34
3.3)	Results and Discussion.....	39
3.4)	Summary.....	43
Chapter 4:	Research Summary.....	44
Chapter 5:	References.....	46
Appendix A:	Directional Solidification Instructions.....	50
Appendix B:	Matlab Code.....	55

List of Tables

Table 1. Cooling parameters of equilibrium freezing experiments using FTIR.....	13
Table 2. Calibration experiments trehalose and albumin concentrations in 1x DPBS.....	31
Table 3. Directional solidification trehalose and albumin concentrations in 1x DPBS.....	32

List of Figures

Figure 1. Binary DMSO and water phase diagram, adapted from the polynomial curve fit created by Kleinhans and Mazur to fit Rasmussen's phase diagram.....	8
Figure 2. Partially frozen solutions at -6°C : A) 6 wt% DMSO, 1:3 Albumin/DMSO, B) 8 wt% DMSO, 1:3 Albumin/DMSO, C) 10 wt% DMSO, 1:3 Albumin/DMSO, D) 12 wt% DMSO, 1:6 Albumin/DMSO.....	9
Figure 3. FTIR and Raman Albumin/DMSO ratio calibration: A-B) Ratio of baseline-corrected areas for γ and linear calibration curve. C-D) Ratio of baseline-corrected areas for ζ and quadratic calibration curve.....	16
Figure 4. A-C) FTIR Results: Change in Albumin/DMSO ratio at -4°C , -6°C and -8.5°C . D) Raman Results: Change in Albumin/DMSO at -17.5°C	19
Figure 5. Bulk freezing experiments: the albumin content in the FCL extracted from the samples after 30 hours at -20°C is plotted versus a measure of the effective surface area that could interact with the FCL. The γ values are normalized by the γ of the FCL extracted from the solution with the least amount of added ice (shown as 100%). The starting bulk solution is also included in the plot.....	23
Figure 6. Schematic of directional solidification setup with confocal Raman microscope. Confocal Raman maps of the distribution of ice, trehalose, and albumin/trehalose ratio are included for 20 wt% trehalose, 4 wt% albumin at -4°C , -9°C , -16°C , and -18°C	33
Figure 7. Temperature profile along microchannel.....	34
Figure 8. Organic content calibration using α : A) Raman spectral ratio, B) Linear calibration curve at 0 to -20°C	35
Figure 9. Calculation of albumin/trehalose ratio using σ in high and low concentration trehalose: A) Raman spectral ratio, σ , in high concentration trehalose B) Linear calibration curve of σ in high concentration trehalose at 0 to -20°C . C) Raman spectral ratio, σ , in low concentration trehalose B) Linear calibration curve of σ in low concentration trehalose at 0 to -20°C	37

Figure 10. Heterogeneity of albumin/trehalose ratio with respect to local environment. For each experiment, albumin/trehalose ratios in each equivalent trehalose concentration normalized by the mean value at that temperature. A) 10 wt% trehalose, 3 wt% albumin, B) 10 wt% trehalose, 4 wt% albumin, C) 20 wt% trehalose, 3 wt% albumin, D) 20 wt% trehalose, 4 wt% albumin, E) 30 wt% trehalose, 3 wt% albumin, F) 30 wt% trehalose, 4 wt% albumin.....42

Chapter 1: Introduction

1.1) Motivation

Freezing and freeze-drying are widely used to stabilize biospecimens, pharmaceutical compounds, and even food^{1,2}. In biobanking, fluid biospecimens such as serum, plasma, bronchial lavage fluid, and urine are stored in the frozen state for proteomics research, whereas protein solutions for therapeutic use are generally freeze-dried³⁻⁵. While the purpose of stabilization is to inhibit damage to samples, the freezing and freeze-drying processes subject proteins to chemical and physical stresses⁵⁻¹³ that can alter their structure and activity irreversibly^{6,14-21}. As a result, stored biospecimens may lose biomarkers and may see a reduction in their clinical or diagnostic utility. Subsequent proteomics studies on frozen and thawed biospecimens can therefore be biased^{22,23} and impede scientific research.²⁴ Similarly, therapeutic proteins can be negatively affected by freeze-processing, causing an economic loss and reducing their therapeutic impact²⁵. As a result, understanding the interactions that occur between ice surfaces and macromolecules such as proteins during after freezing may therefore help to reduce product losses and to improve therapeutic outcomes.

1.2) Freezing Basics

Freezing is the process by which liquid water crystallizes into a solid. While it is often thought that pure water freezes upon cooling to 0°C at atmospheric pressure, this is not truly the case and in fact water freezes spontaneously only once a sufficient number of water molecules arrange themselves into a crystal with a radius large enough to overcome the Gibbs-Thomson effect²⁶. Because the critical number of molecules is reduced with temperature, as water is cooled below 0°C it becomes more and more likely

that a sufficient number of water molecules will overcome nucleation barrier and ice will spontaneously form, making the practical limit of supercooling of ultra-pure water about -40°C .²⁷ Once formed, however, the ice will remain until it is warmed back to its equilibrium freezing/melting temperature.

The addition of solutes to water depresses the equilibrium freezing/melting temperature of an aqueous solution by making it more difficult for the sufficient number of water molecules to spontaneously assemble by the colligative effect²⁸, or in addition by specific interactions between the water molecules and the solutes.

1.2.1) Supercooling

Below the equilibrium freezing/melting temperature and before ice has formed, a solution exists either in an unstable supercooled state, or in a more stable glassy state²⁹. While in the supercooled state, it is susceptible to rapid crystallization once ice initially forms. Higher degrees of supercooling, i.e. the difference between the equilibrium freezing/melting point and the actual temperature, generally result in faster crystallization³⁰, provided the temperature is not so low and/or the concentration so high as to slow the kinetics of the crystal growth³¹.

1.2.2) Ice Nucleation

Ice nucleation is considered homogeneous when ice crystals form spontaneously in a uniform manner without the influence of impurities or added ice crystals. Due to the stochastic nature of homogeneous ice nucleation³², it is not a controlled process. Heterogeneous nucleation occurs when impurities or surfaces exist in a solution that serve as favorable nucleation sites by reducing the critical number of molecules that need

to assemble for crystallization to proceed. Heterogeneous nucleation can be a controlled process by means of seeding a solution with a known degree of supercooling with ice, a chilled surface, or a chemical that promotes crystallization^{33,34}.

1.2.3) Freeze Concentration

In aqueous solutions, the solutes are excluded from the ice phase when ice forms. As the ice phase grows, the solutes are concentrated in a progressively smaller volume of liquid water. Concentration gradients can develop at the moving ice front, and solutes such as buffer components can exceed their solubility limits and selectively precipitate, causing potentially damaging fluctuation in the pH of the freeze-concentrated liquid (FCL) phase³⁰. As the concentrations increase dramatically, the viscosity of the FCL may increase substantially, and a glassy state may be reached⁵.

1.2.4) Ice Morphology

The shape and structure of ice formed in aqueous solutions is influenced by the temperature at which the ice forms, the degree of supercooling, the subsequent cooling rate once ice has been nucleated, and the specific solutes and their concentrations^{35,36}. In general, slow ice growth resulting from minimal supercooling before ice nucleation followed by a low cooling will create large ice structures³⁷. Ice growth following significant supercooling with a subsequent high cooling, will result in ice crystals with side-arms and dendritic features that greatly increase the surface area of the ice phase³⁸. The range in relative sizes and shapes of the ice phase and the FCL phase that can be obtained by varying freezing parameters means there is flexibility available when developing freezing protocols to alter the interactions between proteins and ice. As a result, an efficient method of evaluating the effects of freezing protocols *in situ* could

facilitate improvement in the quality of biospecimens and therapeutic proteins following freezing processes.

1.3) Spectroscopy as a Method for Studying Freezing Phenomena

For evaluating interactions between proteins and ice, spectroscopy offers the distinct benefit of measuring interactions *in situ* during freezing. In Chapter 2, Fourier transform infrared (FTIR) spectroscopy and confocal Raman microspectroscopy (CRM) are developed as techniques to measure protein adsorption to ice during near-equilibrium freezing. In Chapter 3, protein-ice interactions are evaluated under non-equilibrium conditions using directional solidification. Through detailed mapping of the distribution of solute concentrations in the freeze-concentrated liquid, heterogeneity in the relative distribution of proteins is identified. The results of the studies suggest that significant direct interactions between proteins in solution and the ice phase do occur, and that in addition, these interactions can be quantified and adjusted by modifying freezing protocols.

Chapter 2: *In situ* Spectroscopic Quantification of Protein-Ice

Interactions*

2.1) Introduction

Freezing plays a significant role in the stabilization and long-term preservation of biological and pharmaceutical specimens and compounds. In biobanking, fluid biospecimens such as serum, plasma, bronchial lavage fluid and urine are frequently frozen and stored for future proteomics research, while protein solutions for therapeutic use are generally freeze-dried³⁻⁵. Freezing and freeze-drying processes impose very harsh chemical and physical stresses on proteins⁵⁻¹³, altering their characteristics (structure and activity) often irreversibly^{6,14-21}. These stresses affect the quality of the stored biospecimens and may result in the loss of biomarker information or clinical/diagnostic utility. Subsequent proteomics studies on frozen and thawed samples can therefore be biased.^{22,23} The low quality of the biospecimens currently stored in biobanks has been identified as one of the major issues inhibiting scientific progress²⁴. Similarly, therapeutic proteins can be damaged during freeze-processing, causing an economic loss and reducing their therapeutic impact²⁵. Understanding the interactions between an ice surface and the macromolecules in the solution may therefore help to reduce product losses and to improve therapeutic efficacy.

The ice phase is expected to incorporate few or no solutes when an aqueous solution is frozen³⁹. As the ice phase forms and grows, the solutes excluded from the ice phase are concentrated in the remaining liquid phase, termed the freeze-concentrated liquid (FCL) phase. When an aqueous solution containing proteins is frozen, either: **I**) the

**This chapter has been submitted for publication.*

proteins may end up homogeneously distributed within the FCL phase, or **2)** the proteins may end up heterogeneously distributed in the FCL and may aggregate at the surface of or get entrapped within the ice phase. In the latter case, the protein concentration in the FCL phase would decrease. This is known to occur with antifreeze proteins⁴⁰, which are known to adsorb to the surface of the ice⁴⁰ through the formation of hydrogen bonds between the ice surface and their ordered hydration layers⁴¹. With other proteins and enzymes, a handful of studies were conducted and these have reported significant interactions mainly through centrifugation and filtration of a partially frozen solution, followed by measurement the protein content in the FCL^{40,42}. Other studies have used molecular techniques such as confocal Raman microspectroscopy by measuring the changes in protein conformation at the ice interface⁴³ and the resultant protein aggregation, which may even persist post-thaw^{6,44,45}.

In this study, we show the feasibility of using FTIR spectroscopy and confocal Raman microspectroscopy (CRM) in a non-destructive fashion to quantify the adsorption of albumin onto the ice surface in partially frozen aqueous solutions of dimethyl sulfoxide (DMSO). While FTIR has been used to investigate changes in secondary structure of proteins in frozen solutions⁴⁶ and freeze-dried formulations⁴⁷, to our knowledge it has not been used to study protein interaction with ice in the freeze-concentrated liquid in a quantitative manner. Albumin is the most abundant protein found in the plasma. It facilitates transport for thyroid and steroid hormones^{48,49}, fatty acids⁵⁰, and to regulate oncotic pressure in the capillaries⁵¹, and is also used as a biomarker to detect and monitor renal and cardiovascular diseases⁵². DMSO is a cryostabilizing agent that is used very widely for preservation of cells, biofluids and tissues⁵³⁻⁵⁹. The advantage

of using DMSO to study interactions between proteins and ice is its substantial ability to depress the equilibrium freezing point of binary solutions of water and DMSO⁶⁰. This enables investigation of protein-ice interactions in the freeze-concentrated liquid during freezing over a wide range of temperatures. Nonetheless, concern has been expressed about the clinical side effects of DMSO, particularly in autologous stem cell transplants^{53,61,62}. At high very concentration, DMSO has also been found to denature proteins⁶³, but these concentrations are outside the concentration range used in this study.

2.2) The Approach

The technique developed in this study is intended to aid in understanding the interactions between proteins and ice during freezing, as well as serve as a methodology to identify freezing parameters that minimize the harmful interactions between proteins and ice that may occur during the preservation and storage of biospecimens and pharmaceuticals.

When freezing a solution of DMSO and water under equilibrium conditions, a 35 wt% DMSO solution will follow the equilibrium freezing curve of the binary phase diagram as it is cooled to -20°C (*Figure 1*). According to the phase diagram, the FCL region should contain about 37 wt% DMSO in equilibrium with ice^{60,64}. To obtain the same concentration of DMSO in liquid water at -20°C, an alternative would be to dilute the initial solution to 15 wt% or 25 wt% DMSO and cool these under equilibrium conditions to -20°C. Due to the freeze-concentration of the DMSO as it is excluded from the ice phase, the composition of the FCL of these diluted solutions at equilibrium at -20°C should also be 37 wt% DMSO. The only difference among the different solutions at

equilibrium at the same temperature would be the relative sizes of the FCL and ice phases. In **Figure 2**, aqueous solutions of 6-12 wt% DMSO with a small amount of added albumin are all at equilibrium at -6°C . While the 12 wt% DMSO solution has just a few small ice crystals and a large FCL phase, the more dilute 6 wt% DMSO solution has an FCL phase and an ice phase that are almost equal in size.

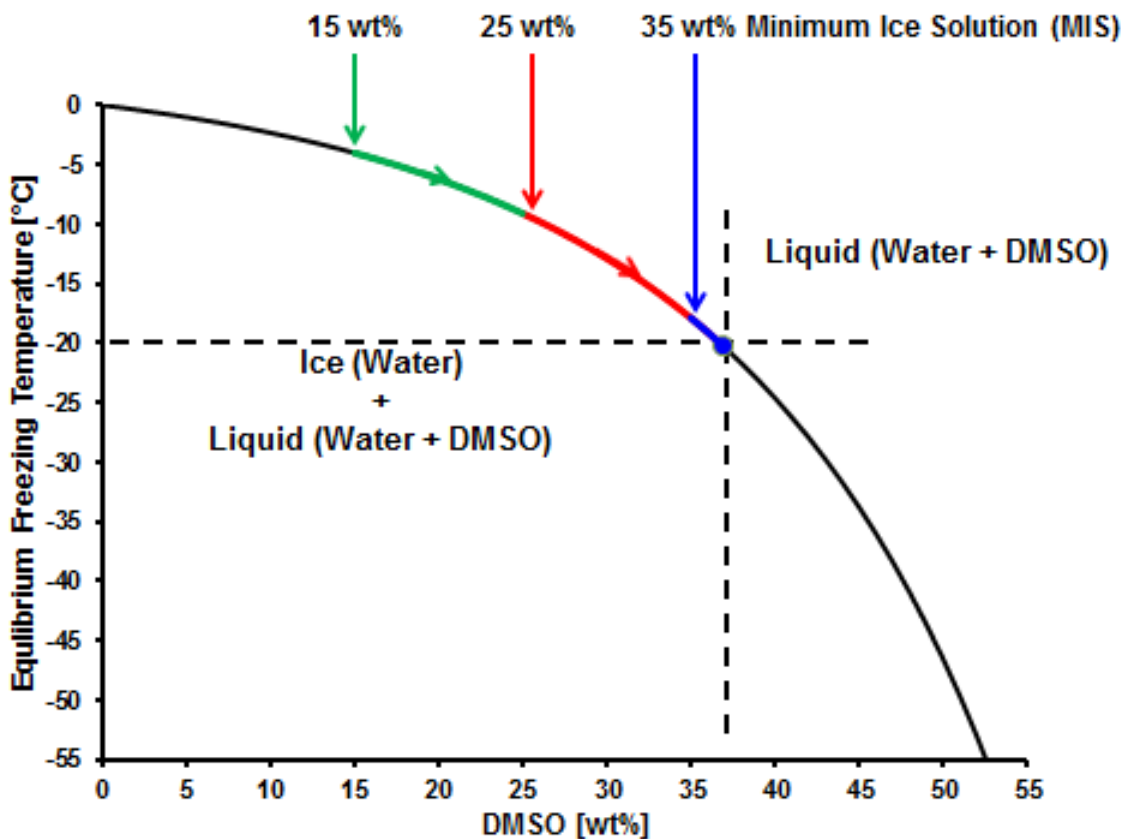


Figure 1. Binary DMSO and water phase diagram, adapted from the polynomial curve fit created by Kleinhans and Mazur to fit Rasmussen's phase diagram.

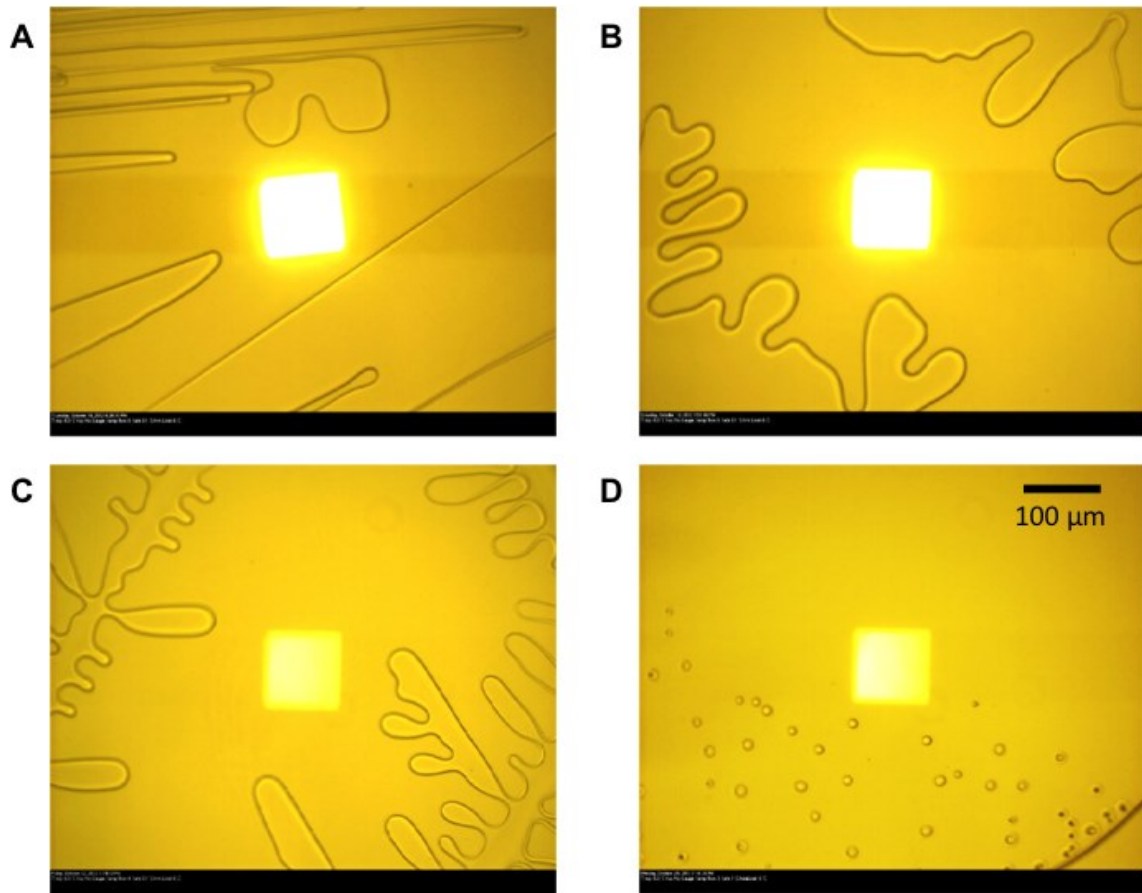


Figure 2. Partially frozen solutions at -6°C : A) 6 wt% DMSO, 1:3 Albumin/DMSO, B) 8 wt% DMSO, 1:3 Albumin/DMSO, C) 10 wt% DMSO, 1:3 Albumin/DMSO, D) 12 wt% DMSO, 1:6 Albumin/DMSO

No ternary phase diagram exists in the literature for aqueous solutions of DMSO and albumin. Even so, the addition of a small amount of albumin to aqueous solutions of DMSO should result in an additional slight depression of the equilibrium freezing point by the colligative effect²⁸. During freezing of such a ternary solution, the mass (and molar) ratio of albumin/DMSO in the FCL should be constant if the albumin and the DMSO are excluded equally from the ice phase, even as their absolute concentrations increase due to freeze-concentration. By measuring the mass ratio of albumin/DMSO in the FCL, it is possible to detect if either albumin or DMSO is preferentially excluded

from the ice phase, since this would result in a change in the mass ratio of albumin/DMSO in the FCL. If there is preferential exclusion of albumin or DMSO from the ice phase, this effect should be greatest in solutions with greater amounts of ice. If the observed effect were due to entrapment within the ice phase, it should be most significant with the greatest volume of ice. If the effect were due to accumulation of albumin or DMSO at the interface between the ice and the FCL phases, then it should be most significant with the greatest interfacial area.

Similar to during the freezing of binary DMSO solutions, dilute ternary solutions of DMSO and albumin will undergo more freeze-concentration than do more concentrated solutions to reach a common temperature, and will have a larger ice phase and smaller FCL phase. Provided that the mass ratio of albumin/DMSO is the same in both the dilute and the concentrated solutions, as is the case when a concentrated solution is diluted with water, it is possible to vary the amount of ice in partially frozen systems at a given temperature and then measure the effect on the composition of the FCL. As a reference point for comparison, it is advantageous to use the composition of the FCL in which the effects of ice are minimized. This reference point is called here the Minimum Ice Solution (MIS) and is the composition of the FCL of the partially frozen system with the least amount of ice at a given temperature. For example, the MIS on the binary DMSO and water phase diagram at -20°C is the 35 wt% solution, which would be 2 wt% ice according to the lever rule (*Figure 1*). By comparing the FCL of the MIS with the FCL of the more dilute 15 wt% and 25 wt% solutions as shown in the figure, preferential exclusion from the ice phase of either albumin or DMSO can be detected by a change in the mass ratio of albumin/DMSO. With this method, we used IR and Raman

spectroscopy in a non-destructive fashion to investigate the interactions of albumin with the ice interface *in situ* in aqueous DMSO solutions in a temperature range of -4°C to -40°C.

2.3) Materials and Methods

Experiments were conducted using Fourier Transform Infrared (FTIR) spectroscopy and Confocal Raman Microspectroscopy (CRM) with solutions over a range of DMSO concentrations (6-35 wt%) and albumin concentrations (20-63 mg/mL) at temperatures of -4°C to -40°C. FTIR was chosen for its speed and lower signal to noise ratio in data acquisition, as well as its ability to measure freeze-concentrated liquid *in situ* without heating the sample. The disadvantage of using FTIR was its relatively poor spatial resolution of 100 μm x 100 μm . CRM can reach a spatial resolution of less than 1 μm x 1 μm , however, the weak intensity of the albumin Raman spectrum resulted in a low signal to noise ratio. Spatial averaging of each 4 μm x 83 μm Raman scan was required to get a sufficiently strong signal to noise ratio, reducing one of the benefits of CRM. The remaining benefit of CRM was that it enabled studying much thicker samples (50 μm) in which ice crystal growth was less constrained than in the very thin geometry of the FTIR experiments.

2.3.1) FTIR Spectroscopy

Experimental solutions were prepared gravimetrically with DMSO (99.9% purity, Sigma-Aldrich, St. Louis, MO), bovine serum albumin (MW 66.5 kDa, $\geq 99\%$ Purity, Sigma-Aldrich, St. Louis, MO) and in ultrapure water (UPW). UPW was prepared by filtering deionized water through a Milli-Q water purification system (Millipore, Billerica, MA) to a final electrical resistance higher than 18.2 Mohms. All DMSO

concentrations reported as wt% correspond to the mass of DMSO as a percentage of total mass of solvent (DMSO and water). Albumin concentrations are given as (mass of albumin)/(volume of DMSO and water).

Each experiment involved placing 100 nL of the experimental solution between two CaF₂ windows. The windows were sealed with vacuum grease to eliminate evaporation and to generate a thin film approximately 1 μm thick. The sealed sample was then transferred to an infrared microscope attached to an FTIR spectrometer (Thermo-Nicolet Continuum equipped with a Mercury Cadmium Telluride detector, Thermo Electron, Waltham, MA) equipped with a FDCS 196 (Linkam Scientific Instruments Ltd., UK) freeze-drying cryostage. The FTIR sampling resolution was 4 cm⁻¹, and 128 IR scans were averaged per spectrum in the 4000-930 cm⁻¹ wavenumber range. The IR spectra were analyzed using OMNIC (Thermo-Nicolet) software.

2.3.1.1) Equilibrium Freezing Experiments

The sample solutions were cooled at 30°C/min until frozen (formation of ice crystals was observed visually and spectroscopically). The samples were then warmed back up slowly to close to the melting temperature until a few small crystals remained in the solution. The samples were then re-cooled down to a common final temperature at the cooling rate described in Table 1. The cooling rates were chosen so that ice growth occurred slowly over 20-40 minutes in order to minimize any concentration gradients in the FCL resulting from diffusion limitations. The small crystals acted as nucleation points for crystal growth and ensured that equilibrium-freezing experiments were conducted in a repeatable manner. At the final temperature, the most concentrated starting solution was made up primarily of FCL and only a few small ice crystals. The effect of ice growth on

the FCL was minimized in this case, which allowed the FCL of this solution to serve as a control and a basis for comparison. See *Figure 1*.

Final Temperature [°C]	DMSO Concentration [wt%]	Cooling Rate [°C/min]	Temperature of Spectra Collection [°C]
-6.0	6, 8, 10, 12	0.1	-4.0, -6.0
-8.5	12, 18	0.2	-8.5
-13.0	10, 20	0.2	-13.0
-17.5	20, 30	0.5	-17.5
-20.0	15, 30	0.5	-20.0
-40.0	20, 25, 30, 35	0.5°C/min to -20°C; 1.0°C/min to -40°C	-20.0, -25.0, -30.0, -35.0, -40.0

Table 1. Cooling parameters of equilibrium freezing experiments using FTIR

2.3.1.2) Bulk Freezing Experiments at -20°C

Biological specimens and pharmaceutical formulations are frequently stored at length in freezers at -20°C. Once a sample has reached equilibrium at these conditions, there should be no additional ice growth. To evaluate the interactions that may occur between ice and albumin over time in the absence of ice growth, similar to what would occur during long-term storage, solutions of DMSO and albumin were added to ice at -20°C. The amount of ice was controlled by freezing known quantities of water (0.1 ml to 1.5 ml) in 15 ml polypropylene centrifuge tubes in a temperature and humidity-controlled walk-in freezer maintained at -20°C. A 35 wt% DMSO solution with 30 mg/ml albumin was allowed to thermally equilibrate overnight in the freezer, and then was added in varying quantities (0.25 ml to 1.0 ml) to the centrifuge tubes containing ice. The concentration of DMSO was chosen to minimize any ice growth or melting of the ice at -20°C. After 30 hours, the liquid phase from all samples was extracted with a 25 gauge needle and syringe, removed from the freezer, and then stored at 4°C until use. FTIR was then used to determine the composition of the extracted liquid in order to detect any

changes in the mass ratio of albumin/DMSO that resulted from the 30 hours of contact with ice. Samples were cooled at 30°C/min until frozen, then warmed until a few ice crystals remained, and then cooled at 1°C/min to -35°C, after which spectra were collected in the resulting FCL.

2.3.2) Confocal Raman Microspectroscopy

Experimental solutions were prepared gravimetrically with DMSO ($\geq 99.7\%$ purity, Sigma-Aldrich, St. Louis, MO), bovine serum albumin ($\geq 98\%$ Purity, Sigma-Aldrich, St. Louis, MO) and deionized (DI) water. Each experiment involved placing 1 μL of the experimental solution in a microchannel machined in a 50 μm thick silicone film, which was sandwiched between two quartz windows. The sample was then transferred to a confocal Raman microscope (Nanophoton, Osaka, Japan) equipped with a FDCS 196 (Linkam Scientific Instruments Ltd., UK) freeze-drying cryostage. The microscope had a 100 \times Nikon air objective (NA 0.90) and a 532 nm AR-ion laser operated at 10 mW for excitation and a CCD detector electrically cooled to -70°C. Spatial resolution was 350 nm in the x-direction and 800 nm in the vertical direction. Scans were conducted over a 4 μm x 83 μm region with a spectral resolution of 6 cm^{-1} in the 4662-70 cm^{-1} wavenumber range at an exposure time of 0.025 s per pixel. The spectra collected from all pixels were averaged for each scan (7980 spectra per scan) and were analyzed using CytoSpec software (Boston, MA) and Matlab (MathWorks, Natick, MA).

In Confocal Raman Microspectroscopy experiments, the sample solutions were frozen and then warmed in the same fashion as the FTIR spectroscopy experiments. The samples were then cooled at 0.5°C/min to -17.5°C after nucleation at the freezing temperature following the same procedures described in the FTIR experiments above.

The small crystals remaining in the liquid after freeze and thawing back to freezing temperature acted as nucleation points for crystal growth and ensured that equilibrium-freezing experiments were conducted in a repeatable manner.

2.3.3) IR Spectral Analysis

The composition of the FCL at a given temperature was measured by the ratio of the baseline-corrected areas of the albumin Amide II band ($1525\text{-}1570\text{ cm}^{-1}$)⁶⁵ and the DMSO HCH deformation band ($1367\text{-}1485\text{ cm}^{-1}$)^{66,67}, $\gamma \equiv A_{\text{Amide II}} / A_{\text{HCH}}$, as shown in **Figure 3A**. To demonstrate the accuracy of this approach, at -6°C , a linear calibration curve was constructed by varying the amount of albumin added to a 12 wt% DMSO solution. For the highest albumin/ DMSO ratio (1:2), an 11 wt% DMSO solution was substituted due to the depression of the melting point to just below -6°C . The solutions were frozen at $30^\circ\text{C}/\text{min}$ and then warmed until a few small ice crystals remained (typically between -5.3°C and -5.8°C), and then re-cooled at $0.1^\circ\text{C}/\text{min}$ to -6°C to ensure that the system was in thermodynamic equilibrium, at which point spectra were collected. The variable γ was then plotted with respect to the known ratio of albumin to DMSO (mg/mg) (**Figure 3B**). The direct proportionality between γ and the albumin to DMSO ratio of the prepared solutions indicated that the chosen variable γ could be used to quantify protein concentration with high fidelity. Since the baseline of the Amide II band is influenced by the $\delta\text{-OH}$ band of water, having a small amount of ice present was important to reduce variability in the water content. The varying protein amounts would shift the equilibrium freezing curve slightly, but this effect was deemed to be less significant than potential variability in water content due to evaporation during preparation of the sample.

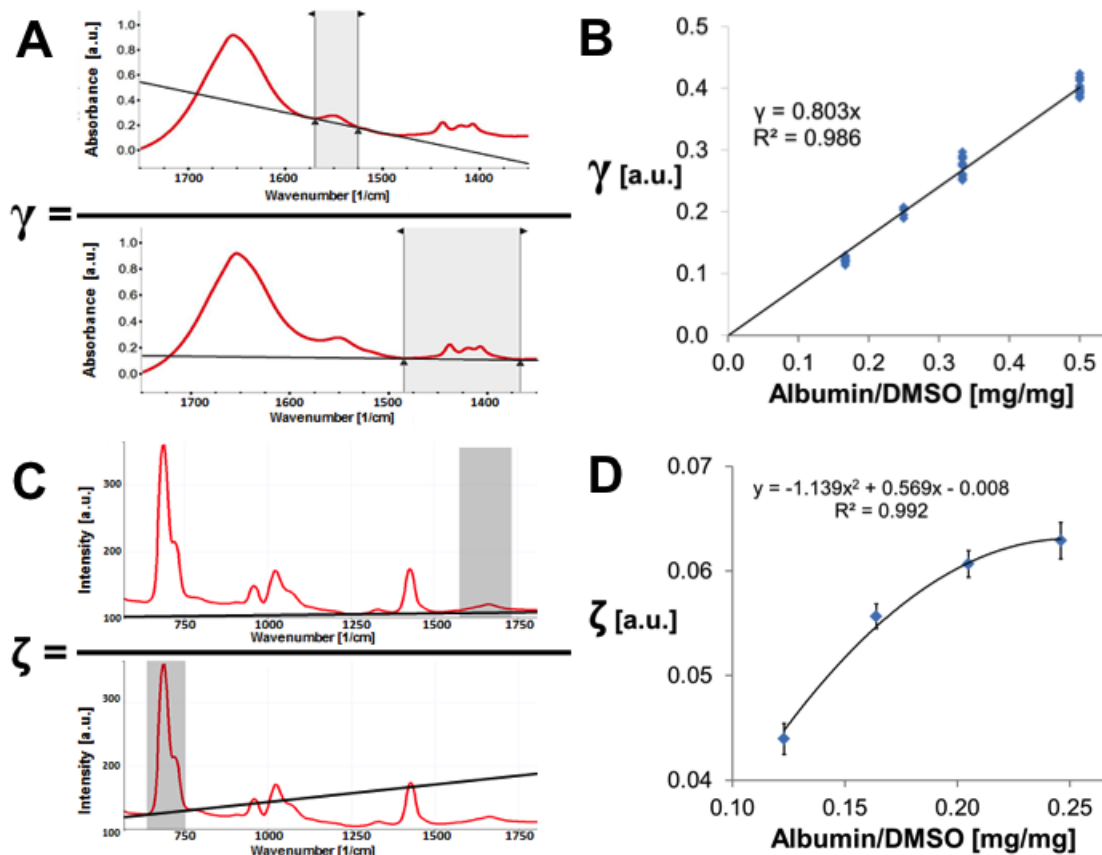


Figure 3. FTIR and Raman Albumin/DMSO ratio calibration: A-B) Ratio of baseline-corrected areas for γ and linear calibration curve. C-D) Ratio of baseline-corrected areas for ζ and quadratic calibration curve.

As γ could be directly calculated from the IR spectra, it could then be used to calculate the protein content changes in the FCL *in situ*. Changes in FCL composition in the presence of varying amounts of ice were then calculated as a percentage change from the FCL of the Minimum Ice Solution (MIS) described previously.

2.3.4) Raman Spectral Analysis

The same experimental protocol followed for the equilibrium freezing FTIR experiments was used to evaluate 15-25 wt% DMSO solutions with CRM. A 30 wt% DMSO solution that contained 63 mg/ml of albumin was frozen at 30°C/min and then

warmed until a few small ice crystals remained at -17.5°C . Solutions of 25 wt%, 20 wt%, and 15 wt% DMSO were then tested with the same albumin/ DMSO ratio.

The albumin concentration in the FCL was measured by a ratio of the baseline-corrected integrated intensity of the strong Amide I band and the weak tyrosine residue of the albumin ($1575\text{-}1735\text{ cm}^{-1}$)⁶⁸ to the baseline-corrected integrated intensity of the band that included strong contributions from the antisymmetric and symmetric S-C stretching bands of the DMSO and a weak contribution from the $\nu\text{-S-C}$ of the albumin ($635\text{-}750\text{ cm}^{-1}$)^{67,68}. This ratio is denoted as $\zeta \equiv A_{\text{Albumin}} / A_{\text{DMSO+Albumin}}$ (**Figure 3C**). The Amide I band used to quantify albumin also overlaps with the $\delta\text{-OH}$ band of water, but this band is very weak in the Raman spectra, and its effect was minimized by the constant water content at equilibrium at -17.5°C ⁶⁹. A calibration curve was constructed by varying the amount of albumin added to a 30 wt% DMSO solution and then plotting ζ with respect to the albumin to DMSO ratio (mg/mg) (**Figure 3D**). A second degree polynomial was required due to the overlap of the albumin and DMSO peaks used.

2.4) Results

In order to measure the exact amount of protein missing from the freeze-concentrated liquid phase due to the presence of ice, we have developed a technique to utilize *in situ* IR and Raman spectroscopy. Aqueous solutions containing 20-63 mg/ml of albumin and 6-35 wt% DMSO were studied. Temperatures at which data were collected were chosen to maximize the amount of the FCL phase in the frozen state (to maximize the signal to noise ratio of the spectra). Therefore, we conducted experiments with frozen solutions at -4°C to -6°C for 6-12 wt% DMSO solutions, at -8.5°C for 12-18 wt% DMSO

solutions, at -13°C for the 10-20 wt% DMSO solutions, at -17.5°C for 15-30 wt% DMSO solutions, and at -20°C to -40°C for 15-35 wt% solutions.

2.4.1) FTIR Experiments at -4°C and -6°C

For low DMSO concentration experiments with equilibrium freezing temperatures in the range of -2°C and -6°C, two ratios of albumin/DMSO, 1:3 and 1:2, were used in solutions of 6 wt%, 8 wt%, 10 wt%, 11 wt% (for 1:2), and 12 wt% (for 1:3) DMSO, such that the FCL at equilibrium at -6°C would contain approximately 40 mg/ml or 56 mg/ml albumin (for the 1:3 and 1:2 albumin/ DMSO ratio, respectively). At the temperature where data were collected, the albumin/DMSO ratio decreased slightly with respect to the Minimum Ice Solution (MIS) in two conditions, but these were statistically insignificant ($p=0.33$ and $p=0.46$, $n=15$) (**Figure 4A-B**). In all other conditions at -4°C and -6°C, there was a net increase in the albumin/DMSO ratio that was correlated with greater ice content. The most significant increase in the albumin/DMSO ratio was observed in the FCL of the 6 wt% DMSO solutions, where ice comprised approximately 50% of the volume of the partially frozen system. This increase was statistically significant in the 6 wt% DMSO solution at both protein concentrations and temperatures ($p < 0.001$, $n=15$ for each protein concentration and temperature). Since a net increase in the albumin/DMSO ratio would only be possible if more DMSO than albumin were missing from the FCL, either by accumulation at the ice surface or entrapment in the ice phase, this suggests that the albumin was preferentially excluded from the ice phase during freezing. This effect was greatest in the warmer temperature (-4°C) with the most amount of ice (6 wt% DMSO). To evaluate the influence of temperature, additional FTIR experiments were run at -8.5°C, -13°C, -17.5°C, and -20°C.

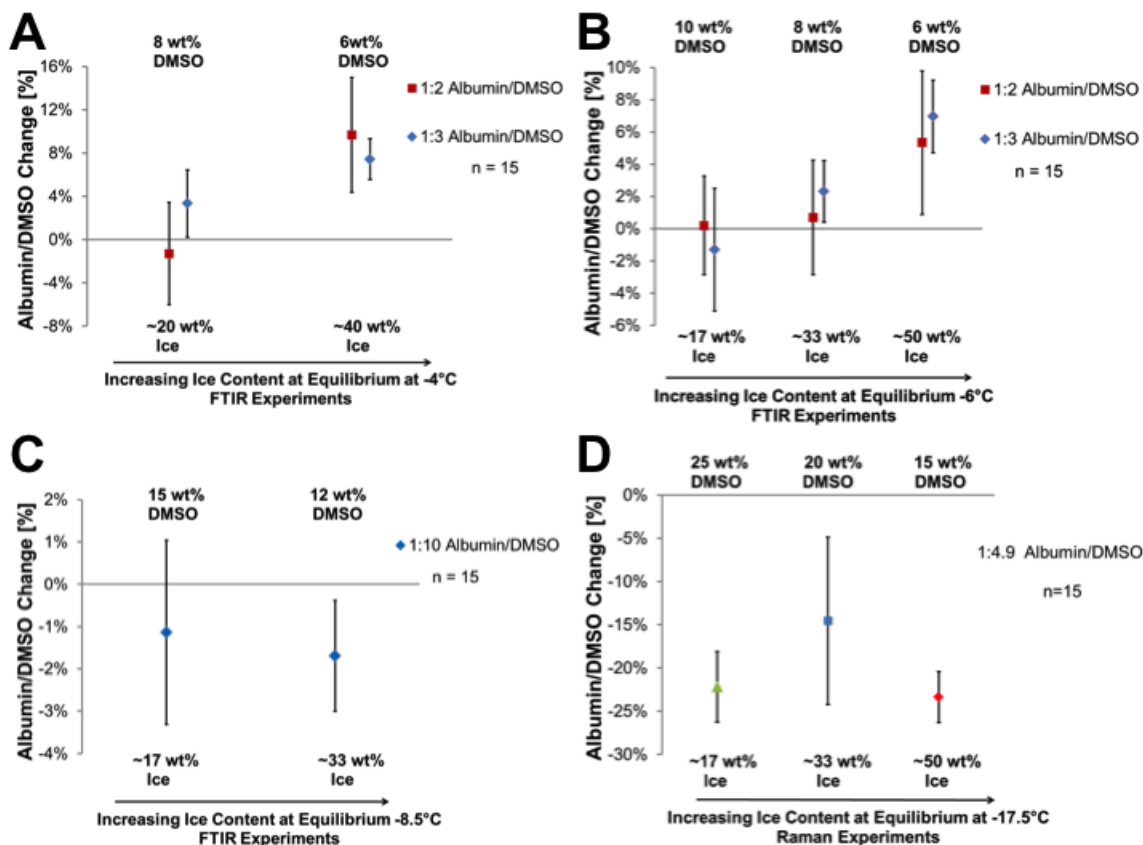


Figure 4. A-C) FTIR Results: Change in Albumin/DMSO ratio at -4°C, -6°C and -8.5°C. D) Raman Results: Change in Albumin/DMSO at -17.5°C.

2.4.2) FTIR Experiments at -8.5°C, -13°C, -17.5°C, and -20°C

To evaluate changes in FCL composition at lower temperatures, more concentrated DMSO solutions were necessary to ensure that there would be a sufficient volume of FCL in which to collect spectra. To evaluate partially frozen solutions at -8.5°C, an 18 wt% DMSO solution with 30 mg/ml albumin was diluted to 15 wt% DMSO, 12 wt%, and 9 wt%. It was not feasible to collect spectra in the FCL of the 9 wt% DMSO solution due to an insufficient volume of FCL. In the 12 wt% DMSO solution there was a small, but significant decrease (-1.7% +/- 1.3%, $p = 0.017$, $n = 15$) in the albumin/DMSO ratio in the FCL with respect to the FCL of the MIS (18 wt% DMSO). In the 15 wt%

DMSO solution, which had only a small amount of ice at this temperature, only an insignificant decrease in the albumin/DMSO ratio of the FCL was observed (-1.1% +/- 2.2%, $p=0.17$, $n=15$). See *Figure 5C*.

To evaluate partially frozen solutions at -13°C , a 20 wt% DMSO solution with 25 mg/ml albumin was diluted to 10 wt% DMSO. There was no significant difference in the albumin/DMSO ratio ($p=0.43$, $n=15$) in the FCL of these solutions, although the standard deviation was much higher in the 10 wt% solutions (with more ice), suggesting the presence of heterogeneity in the FCL. Additional experiments at -17.5°C were conducted with a 30 wt% DMSO solution with 30 mg/ml albumin that was diluted to 20 wt% DMSO. At this temperature, a small decrease in the albumin/DMSO ratio in the FCL of the 20 wt% DMSO solution with respect to the 30 wt% DMSO solution was observed, but it did not reach statistical significance (-1.5% +/-3.1%, $p=0.18$, $n=15$). At -20°C , a significant decrease was observed in the albumin/DMSO ratio in a diluted 15 wt% DMSO solution with respect to the original 30 wt% DMSO with 25 mg/ml albumin solution (-5.3% +/-2.7%, $p<0.0001$, $n=10$).

These results, when considered with those of the 6 wt% DMSO solutions at -4°C and -6°C , suggest that the presence of ice has an effect on the composition of the FCL that changes over the -4°C to -20°C temperature range. At temperatures of -4°C and -6°C , the presence of ice is associated with an increase in the albumin/DMSO ratio in the FCL of partially frozen solutions. At lower temperatures, the observed effect of ice changes and is now associated with a decrease in the albumin/DMSO ratio. This loss of the albumin from the FCL at lower temperatures is also supported by the results of the CRM experiments (*Figure 5D*).

2.4.3) Confocal Raman Experiments at -17.5°C

Solutions of 15 wt%, 20 wt%, and 25 wt% DMSO with an albumin/DMSO ratio of 1:4.9, such that the FCL at -17.5°C would contain 63 mg/ml albumin, all showed significant decreases in the albumin/DMSO with respect to the MIS (30 wt% DMSO), suggesting a loss of the albumin from the FCL ($p < 0.001$, $n = 15$) (*Figure 5D*). The magnitude of the decrease was greater than that observed in FTIR experiments, which may be the result of the different geometry of the experiment. In the very thin geometry of the FTIR experiments, ice crystal growth is constrained to the X-Y plane of the microscope window and the majority of the ice surface area is in contact with the top and bottom windows and not the FCL. The thicker geometry of the CRM experiments means that more of the ice surface area is in contact with the FCL instead of the top and bottom windows, which may be why the ice has a larger effect.

2.4.4) Additional FTIR Experiments between -20°C and -35°C

To investigate temperatures below -20°C, a 40 wt% DMSO with 25 mg/ml albumin solution was prepared and successively diluted to 35 wt%, 30 wt%, 25 wt%, and 20 wt% DMSO. The highest concentration solution of 40 wt% DMSO did not freeze consistently, and so the next most concentrated solution, the 35 wt% DMSO, was used as a basis for comparison at -30°C. At this temperature, there was no statistically significant difference between solutions. Due to unexpectedly large variations in equilibrium melt temperatures, as well as a worse signal/noise ratio with the lower protein concentration, a new 35 wt% DMSO solution with 30 mg/ml albumin was prepared and successively diluted. FCL comparison with 35 wt% DMSO solutions was possible at -30°C, temperature at which minimal ice content was present in the 35 wt% solution, and with

the 30 wt% DMSO solution at -25°C and -20°C. The most diluted solution, the 20 wt% DMSO, showed slight increases in protein concentration with respect to the more concentrated 30 wt% and 35 wt% DMSO solutions, whereas the 25 wt% DMSO showed slight decreases. The significant standard deviations and the absence of a consistent trend with respect to concentration, make it difficult to draw any conclusions from these results alone.

2.4.5) Bulk Freezing Experiments at -20°C

FTIR analysis revealed two interesting findings. There was a net increase in protein content with respect to DMSO in the extracted FCL with respect to the bulk solution. This increase was most significant in the sample with the smallest amount of ice ($p < 0.0001$, $n = 20$), such that with respect to the FCL of this sample, there was a decreasing trend in protein content with additional ice. In an attempt to elucidate this relationship, the protein content was normalized by the composition of the extracted FCL with the smallest amount of ice, and then plotted with respect to the ratio of the minimum surface area of the ice to the volume of liquid added to the ice (**Figure 5**). The minimum surface area was calculated by assuming the most thermodynamically favored geometry of a sphere, using the volume of the frozen water that was initially added to the centrifuge tubes. Although the actual surface area was unknown, just prior to extracting the FCL at 30 hours, it was visually observed that the ice was surrounded by solution as a result of restructuring.

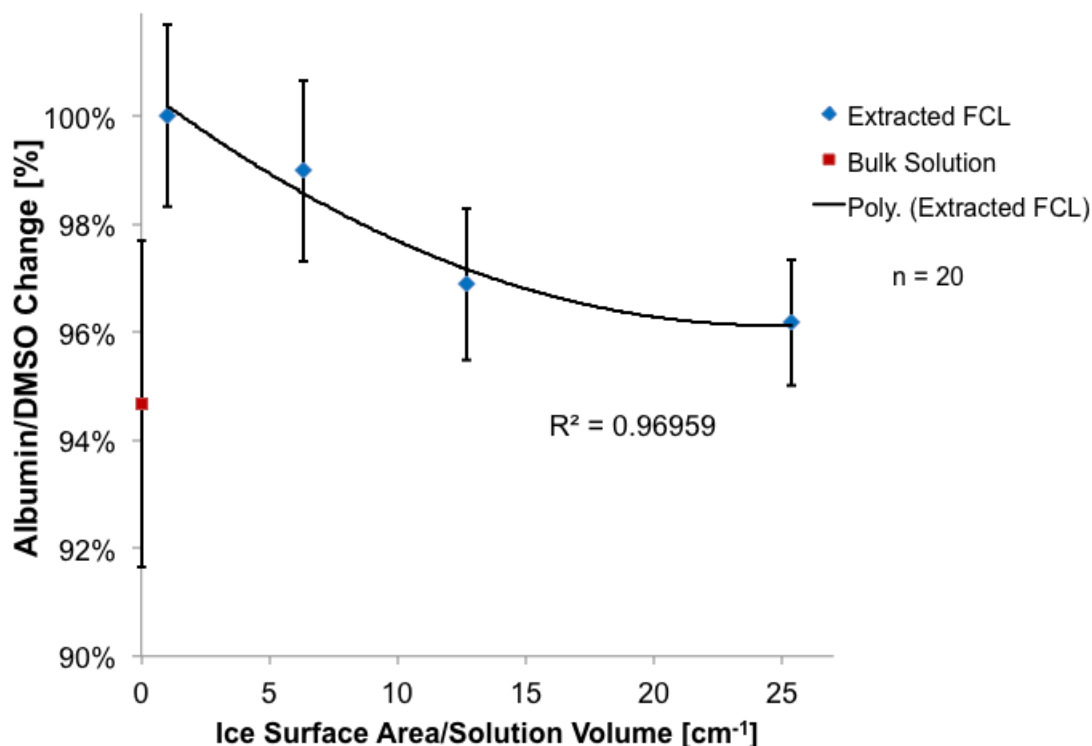


Figure 5. Bulk freezing experiments: the albumin content in the FCL extracted from the samples after 30 hours at -20°C is plotted versus a measure of the effective surface area that could interact with the FCL. The γ values are normalized by the γ of the FCL extracted from the solution with the least amount of added ice (shown as 100%). The starting bulk solution is also included in the plot.

2.5) Discussion

The hypothesis that motivated this investigation was that albumin was not simply distributed homogeneously in the FCL and that it either accumulated or aggregated at the ice interface, or became entrapped within the ice during slow, near-equilibrium freezing. The anticipated experimental results would show either a decrease in protein content in the FCL that would support the hypothesis, or no change in the FCL. The results that were obtained however, suggest that more complicated interactions -that also involve the

solvent DMSO- are occurring during freezing. In the experiments with low concentration DMSO at -4°C and -6°C , the presence of ice was correlated with a net increase in protein content with respect to albumin in the FCL. As the ice phase grew and the FCL phase became more concentrated, the protein concentration increased more than the DMSO concentration. This same phenomenon was also observed in the bulk freezing experiments, where larger volumes of solution were added to ice and then extracted as an FCL after being in contact with ice for 30 hours at -20°C .

This would suggest that the protein became more concentrated than expected in the FCL as a result of a loss of DMSO from the FCL phase, either during ice growth or simply in the presence of ice. In addition, the results from the equilibrium freezing experiments using FTIR and CRM at -8.5°C , -17.5°C , and -20°C , as well as the bulk freezing experiments at -20°C , supported the original hypothesis of a loss of protein to the ice interface or ice phase. This evidence, nonetheless, appears to be complicated by what was occurring with the DMSO, which is perhaps why the results between -20°C and -40°C did not yield a consistent trend.

A possible explanation for these observations is that albumin accumulates at the ice interface. This phenomenon is either negligible at warmer temperatures approaching 0°C , or is disguised by the more significant loss of DMSO from the FCL, resulting in the observed net increase in protein content in the FCL at -4°C and -6°C in the presence of ice. The decrease in the albumin/DMSO ratio as the temperature approached -20°C , suggests that the loss of albumin from the FCL becomes more significant with decreasing temperature.

The loss of DMSO from the FCL during freezing experiments at -4°C and -6°C , as well as from the FCL of bulk solutions held at -20°C in the presence of ice, could have multiple explanations. The first possible explanation would be the formation of DMSO-rich clusters or chains of molecules in solutions of DMSO+water+albumin. DMSO has been shown to form DMSO-water complexes with 1:2^{70,71} and 1:3 ratios⁶⁰ in binary solutions, but to our knowledge, it is not established what effect the presence of protein molecules has on these arrangements at sub-zero temperatures. If larger clusters rich in DMSO molecules were formed, these could have an affinity for ice surfaces, such that they could congregate preferentially at the interface. Or they could simply have reduced mobility, and thereby could get caught at the interface of growing ice crystals. In both cases, there would be heterogeneous distribution of DMSO in the FCL.

The results of the bulk freezing experiments support the conclusion that the heterogeneous distribution of DMSO-rich regions during slow freezing was the result of an affinity of DMSO for the ice surface and not reduced mobility. While it is possible that reduced mobility of the DMSO caused the increased protein content relative to DMSO observed in the FCL extracted from solutions held at -20°C for 30 hours in the absence of significant ice growth, this seems unlikely, unless the clusters of DMSO-rich regions were large enough to rival the size of the albumin macromolecules.

Another possible explanation for the increase in albumin observed in the FCL of solutions held at -20°C is that some of the DMSO crystallized out of the liquid phase. This would not need to have been triggered by the presence of ice, since it could have also occurred and gone undetected in the bulk solution held at -20°C . Samples for FTIR analysis were only taken from this solution once it had been warmed back to 4°C and

stirred again. Subsequent X-ray diffraction experiments at -6°C and -20°C (data not shown here), however, showed only the presence of ice and did not confirm the presence of any non-ice crystals.

The most compelling evidence of a loss of albumin from the freeze-concentrated liquid comes from the experiments conducted over 30 hours in a large-scale freezer, held at the common industry standard temperature of -20°C . These experiments were designed to isolate the interactions between the ice interface and albumin in the absence of ice growth. Thus the results, which showed a correlation between increased ice surface area and loss of albumin from the FCL over the relatively short time-scale of 30 hours, have implications for the long-term storage of albumin.

2.6) Summary

In this study, we have developed a novel technique using FTIR and Confocal Raman Microspectroscopy to measure interactions between ice and proteins *in situ* during freezing. We have shown that during freezing, as a function of temperature, dimethyl sulfoxide (DMSO) and bovine serum albumin are preferentially excluded from the ice phase, resulting in significant deviations from the theoretical composition of the freeze-concentrated liquid phase. As a result, as much as 20% of the albumin in solution may leave the freeze-concentrated liquid following freezing, and may be adsorbed onto the ice interface or entrapped in the ice phase.

Chapter 3: Mapping of Protein and Cryoprotectant Distribution in Directional Solidification using Confocal Raman Microspectroscopy

3.1) Introduction

Freezing and lyophilization are commonly employed to stabilize biological specimens and therapeutic proteins that would otherwise degrade over time in ambient or refrigerator conditions. Biospecimens like serum, plasma, bronchial lavage fluid and urine are often frozen and stored in the frozen state, while therapeutic proteins are often frozen and subsequently freeze-dried³⁻⁵. The end quality of the processed proteins and biospecimens can be diminished as a result of the physical and chemical stresses placed upon them during freezing⁵⁻¹³. In biospecimens, biomarkers may be lost and diagnostic and clinical utility may be reduced, thereby negatively impacting subsequent proteomic studies^{22,23}. In the case of proteins, these stresses can lead to irreversible alterations in the proteins' structure and activity^{4,12-19}, resulting in product losses and diminished reduced therapeutic impact²⁵. Identifying conditions under which the potentially damaging effects of freezing are minimized therefore represents an opportunity to improve the diagnostic and clinical utility of biospecimens, as well improve the product yields of proteins in the pharmaceutical industry and their therapeutic impact.

Freezing is a complex phenomenon that is influenced by multiple variables. When freezing aqueous solutions, the ice phase that forms generally incorporates few or no solutes³⁹. The solutes are excluded from the ice phase and are concentrated in the remaining freeze-concentrated liquid (FCL) phase. The morphology of the ice phase is greatly influenced the aqueous solution's composition^{72,73} and by the freezing conditions⁷⁴. The concentration of the solutes affects the equilibrium freezing

temperature, as well as the relative sizes of the freeze-concentrated liquid and ice phases, in accordance with the respective phase diagram.

Generally, ice does not form spontaneously upon reaching the equilibrium freezing temperature, and some degree of supercooling is required before homogeneous nucleation of ice will occur⁷⁵. To control the freezing process, seeding can be used to heterogeneously nucleate ice at a known temperature^{33,34}. The degree of supercooling, i.e. the difference between the nucleation temperature and the equilibrium freezing temperature, influences the morphology of the ice crystals that form. Solutions with higher degrees of supercooling freeze rapidly upon nucleation and have finer ice crystals with greater surface area than solutions with low degrees of supercooling³⁶.

Likewise, following heterogeneous nucleation at a given temperature, the morphology of the ice crystals that grow is affected by the cooling rate³⁶. In directional solidification, ice growth occurs in one primary direction and is controlled by cooling along the axis of ice growth^{35,76}. At very slow cooling rates with minimal solute concentration, the ice that forms is planar or cellular with large and smooth surfaces. With faster cooling rates and higher solute concentrations, the surface of the advancing ice front breaks down and becomes dendritic with much greater surface³⁵.

The interactions between proteins and the ice phase are of particular interest when freezing. Previous studies have shown that freezing can result in aggregation of proteins that may remain following thawing^{6,44,45}, as well as changes in protein conformation at the ice interface⁴³. The class of antifreeze proteins, for example, is known to adsorb to the surface of the ice, possibly through the formation of hydrogen bonds with the ice

surface^{40,41}. As a result, it would be beneficial to identify freezing conditions that affect the potentially harmful interactions between proteins and the ice phase.

In this study, we demonstrate the use of confocal Raman microspectroscopy (CRM) to quantify and map the distribution of proteins and cryoprotective agents in a sample frozen along a temperature gradient. By freezing along a temperature gradient, we are able to evaluate multiple freezing conditions simultaneously. CRM has been used previously to map solid⁷⁷⁻⁷⁹ samples and has been developed recently as a technique to map thermally uniform frozen tissue^{80,81}, cells⁸², and partially frozen solutions⁴³. To our knowledge, it has not been used previously to evaluate solutions frozen along a temperature gradient.

For a model protein, we use bovine serum albumin. Albumin is the most abundant protein found in the plasma^{83,84}, and in addition to facilitating transport for thyroid and steroid hormones^{48,49}, fatty acids⁵⁰, and regulating oncotic pressure in the capillaries⁵¹, it is used as a biomarker to detect and monitor renal and cardiovascular diseases⁵².

For a cryoprotective agent, we use trehalose, which is a disaccharide that is widely used for its ability to protect proteins from freezing-induced damaged⁸⁵⁻⁸⁷.

3.2) Materials and Methods

Experiments were conducted using Confocal Raman Microspectroscopy (CRM) with solutions over a range of trehalose concentrations (10-35 wt%) and albumin concentrations (2-12 wt%). Directional solidification experiments and calibration experiments were performed using solutions that were prepared gravimetrically with trehalose dihydrate ($\geq 97\%$ Purity, Wako, Osaka, Japan), bovine serum albumin ($\geq 98\%$ Purity, Sigma-Aldrich, St. Louis, MO) and 1x Dulbecco's phosphate buffered saline

(14190-144, Invitrogen Corporation, Burlington, Ontario, Canada). For directional solidification experiments, a 50 μm wide by 10 mm long microchannel with reservoirs at each end was machined in a 50 μm thick silicone film that was then sandwiched between two quartz windows (**Figure 6**). Each directional solidification experiment involved wicking 3 nL of solution into the microchannel through the reservoir. Calibration experiments were performed with a similar channel without the fluid reservoirs at each end, such that the solution was added to the microchannel before the top quartz window was placed.

For all experiments, the sample was then transferred to a confocal Raman microscope (Nanophoton, Osaka, Japan) equipped with a 100 \times Nikon air objective (NA 0.90) and a 532 nm AR-ion laser operated at 12 mW for excitation and a CCD detector electrically cooled to -70°C . Spatial resolution was 350 nm in the x-direction and 800 nm in the vertical direction. Each scan was conducted over a 4 μm x 83 μm region of the sample with a spectral resolution of 6 cm^{-1} in the 4666-70 cm^{-1} wavenumber range at an exposure time of 0.05 s per pixel. To improve the signal to noise ratio in individual spectra, the collected spectra were spatially averaged by a factor of 2 in each direction, thereby reducing the number of spectra per scan from 8000 to 2000. The spectra were then processed by applying 15 point Savitsky Golay smoothing and analyzed using CytoSpec software (Boston, MA) and Matlab (MathWorks, Natick, MA).

For calibration experiments, a FDCS 196 (Linkam Scientific Instruments Ltd., UK) freeze-drying cryostage was installed and used for temperature control of the sample. For directional solidification experiments, a cooling stage was built with two copper plates separated by 4mm. The temperature of each plate was controlled

independently by internal resistance heating elements and liquid nitrogen. By setting these two plates to different temperatures and placing the ends of the microchannel of solution on each plate, a temperature gradient was imposed across the microchannel (*Figure 6*).

3.2.1) Calibration Experiments

During solidification experiments, solutes are excluded from the ice phase and redistributed within the freeze-concentrated liquid phase. To quantify and map the resulting distribution of trehalose and albumin in solutions in the solutions frozen along a temperature gradient, calibration was required. Solutions of trehalose and albumin were cooled at 10°C/min to -20°C. Cooling was paused to collect spectra at 0°C, -5°C, -10°C, -15°C, and -20°C. See *Table 2* for a description of the calibration concentrations.

Trehalose [wt%]	Albumin [wt%]	Albumin/Trehalose [w/w]
10	2	0.2
10	3	0.3
10	4	0.4
20	2	0.1
20	4	0.2
20	6	0.4
30	3	0.1
30	6	0.2
30	12	0.4
35	7	0.2

Table 2. Calibration experiments trehalose and albumin concentrations in 1x DPBS.

3.2.2) Directional Solidification Experiments

Directional solidification experiments were performed with combinations of 10-30 wt% trehalose and 2-4 wt% albumin (about 20-40 mg/ml) and are shown in *Table 2*. The microchannel of solution was positioned on the two temperature-controlled plates

while at room temperature. The plates were then slowly cooled until reaching set temperatures of 16°C and -20°C and held to +/- 2°C throughout the remainder of the experiments. The difference in temperature between the two plates created a temperature gradient along the microchannel, dT/dx , with a near linear segment in the region that straddled the two plates (**Figure 6**). The temperature profile was confirmed by embedding 0.25mm diameter thermocouples at a spacing of 1mm in a microchannel of deionized water (**Figure 7**).

Once the temperature gradient was established, ice was nucleated at the cold end by injecting a small amount of silver iodide into the cold reservoir (at right on **Figure 6**). Ice formed rapidly and propagated along the microchannel at a speed of v toward the warm reservoir until reaching the equilibrium melt temperature of the solution. Confocal Raman scans were then collected every 0.5 mm, starting from the cold end.

Trehalose [wt%]	Albumin [wt%]	Albumin/Trehalose [w/w]
10	2	0.20
10	3	0.30
10	4	0.40
20	2	0.10
20	3	0.15
20	4	0.20
30	3	0.10
30	4	0.13

Table 2. Directional solidification trehalose and albumin concentrations in 1x DPBS.

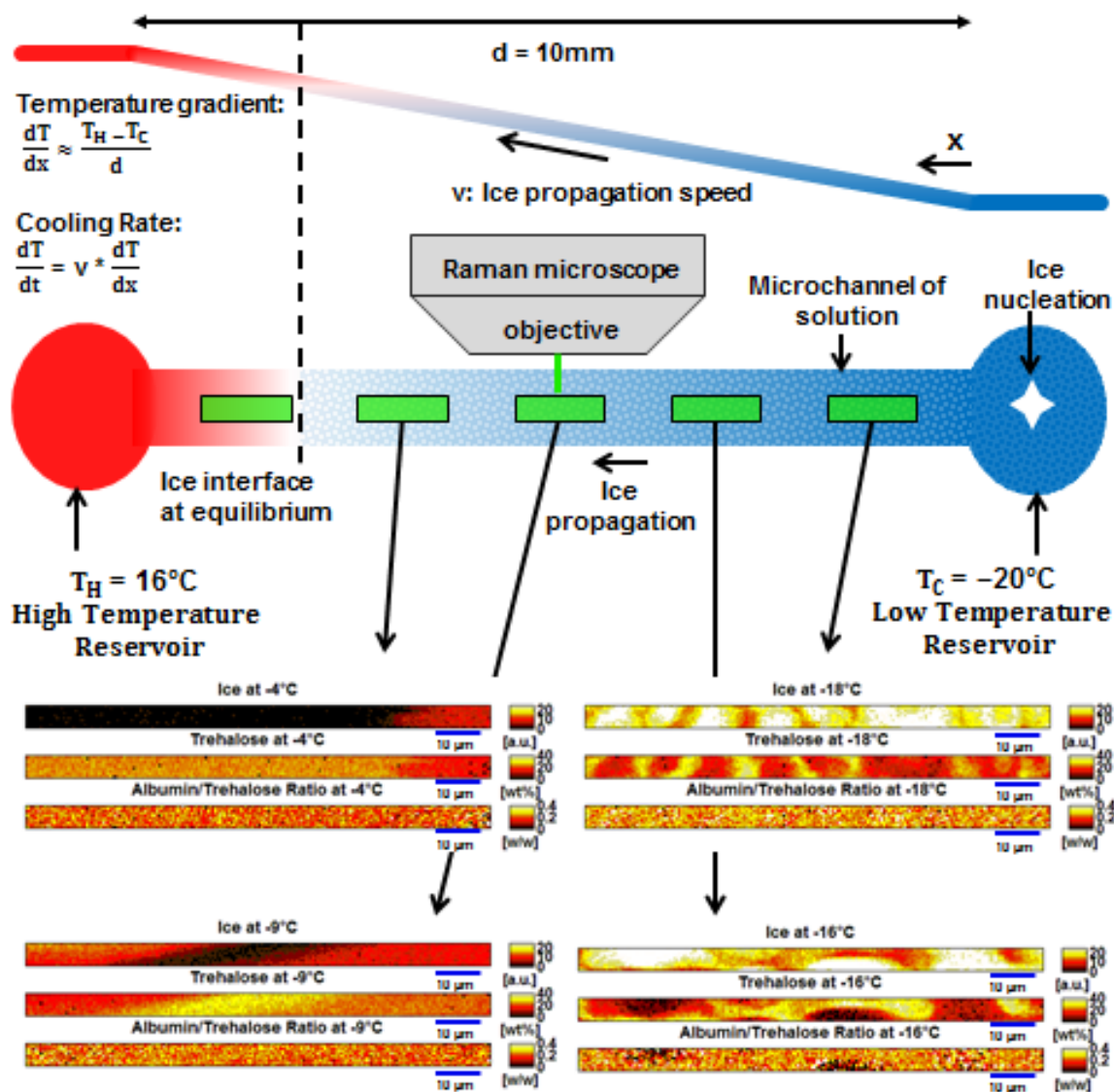


Figure 6. Schematic of directional solidification setup with confocal Raman microscope. Confocal Raman maps of the distribution of ice, trehalose, and albumin/trehalose ratio are included for 20 wt% trehalose, 4 wt% albumin at -4°C , -9°C , -16°C , and -18°C .

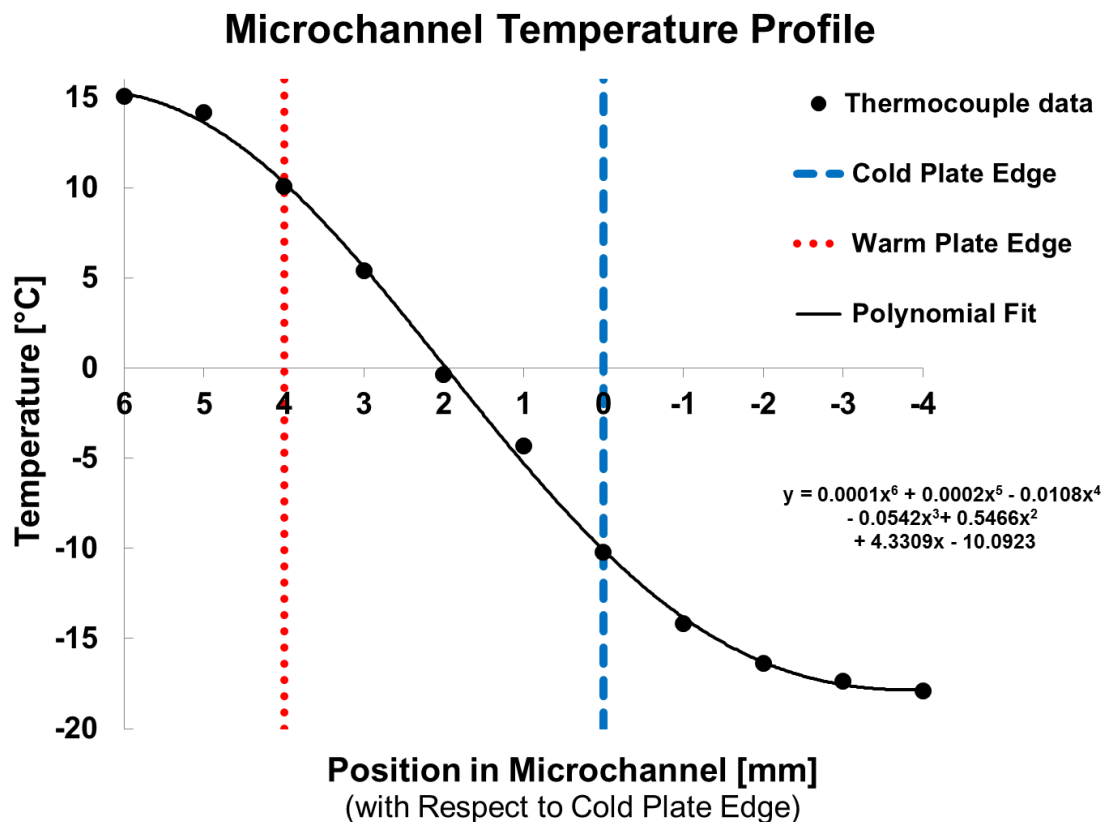


Figure 7. Temperature profile along microchannel.

3.2.3) Raman Spectral Calibration and Analysis

The goal in mapping the distribution of trehalose and albumin in the solutions frozen along a temperature gradient was to determine how the two solutes were redistributed during freezing. Since a cryoprotective agent like trehalose would only protect proteins in its vicinity, attention was paid to identify heterogeneity that occurred during the freeze-concentration of trehalose and albumin, which could leave the proteins more vulnerable to stresses at the ice interface.

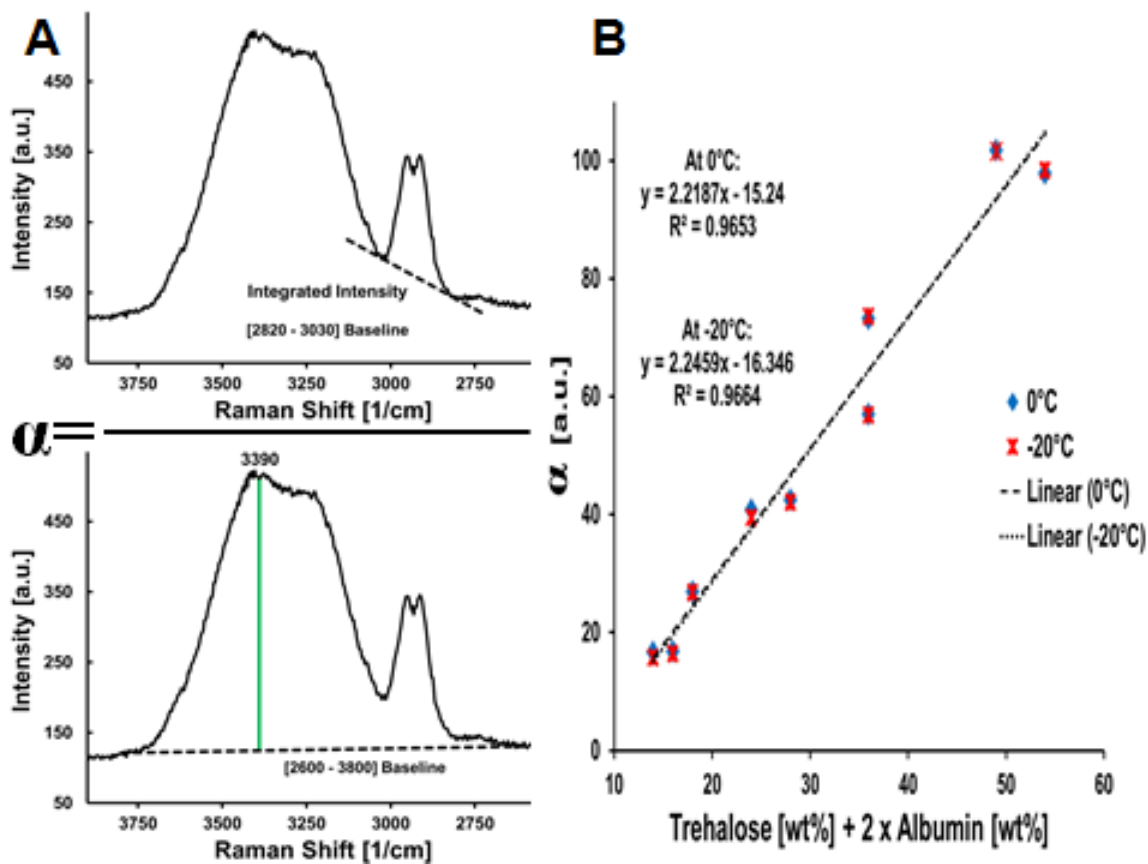


Figure 8. Organic content calibration using α : A) Raman spectral ratio, B) Linear calibration curve at 0 to -20°C.

Albumin and trehalose, being both organic molecules, have strong ν -CH bands in their Raman spectra. Due to the overlap of these bands, trehalose and albumin concentrations were not determined directly. Instead, the overall organic content was determined first by calculating the baseline-corrected integrated intensity of the overlapping ν -CH bands (2820-3030 cm^{-1})⁸⁸⁻⁹¹ and dividing this by the intensity of the OH stretching band at 3390 cm^{-1} , coming primarily from the water with some contribution from the trehalose^{69,88,92}. A baseline of 2600-3800 cm^{-1} was used to calculate the intensity of the peak at 3390 cm^{-1} . The resulting ratio was denoted as $\alpha \equiv \text{Integrated Intensity}_{\nu\text{-CH}} / \text{Intensity}_{\nu\text{-OH}}$ and was plotted with respect to the concentration of

trehalose and twice the concentration of albumin in calibration experiments (*Figure 8, A-B*). The ν -CH band of the albumin Raman spectrum in this temperature range was strongest just surrounding 2935 cm^{-1} , as has been found for human serum albumin⁹³, and was found to contribute proportionally more to α than the trehalose, perhaps in part due to the contribution of the trehalose^{88,92} to the ν -OH band intensity at 3390 cm^{-1} . Due to the slight shifting of the spectra with decreasing temperature, a linear calibration curve was made at each temperature (0°C , -5°C , -10°C , -15°C , -20°C). For clarity, only the calibration curves of the extreme temperature are shown and the very minimal standard deviations are omitted from the plot.

After determining the organic content (the sum of the unknown trehalose and twice the albumin concentration) in the sample, the mass ratio of albumin/trehalose was determined by the ratio of the intensities at 2935 cm^{-1} (from primarily albumin)⁹³ and at 2915 cm^{-1} (albumin and trehalose)^{88,94}. The intensities were calculated using the baseline of $2890\text{-}2990\text{ cm}^{-1}$ for regions with high organic concentration corresponding to about 20 wt% trehalose or greater, and using the baseline of $2880\text{-}3010\text{ cm}^{-1}$ for regions with low organic concentration corresponding to less than 20 wt% trehalose (*Figure 9, A and C*). This ratio was denoted as σ_{low} or $\sigma_{\text{high}} \equiv \text{Intensity}_{2935}/\text{Intensity}_{2915}$ and was plotted with respect to the mass ratio of albumin/trehalose at each temperature, at both high and low trehalose concentrations, to create a series of linear calibration curves (*Figure 9, B and D*).

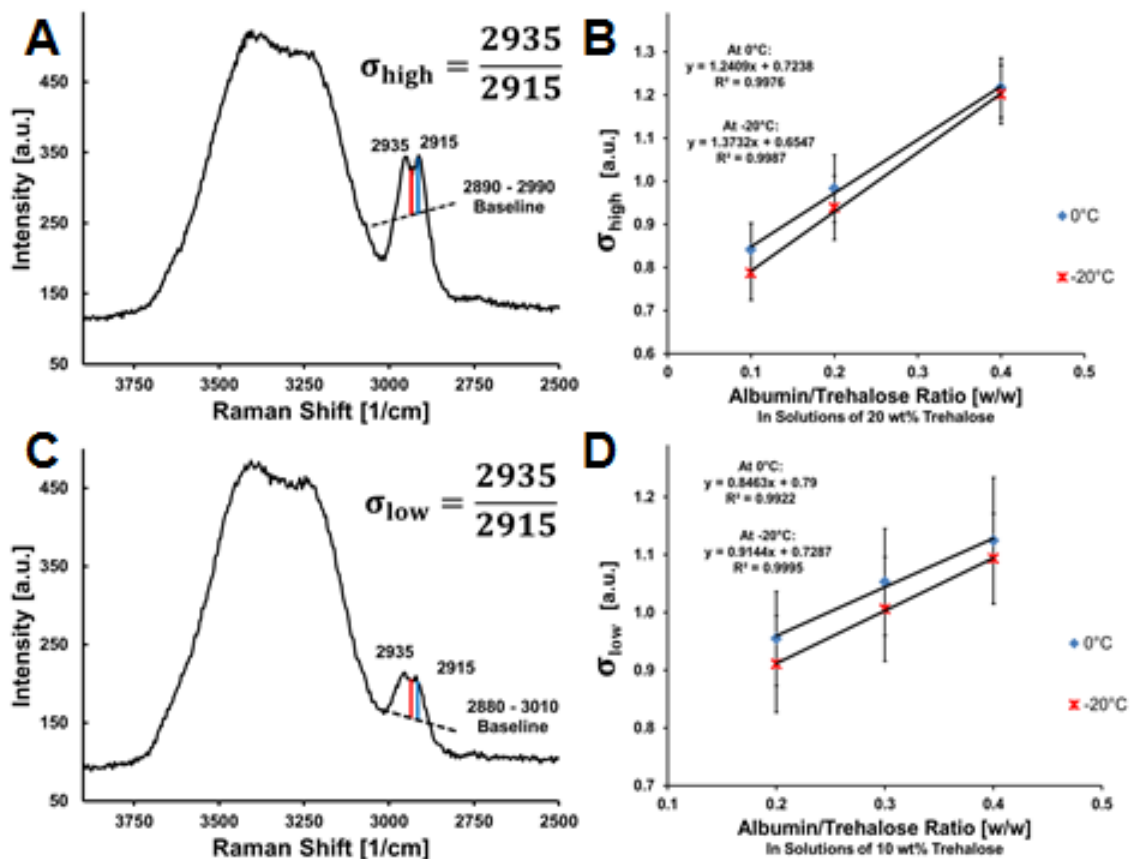


Figure 9. Calculation of albumin/trehalose ratio using σ in high and low concentration trehalose: A) Raman spectral ratio, σ , in high concentration trehalose B) Linear calibration curve of σ in high concentration trehalose at 0 to -20°C. C) Raman spectral ratio, σ , in low concentration trehalose B) Linear calibration curve of σ in low concentration trehalose at 0 to -20°C.

With the known amount of organic content and albumin/trehalose ratio, a trehalose concentration could be calculated. This is the trehalose concentration of the solution in a $0.5 \times 0.5 \mu\text{m}$ scanned area assuming a homogeneous distribution of trehalose. Since in partially frozen solutions a given area was not necessarily all liquid, but instead a mixture of even smaller regions of highly concentrated freeze-concentrated liquid and ice, the calculated concentration was in fact an equivalent concentration. Low

equivalent trehalose concentrations served as a proxy to indicate that there were significant regions of ice in the scanned area. Conversely, scanned areas with high equivalent trehalose concentration were primarily freeze-concentrated liquid with little or no ice present.

When calculating the equivalent trehalose concentrations and albumin/trehalose ratios in the sample, the calibration curves at each temperature ($2.5^{\circ}\text{C} \leq \text{Calibration Temperature} < +2.5^{\circ}\text{C}$) were used. The temperature in a given region of the sample was calculated using a polynomial fit to the thermocouple data (*Figure 7*). Due to variability between experiments in the reference point used for position, the position data for each experiment were shifted so that the equilibrium melt temperature of each solution was aligned with the ice interface. This temperature was calculated using the binary trehalose and water phase diagram, where the wt% concentration of trehalose was adjusted so that only the weight of the trehalose and the 1x DPBS was used⁹⁵.

To visualize the distribution of ice, which should show an inverse relationship with the equivalent trehalose concentration, a ratio was calculated of the baseline-corrected integrated intensity of the ice band⁴³ from $3100\text{-}3200\text{ cm}^{-1}$ over the intensity coming primarily from water^{89,90} at 3390 cm^{-1} with the $2600\text{-}3800\text{ cm}^{-1}$ baseline that was also used for measuring organic content.

The accuracy of the trehalose concentration and albumin/trehalose ratio diminished in very low concentration due to a poor signal to noise ratio. Since after freezing, a scanned $0.5\text{ }\mu\text{m} \times 0.5\text{ }\mu\text{m}$ area could be composed of anything from pure ice with no solutes to all freeze-concentrated liquid, regions with very low concentrations of albumin and trehalose were present. To avoid biasing the results by including these areas

with weak signal, the areas with less than 10 wt% equivalent trehalose concentration were filtered out and excluded from further analysis. Likewise, areas where the calculated mass ratio of albumin/trehalose differed from the nominal value by more than a factor of three were considered spurious and excluded from analysis. For example, a 20 wt% trehalose and 3 wt% albumin solution would have a nominal albumin/trehalose ratio of 0.15, so that any area would need to have a calculated albumin/trehalose mass ratio of between 0.05 and 0.45, regardless of the absolute concentrations of the albumin and trehalose, to be included in further analysis.

3.3) Results and Discussion

The complexity of the data acquired in just one directional solidification experiment means that a number of variables can be evaluated, such as ice crystal size, solute redistribution, freezing temperature, the degree of supercooling, ice interface velocity, and cooling rate. The choice of which variables to consider affects the manner in which the Raman data is processed. In addition, the scale at which these variables are evaluated also affects the processing, since more subtle features in the Raman spectra like those stemming from conformational changes in proteins would be perhaps apparent only with a very good signal to noise ratio achieved with substantial spatial averaging.

Between 8 and 14 confocal Raman scans were taken in each experiment, resulting in between 64,000 and 112,000 individual spectra. We chose to focus our efforts on evaluating the heterogeneity of the freeze-concentrated liquid phase, in order to see under what conditions the relative composition (ratio of protein to cryoprotectant) of the freeze-concentrated liquid would vary with proximity to the ice phase. Due to the high degree of supercooling in the experiments (at the cold end), very small ice crystals and freeze-

concentrate liquid regions were formed upon ice nucleation. As a result, it was important to maintain spatial resolution at the sub-micron scale while processing the spectra.

As seen in the maps included at the bottom of *Figure 6*, a wide variety in ice and freeze-concentrated liquid morphology could be measured and mapped along the microchannel at different temperatures. The relative intensity of the ice phase was in very good agreement with the measured equivalent trehalose concentration in all experiments, so that a faint ice signal was detected in regions with high trehalose concentration and vice versa. That the variety in morphology along the temperature gradient could be detected with good accuracy in a single experiment demonstrated the potential utility that this experimental technique could have in identifying freezing conditions to obtain a given ice morphology.

The spatial averaging by a factor of 2 in each direction meant that 4 individual spectra were averaged before analysis. In many of the experiments, particularly at the low temperature end of the microchannel, the freeze-concentrated liquid and the ice phases were not clearly distinct even at the scale of 0.5 μm . This led to the measurement of regions with a range of equivalent trehalose concentrations and varying ice signals. Since quantifying the ice content directly was not readily feasible, the lower trehalose equivalent concentrations were used to identify regions with greater ice content. By sorting the albumin/trehalose data according to equivalent trehalose concentration, it was possible to identify variation in the relative composition of the freeze-concentrated liquid (i.e., the proportions of albumin and trehalose) indirectly as a function of ice content.

In *Figure 10*, the mean albumin/trehalose value in each sorted category of equivalent trehalose concentration at each temperature is shown. The values are

normalized by the mean value of all concentrations at each temperature to facilitate comparison. Concentration ranges were sorted as greater or equal to the lower limit in the displayed range and less than the upper limit (e.g., $10 \text{ wt}\% \leq X < 15 \text{ wt}\%$). While the spatial averaging did improve the signal to noise ratio, it was still important to have data from many spectra in order to reduce the influence of noise. For this reason, to be included in the plot, a minimum of 2% of the values at a given temperature had to fall within the concentration range, so that only data representing the mean of at least 40 data points would be included.

Multiple trials of each condition would be required to make definitive observations, but there are some noticeable trends that can be seen in *Figure 10*. With few exceptions, the lowest equivalent trehalose concentration range, 10-15 wt%, has an albumin/trehalose ratio higher than the mean value. Likewise, the highest equivalent trehalose concentration range (comprised of the least amount of ice), 30 wt% and greater, has an albumin/trehalose ratio that is equal to or less than the mean value in all experiments. Between these two extremes, there is a general trend of lower albumin/trehalose ratios in higher equivalent trehalose concentration. Notably, the variation in the albumin/trehalose ratio is more pronounced in the higher concentration trehalose experiments (20 wt% and 30 wt%) than in the lower concentration trehalose experiments (10 wt%).

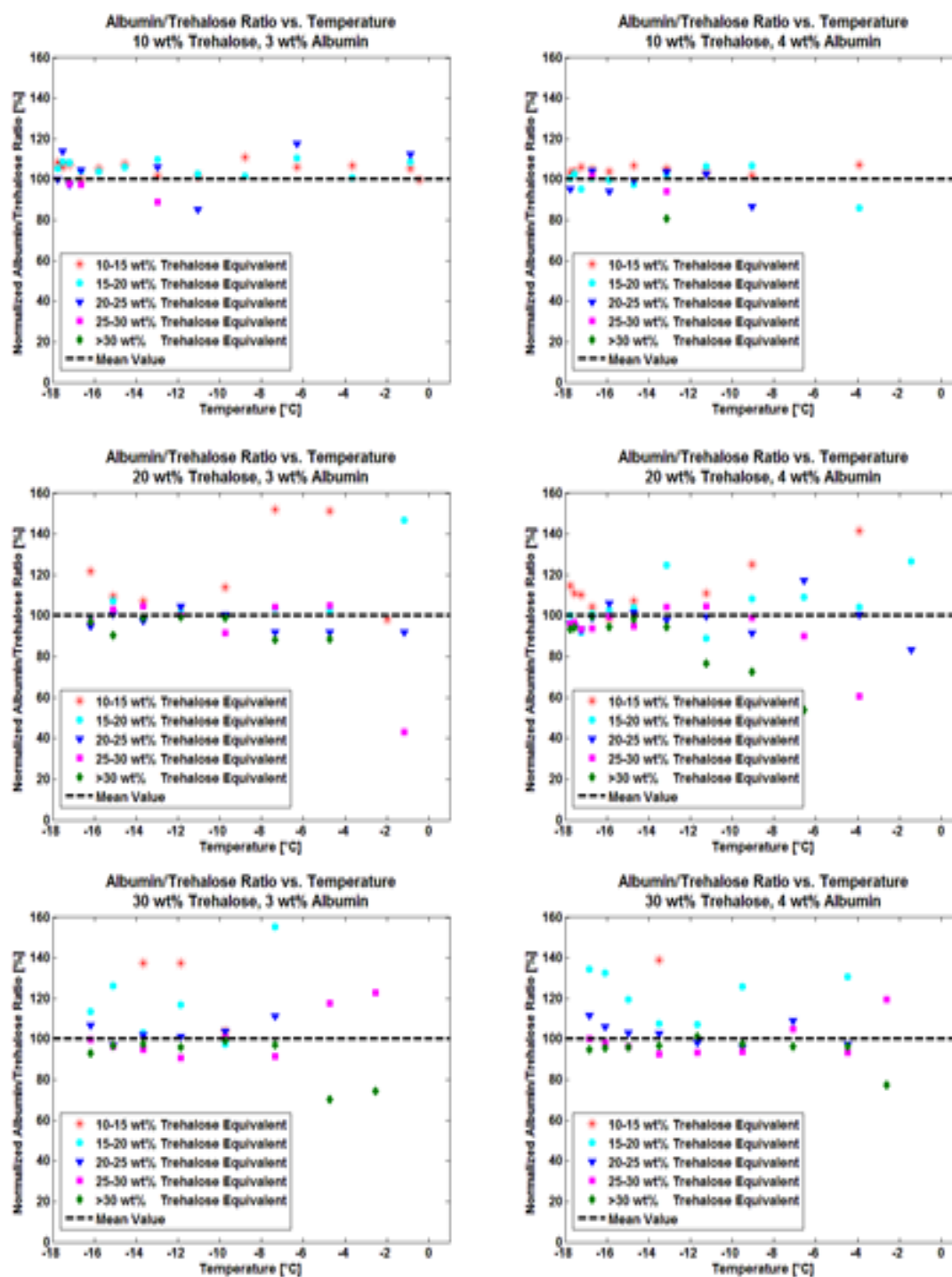


Figure 10. Heterogeneity of albumin/trehalose ratio with respect to local environment. For each experiment, albumin/trehalose ratios in each equivalent trehalose concentration normalized by the mean value at that temperature. A) 10 wt% trehalose, 3 wt% albumin, B) 10 wt% trehalose, 4 wt% albumin, C) 20 wt% trehalose, 3 wt% albumin, D) 20 wt% trehalose, 4 wt% albumin, E) 30 wt% trehalose, 3 wt% albumin, F) 30 wt% trehalose, 4 wt% albumin.

Interestingly, the heterogeneity of the albumin distribution in the freeze-concentrated liquid, as evidenced by the varying albumin/trehalose ratio with respect to the equivalent trehalose concentration, is greatest at warmer temperature and in higher trehalose concentration. Both of these conditions result in slower ice formation with larger freeze-concentrated liquid regions. That under these conditions the albumin is disproportionately distributed in areas of less trehalose concentration and more ice could have multiple explanations. It could be the result of a bias introduced in the Raman spectra by the ice peak that altered the baseline used to calculate the albumin/trehalose ratio. This explanation does not seem likely, however, since a bias introduced by the ice peak should be greatest at the lower temperatures with the greatest amount of ice, and this was not the case. Another explanation could be an increase in the diffusion length scale with the larger freeze-concentrated regions, combined with the reduced mobility of the albumin in high concentration trehalose. Lastly, it could be the result of an affinity of the albumin for the ice surface, as has been shown to occur in anti-freeze proteins^{40,41}, and has been shown to occur with albumin in dimethyl sulfoxide during slow, quasi-equilibrium freezing (Chapter 2).

3.4) Summary

In this investigation, we have introduced a novel technique that uses confocal Raman microscopy in combination with directional solidification to evaluate a wide range of freezing conditions in a quantitative fashion at the sub-micron scale in a single experiment. Initial results from experiments with albumin and trehalose suggest that there is heterogeneity in the distribution of the protein in the freeze-concentrated liquid, and that it is preferentially distributed near the ice phase. Further investigation is required to

confirm these findings and to identify under what freezing conditions this heterogeneity is most significant and to evaluate its effects on freeze-labile proteins.

Chapter 4: Research Summary

In this thesis, spectroscopic techniques were developed to measure interactions between proteins and ice. The goal of the investigations undertaken was to identify if and under what freezing conditions a common protein, bovine serum albumin, would be adsorbed to the ice interface or entrapped with the ice phase. The following conclusions were made:

In chapter 2, significant deviations from the expected composition of the freeze-concentrated liquid were found during quasi-equilibrium freezing of aqueous solutions of DMSO and albumin. In low concentration DMSO and warmer temperatures, there was an apparent loss in DMSO from the freeze-concentrated liquid that suggested that the DMSO was getting adsorbed onto the ice interface or entrapped in the ice phase. In higher concentrations of DMSO at lower temperatures, this behavior changed and as much as 20% of the albumin in solution may have been adsorbed to the ice interface or become entrapped in the ice phase.

In chapter 3, the investigation of protein-ice interactions was expanded to non-equilibrium conditions. To study a wide range of freezing conditions, directional solidification was combined in a novel way with confocal Raman microspectroscopy. After mapping the concentrations of both trehalose and albumin frozen in solutions frozen along a temperature gradient, microheterogeneity in the freeze-liquid phase was identified. Under some freezing protocols, this microheterogeneity resulted in the albumin being preferentially distributed in regions with greater nearby ice content. This

conclusion would be in agreement with the findings from Chapter 2, which suggested an affinity of albumin for ice quasi-equilibrium freezing conditions with slow ice growth. Together, these conclusions indicate that significant interactions between albumin and ice can occur, and that these conditions may be rapidly identified through directional solidification and mapping with confocal Raman Microscopy. Thus the technique developed here may be beneficial in the development of freezing protocols that minimize protein-ice interactions for other proteins of interest.

Chapter 5: References

- (1) Lee, M. H.; Baek, M. H.; Cha, D. S.; Park, H. J.; Lim, S. T. *Food Hydrocolloids* **2002**, *16*, 345.
- (2) Mackie, I. M. *Food Reviews International* **1993**, *9*, 575.
- (3) Peakman, T. C.; Elliott, P. *International journal of epidemiology* **2008**, *37*, i2.
- (4) Riegman, P. H. J.; Morente, M. M.; Betsou, F.; de Blasio, P.; Geary, P. **2008**, *2*, 213.
- (5) Chang, L.; Shepherd, D.; Sun, J.; Ouellett, D.; Grant, K. L.; Tang, X.; Pikal, M. J. *Journal of Pharmaceutical Sciences* **2005**, *94*, 1427.
- (6) Bhatnagar, B. S.; Bogner, R. H.; Pikal, M. J. *Pharmaceutical Development and Technology* **2007**, *12*, 505.
- (7) Pikal, M. J. Freeze-Drying of Proteins. In *Stability, Formulation and Delivery of Peptides and Proteins*; Cleland, J. L., Langer, R., Eds.; American Chemical Society: Washington, DC, 1994; pp 120.
- (8) Tang, X.; Pikal, M. J. *Pharmaceutical Research* **2005**, *22*, 1167.
- (9) Ragoonanan, V.; Aksan, A. *Transfus Med Hemoth* **2007**, *34*, 246.
- (10) Carpenter, J. F.; Crowe, J. H. *Biochemistry* **1989**, *28*, 3916.
- (11) Carpenter, J. F.; Crowe, J. H.; Arakawa, T. *Journal of Dairy Science* **1990**, *73*, 3627.
- (12) Crowe, J. H.; Carpenter, J. F.; Crowe, L. M.; Anchordoguy, T. J. *Cryobiology* **1990**, *27*, 219.
- (13) Randolph, T. W.; Carpenter, J. F. *AIChE Journal* **2007**, *53*, 1902.
- (14) Strambini, G. B.; Gabellieri, E. *Biophysical Journal* **1996**, *70*, 971.
- (15) Strambini, G. B.; Gonnelli, M. *Biophysical Journal* **2007**, *92*, 2131.
- (16) Manning, M. C.; Chou, D. K.; Murphy, B. M.; Payne, R. W.; Katayama, D. S. *Pharmaceutical Research* **2010**, *27*, 544.
- (17) Privalov, P. L.; Griko, Y. V.; Venyaminov, S. Y.; Kutysenko, V. P. *Journal of Molecular Biology* **1986**, *190*, 487.
- (18) Hannisdal, R.; Gislefoss, R. E.; Grimsrud, T. K.; Hustad, S.; Morkrid, L.; Ueland, P. M. *J. Nutr.* **2010**, *140*, 522.
- (19) Lee, D. H.; Kim, J. W.; Jeon, S. Y.; Park, B. K.; Han, B. G. *Ann. Clin. Lab. Sci.* **2010**, *40*, 61.
- (20) Manning, M. C.; Patel, K.; Borchardy, R. T. *Pharmaceutical Research* **1989**, *6*, 903.
- (21) Panesar, N. S.; Lit, L. C. W. *Clin. Chem. Lab. Med.* **2010**, *48*, 409.
- (22) McLerran, D.; Grizzle, W.; Feng, Z.; Bigbee, W.; Banez, L.; Cazares, L. *Clinical Chemistry* **2007**, *54*, 44.
- (23) McLerran, D.; Grizzle, W. E.; Feng, Z.; Bigbee, W. L.; Banez, L. L.; Cazares, L. H.; Chan, D. W.; Diaz, J.; Izbicca, E.; Kagan, J. *Clinical chemistry* **2008**, *54*, 44.
- (24) Silberman, S. *Wired Magazine* **2010**.
- (25) Rathore, N.; Rajan, R. S. *Biotechnology Progress* **2008**, *24*, 504.
- (26) Wettlaufer, J. S. *Philosophical Transactions of the Royal Society of London. Series A: Mathematical, Physical and Engineering Sciences* **1999**, *357*, 3403.

- (27) Angell, C. A. *Annual Review of Physical Chemistry* **1983**, 34, 593.
- (28) Kiyosawa, K. **2003**, 104, 171.
- (29) Goff, H. D.; Verespej, E.; Jermann, D. **2003**, 399, 43.
- (30) MacKenzie, A. P.; Derbyshire, W.; Reid, D. S. *Philosophical Transactions of the Royal Society of London. B, Biological Sciences* **1977**, 278, 167.
- (31) Murray, B. J. *Atmospheric Chemistry and Physics Discussions* **2008**, 8, 8743.
- (32) Huang, J.; Bartell, L. S. *The Journal of Physical Chemistry* **1995**, 99, 3924.
- (33) Fabbri, R.; Porcu, E.; Marsella, T.; Primavera, M. R.; Rocchetta, G.; Ciotti, P. M.; Magrini, O.; Seracchioli, R.; Venturoli, S.; Flamigni, C. *Molecular and cellular endocrinology* **2000**, 169, 39.
- (34) Trad, F. S.; Toner, M.; Biggers, J. D. *Human Reproduction* **1999**, 14, 1569.
- (35) Rubinsky, B.; Ikeda, M. *Cryobiology* **1985**, 22, 55.
- (36) Searles, J. A.; Carpenter, J. F.; Randolph, T. W. *Journal of pharmaceutical sciences* **2001**, 90, 860.
- (37) Bald, W. B. *Journal of Microscopy* **2011**, 143, 89.
- (38) Aysel, V.; Lottin, O.; Faucheux, M.; Sallier, D.; Peerhossaini, H. *International journal of heat and mass transfer* **2006**, 49, 1876.
- (39) Hobbs, P. V. *Oxford: Clarendon Press, 1974* **1974**, 1.
- (40) Raymond, J. A.; DeVries, A. L. *Proceedings of the National Academy of Sciences* **1977**, 74, 2589.
- (41) Nutt, D. R.; Smith, J. C. *Journal of the American Chemical Society* **2008**, 130, 13066.
- (42) Lin, Y.; Raymond, J.; Duman, J.; DeVries, A. *Cryobiology* **1976**, 13, 334.
- (43) Dong, J.; Hubel, A.; Bischof, J. C.; Aksan, A. *The Journal of Physical Chemistry B* **2009**, 113, 10081.
- (44) Eckhardt, B. M.; Oeswein, J. Q.; Bewley, T. A. *Pharmaceutical Research* **1991**, 8, 1360.
- (45) Kerwin, B. A.; Heller, M. C.; Levin, S. H.; Randolph, T. W. **1998**, 87, 1062.
- (46) Schwegman, J. J.; Carpenter, J. F.; Nail, S. L. *Journal of Pharmaceutical Sciences* **2009**, 98, 3239.
- (47) Costantino, H.; Firouzabadian, L.; Hogeland, K.; Wu, C.; Beganski, C.; Carrasquillo, K.; Córdova, M.; Griebenow, K.; Zale, S.; Tracy, M. *Pharmaceutical Research* **2000**, 17, 1374.
- (48) Pardridge, W. M.; Mietus, L. J. *Journal of Clinical Investigation* **1979**, 64, 145.
- (49) Pardridge, W. M. *American Journal of Physiology-Endocrinology And Metabolism* **1987**, 252, E157.
- (50) Bhattacharya, A. A.; Grüne, T.; Curry, S. *Journal of molecular biology* **2000**, 303, 721.
- (51) Gekle, M. *Annu. Rev. Physiol.* **2005**, 67, 573.
- (52) Basi, S.; Lewis, J. B. *American journal of kidney diseases: the official journal of the National Kidney Foundation* **2006**, 47, 927.

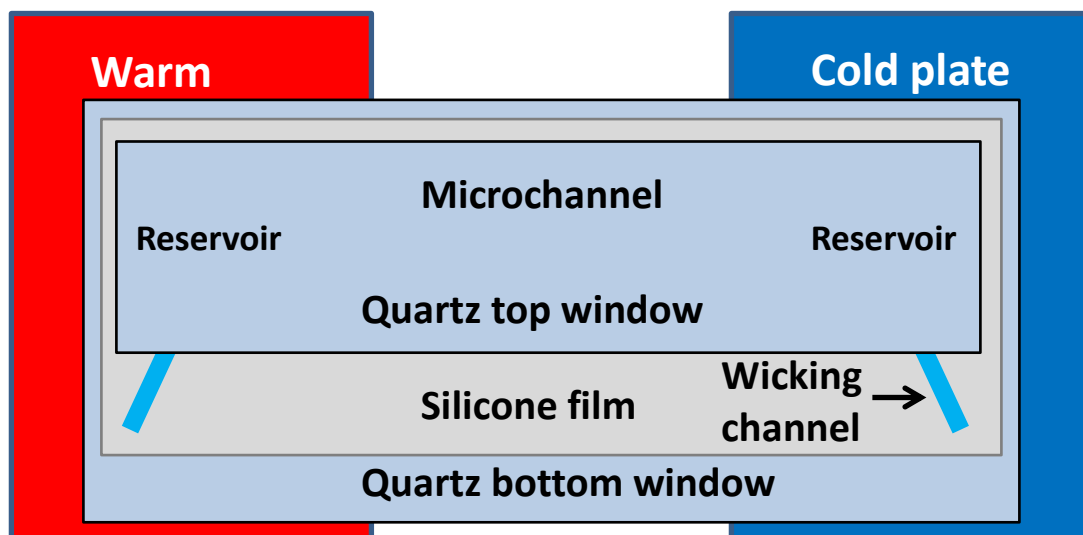
- (53) Santos, N. C.; Figueira-Coelho, J.; Martins-Silva, J.; Saldanha, C. **2003**, *65*, 1035.
- (54) Quatrano, R. S. *Plant Physiology* **1968**, *43*, 2057.
- (55) Weber, T. R.; Lindenauer, S. M.; Dent, T. L.; Allen, E.; Salles, C. A.; Weatherbee, L. *Annals of surgery* **1976**, *184*, 709.
- (56) Ashwood-Smith, M. J. **1975**, *243*, 246.
- (57) Stiff, P. J.; Koester, A. R.; Weidner, M. K.; Dvorak, K.; Fisher, R. I. *Blood* **1987**, *70*, 974.
- (58) Whittingham, D. G.; Leibo, S. P.; Mazur, P. *Selected Readings: Genetic Engineering and Bioethics* **1974**, *178*, 100.
- (59) He, S.; Woods Iii, L. C. **2004**, *48*, 254.
- (60) Rasmussen, D.; MacKenzie, A. **1968**.
- (61) Windrum, P.; Morris, T. C. M.; Drake, M. B.; Niederwieser, D.; Ruutu, T. *Bone marrow transplantation* **2005**, *36*, 601.
- (62) Syme, R.; Bewick, M.; Stewart, D.; Porter, K.; Chadderton, T.; Glück, S. **2004**, *10*, 135.
- (63) Arakawa, T.; Kita, Y.; Timasheff, S. N. **2007**, *131*, 62.
- (64) Kleinhans, F. W.; Mazur, P. **2007**, *54*, 212.
- (65) Grdadolnik, J.; Maréchal, Y. **2001**, *62*, 40.
- (66) Cotton, F. A.; Francis, R.; Horrocks, W. D. *The Journal of Physical Chemistry* **1960**, *64*, 1534.
- (67) Horrocks Jr, W. D.; Cotton, F. A. **1961**, *17*, 134.
- (68) Lin, V. J. C.; Koenig, J. L. **1976**, *15*, 203.
- (69) Scherer, J. R.; Go, M. K.; Kint, S. *The Journal of Physical Chemistry* **1974**, *78*, 1304.
- (70) Luzar, A.; Chandler, D. *The Journal of chemical physics* **1993**, *98*, 8160.
- (71) Vaisman, I. I.; Berkowitz, M. L. *Journal of the American Chemical Society* **1992**, *114*, 7889.
- (72) Sei, T.; Gonda, T.; Arima, Y. *Journal of crystal growth* **2002**, *240*, 218.
- (73) Zhang, H.; Hussain, I.; Brust, M.; Butler, M. F.; Rannard, S. P.; Cooper, A. I. *Nature materials* **2005**, *4*, 787.
- (74) Petzold, G.; Aguilera, J. M. *Food Biophysics* **2009**, *4*, 378.
- (75) Langham, E. J.; Mason, B. J. *Proceedings of the Royal Society of London. Series A. Mathematical and Physical Sciences* **1958**, *247*, 493.
- (76) Chen, C. F.; Chen, F. *Journal of Fluid Mechanics* **1991**, *227*, 567.
- (77) Breitenbach, J.; Schrof, W.; Neumann, J. *Pharmaceutical research* **1999**, *16*, 1109.
- (78) Kress, J.; Rose, A.; Frey, J. G.; Brocklesby, W. S.; Ladlow, M.; Mellor, G. W.; Bradley, M. *Chemistry-a European Journal* **2001**, *7*, 3880.
- (79) Pudney, P. D. A.; Hancewicz, T. M.; Cunningham, D. G.; Brown, M. C. *Vibrational spectroscopy* **2004**, *34*, 123.
- (80) Choi, J.; Choo, J.; Chung, H.; Gweon, D. G.; Park, J.; Kim, H. J.; Park, S.; Oh, C. H. *Biopolymers* **2005**, *77*, 264.
- (81) Terada, N.; Ohno, N.; Saitoh, S.; Ohno, S. *Journal of structural biology* **2008**, *163*, 147.

- (82) Dong, J.; Malsam, J.; Bischof, J. C.; Hubel, A.; Aksan, A. *Biophysical journal* **2010**, *99*, 2453.
- (83) Shen, Y.; Jacobs, J. M.; Camp, D. G.; Fang, R.; Moore, R. J.; Smith, R. D.; Xiao, W.; Davis, R. W.; Tompkins, R. G. *Analytical chemistry* **2004**, *76*, 1134.
- (84) Klajnert, B.; Bryszewska, M. *Bioelectrochemistry* **2002**, *55*, 33.
- (85) Leslie, S. B.; Israeli, E.; Lighthart, B.; Crowe, J. H.; Crowe, L. M. *Applied and Environmental Microbiology* **1995**, *61*, 3592.
- (86) Lins, R. D.; Pereira, C. S.; Hünenberger, P. H. *Proteins: Structure, Function, and Bioinformatics* **2004**, *55*, 177.
- (87) Wolkers, W. F.; Walker, N. J.; Tablin, F.; Crowe, J. H. *Cryobiology* **2001**, *42*, 79.
- (88) Lerbret, A.; Bordat, P.; Affouard, F.; Guinet, Y.; Hédoux, A.; Paccou, L.; Prévost, D.; Descamps, M. *Conformations of Oligo- and Poly-saccharides* **2005**, *340*, 881.
- (89) Caspers, P. J.; Lucassen, G. W.; Carter, E. A.; Bruining, H. A.; Puppels, G. J. *Journal of investigative dermatology* **2001**, *116*, 434.
- (90) Huizinga, A.; Bot, A. C. C.; de Mul, F. F. M.; Vrensen, G. F. J. M.; Greve, J. **1989**, *48*, 487.
- (91) Li-Chan, E. C. Y. *Le Lait* **2007**, *87*, 443.
- (92) Branca, C.; Magazù, S.; Maisano, G.; Migliardo, P. *The Journal of chemical physics* **1999**, *111*, 281.
- (93) Dàvila, E.; Parés, D.; Howell, N. K. *Journal of agricultural and food chemistry* **2006**, *54*, 7890.
- (94) Abbate, S.; Conti, G.; Naggi, A. **1991**, *210*, 1.
- (95) Miller, D. P.; de Pablo, J. J.; Corti, H. *Pharmaceutical research* **1997**, *14*, 578.

Appendix A: Directional Solidification Instructions

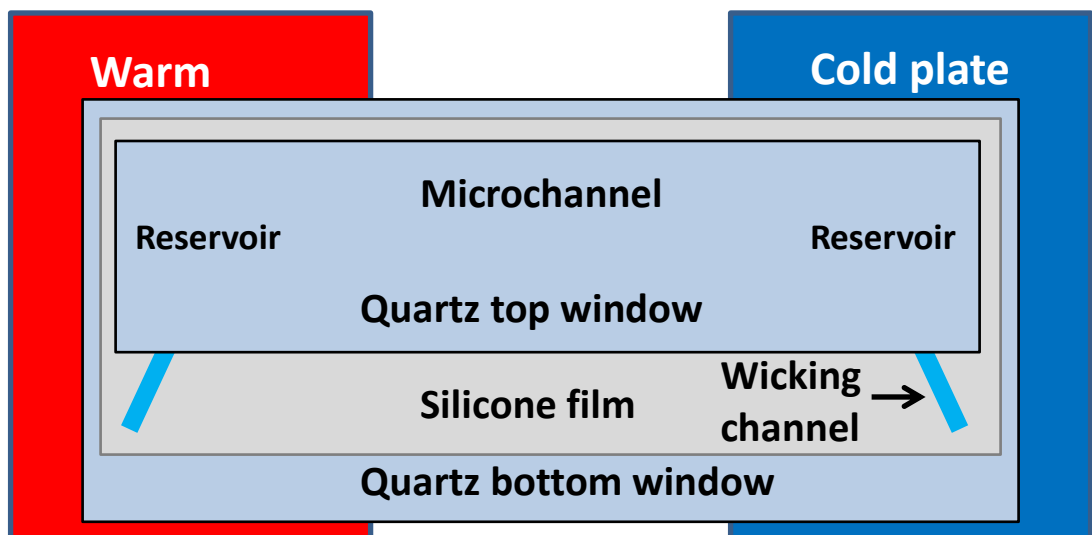
Set up experiment

1. Apply 50 μm thick silicone film to clean quartz window so that it adheres smoothly without bubbles
2. Create 10 mm microchannel with two parallel razor blades
3. Create two larger reservoirs (3-5mm in diameter) at each end of the microchannel
4. Create a thin channel toward the outside of the reservoirs to facilitate future wicking
5. Place top quartz window so that it covers the microchannel and reservoirs, but leaves part of the wicking channels uncovered
6. Wick experimental solution into the microchannel, from the end that will be placed on the cold plate
7. Place microchannel assembly on warm and cool plates already in position in the confocal Raman microscope so that the microchannel bridges the gap
8. Set temperature on the two plates and wait for them to stabilize



Perform experiment

1. Ensure that the microchannel is perpendicular to the plate edges and secure the microchannel assembly with adhesive tape as necessary
2. Determine a point of reference in the x-direction and zero the position
3. Adjust microscope objective and select parameters:
 1. Adjust size of scan area
 2. Select region of Raman spectrum desired (depending on area of spectra of interest).
Smaller regions improve spectral resolution, but may increase noise and exclude useful information in other areas of the spectrum.
 3. Power: as high as necessary to get good spectra without melting
 4. Exposure time: 0.05 seconds per pixel
4. Allow temperatures to stabilize
5. Nucleate ice by wicking small amount of silver iodide suspended in water into the wicking channel at the cold end
6. Once ice interface as reached an equilibrium position, begin scanning at cold end



Process data in RamanViewer and CytoSpec

1. Make sure to save all data (not automatic) and label per the position with respect to the reference point
2. Open data files using Nanophoton's RamanViewer software (Note: USB key may be necessary)
3. If individual spectra are too noisy too use, do spatial averaging
 1. If individual spectra are too noisy too use, do spatial averaging
 2. Edit > Binning > adjust the size of the area to be spatially averaged (2x2, 4x4, etc.)
4. To export data using plugin:
 1. Edit > Select > Select All Image
 2. Plugin > Export JCAMPs in Rect
 3. Create a new folder and save data here; plugin will generate a text file for every spectrum numbered sequentially
5. Process data with CytoSpec
 1. CytoSpec allows more quantitative processing of spectra
 2. 64-bit version is run through Matlab by typing "fir" in the command line
 3. File > Import ASCII > double column ASCII
 4. Deselect increment extension
 5. X-dim: height of the Raman scan (number of spectra)
 6. Y-dim: width of the Raman scan (number of spectra)
 7. Delimiter: space or tab
 8. Lines to skip: 15
 9. Load
 10. Preprocessing > smoothing > Savitsky Golay
 1. 15 smoothing points
 2. Original data
 11. To map things:
 1. Univariate Imaging > chemical maps (or colored symbol on taskbar)
 2. Choose preprocessed data block and then select ranges and type of map desired

12. Now fix the alignment of the pixels (only necessary once, but can only be done after the first value is calculated):

Tools > rotate > 90 ° clockwise

1. Tools > export maps > lower maps

(To facilitate processing, label maps with a letter followed by the number of the scan, e.g., a7)

Final Processing with Matlab

1. Import the maps of individual calculated values from CytoSpec into Matlab
2. Save these as a Workspace so avoid having to import them in the future
3. Use of modify existing Matlab as necessary
4. Things to consider in the code:
 1. Temperature
 2. Concentration variations
 3. Filtering noise or values far outside of expected values
 4. Accommodating different sizes of data
5. What the current code does:
 1. Identifies each experiment upon loading the Workspace and automatically sets the temperature profile, and nominal trehalose and albumin concentrations
 2. Flips all data vertically so the Matlab maps match the light microscopic image from the experiments
 3. Calculates the organic content, albumin/trehalose ratio, and trehalose content using a combination of calibration curves at 0, -5, -10, -15, and -20 °C
 4. Qualitatively determines the ice content
 5. Filters out low trehalose concentration values and extreme values for the albumin/trehalose ratio
 6. Determines the average temperature of each scan
 7. Sorts the albumin/trehalose ratio by trehalose concentration ranges and determines the mean value at each temperature normalized by:
 1. Nominal values
 2. Average value at the temperature in all concentration ranges
 8. Maps of each variable are generated automatically and are images automatically saved to the Matlab folder

Appendix B: Matlab Code

```

% This code was developed to process confocal Raman microspectroscopy
data.
% It uses a polynomial curve for temperature calculations, and a series
of
% linear calibration curves at 0, -5, -10, -15, and -20 deg C to
quantify
% and map trehalose concentration, the albumin/trehalose mass ratio,
and
% qualitatively the presence of ice.

% data was imported into CytoSpec and then rotated clockwise. It now
must be
% vertically flipped to match the original images, with the cold side
being
% on the right (a1 corresponds to -3mm from the edge of the right cold
% temperature plate)

% temperature values shifted so that the ice interface position
corresponds
% to the binary phase diagram temperature, due to the variability in
the
% temperature control

% automatically shifts the temperature profile from the thermocouple
values
% so that the edge of the interface is located at the melt temperature
per
% the binary trehalose/water diagram developed by Miller (1997)
% the albumin is excluded from the calculation, so the concentration
used
% to determine the melt temp is (trehalose)/(trehalose+water)

% all data were spatially averaged 2x2 ("binned"), and then 15 point
% Savitsky Golay smoothed

% each successive file is placed at 0.5mm beyond the previous one
unless
% otherwise noted (the last file was shifted to the ice interface in
some
% cases, which is accounted for in the code)

% the variables a, b, e, and f were used as follows:
% a = (2820-3030)/[3390 with (2600-3800) baseline]
% b = (3100-3200)/[3390 with (2600-3800) baseline]
% e = 2935/2915 with (2880-3010) baseline (for lower concentration)
% f = 2935/2915 with (2890-2990) baseline (for higher concentration)

format compact

% trecon and albcon saved in workspaces
% enter nominal trehalose concentration (wt%)

```

```

% trecon=10;
% enter albumin concentration (wt%)
% albcon=4;
% minimum frequency (%) for alb/tre ratio to be included for a
trehalose
% concentration range:
threshold=2;
% nominal albumin/trehalose ratio
rationominal=albcon/trecon;
% limits of trehalose wt% and albumin/trehalose ratio for filtering:
lowtrehalose=5;
hightrehalose=100;
filterfactor=3;
lowratio=rationominal/filterfactor;
highratio=rationominal*filterfactor;
% plus and minus trehalose concentration limits for nominal
concentration:
treconplus=trecon+5;
treconminus=trecon-5;
% high frequency % for plot:
trehi=100;
% high value for alb/tre plot
plotRatioHi=0.1+1.5*rationominal;
% threshold for organic content, c, to use higher concentration
% calibration:
organic10=22;
organic20=30;

% figure size
fsize=[100, 100, 750, 550];
fsize2=[100, 100, 750,300];
fposition=[0.22 0.14 0.3 0.28];
tsize=16;
xsize=14;
ysize=14;
% map title sizes
msize=14;
mTsize=['FontWeight','bold',...
        'FontSize',msize,...
        'FontName','Arial'];
% Titles
tAlbTre1='Albumin/Trehalose Ratio vs. Temperature';
tAlbTre2=[num2str(trecon), ' wt% Trehalose, ',num2str(albcon), ' wt%
Albumin' ];
tTreDist1='Trehalose Distribution vs. Temperature';
tTreDist2=[num2str(trecon), ' wt% Trehalose, ',num2str(albcon), ' wt%
Albumin'];

% determines the number of files to accommodate and the shift in the
% temperature profile:
% the last file position is also shifted automatically
lastshift=zeros(1,14);
if trecon==10
    if albcon==2
        shift=1.25;

```

```

        files=14;
        lastshift(files)=-3.5+files*0.5-3.12;
    end
    if albcon==3
        shift=1.25;
        files=14;
        lastshift(files)=-3.5+files*0.5-3.08;
    end
    if albcon==4
        shift=0.8;
        files=12;
    %   files=13;
    %   lastshift(files)=-3.5+files*0.5-2.67;
    end
end
if trecon==20
    if albcon==2
        shift=1.05;
        files=13;
        lastshift(files)=-3.5+files*0.5-2.73;
    end
    if albcon==3
        shift=-1.05;
        files=9;
        lastshift(files)=-3.5+files*0.5-0.65;
    end
    if albcon==4
        shift=0.8;
        files=12;
        lastshift(files)=-3.5+files*0.5-2.45;
    end
end
if trecon==30
    if albcon==3
        shift=-1.05;
        files=8;
        lastshift(files)=-3.5+files*0.5-0.4;
    end
    if albcon==4
        shift=-0.6;
        files=9;
        lastshift(files)=-3.5+files*0.5-0.84;
    end
end
% thickness of pixels due to binning:
th=10;
% width of pixels per file
width=200;
% pixels per file:
pixels=th*width;
%number of columns of pixels
z=files*width;
% Plot temperature ranges:
Tlow=-18;
Thigh=1;
% Plot percentage ranges:
PctLow=0;

```

```

PctHigh=160;
% create nominal 100% line for plotting:
Nominal=100*ones(1,3);
NominalTemp=[-20 0 10];
% accommodating input sizes of
if files<9
    a9=NaN(th,width);
    b9=NaN(th,width);
    e9=NaN(th,width);
    f9=NaN(th,width);
end
if files<10
    a10=NaN(th,width);
    b10=NaN(th,width);
    e10=NaN(th,width);
    f10=NaN(th,width);
end
if files<11
    a11=NaN(th,width);
    b11=NaN(th,width);
    e11=NaN(th,width);
    f11=NaN(th,width);
end
if files<12
    a12=NaN(th,width);
    b12=NaN(th,width);
    e12=NaN(th,width);
    f12=NaN(th,width);
end
if files<13
    a13=NaN(th,width);
    b13=NaN(th,width);
    e13=NaN(th,width);
    f13=NaN(th,width);
end
if files<14
    a14=NaN(th,width);
    b14=NaN(th,width);
    e14=NaN(th,width);
    f14=NaN(th,width);
end
a=NaN(th,width,files);
a(:, :, 1)=a1;
a(:, :, 2)=a2;
a(:, :, 3)=a3;
a(:, :, 4)=a4;
a(:, :, 5)=a5;
a(:, :, 6)=a6;
a(:, :, 7)=a7;
a(:, :, 8)=a8;
a(:, :, 9)=a9;
a(:, :, 10)=a10;
a(:, :, 11)=a11;
a(:, :, 12)=a12;
a(:, :, 13)=a13;
% if trecon==10
%     if albcon==4

```

```

%      a(:, :, 13)=[a13;nan(th,width)];
%      end
% end
a(:, :, 14)=a14;
b=NaN(th,width,files);
b(:, :, 1)=b1;
b(:, :, 2)=b2;
b(:, :, 3)=b3;
b(:, :, 4)=b4;
b(:, :, 5)=b5;
b(:, :, 6)=b6;
b(:, :, 7)=b7;
b(:, :, 8)=b8;
b(:, :, 9)=b9;
b(:, :, 10)=b10;
b(:, :, 11)=b11;
b(:, :, 12)=b12;
b(:, :, 13)=b13;
b(:, :, 14)=b14;
e=NaN(th,width,files);
e(:, :, 1)=e1;
e(:, :, 2)=e2;
e(:, :, 3)=e3;
e(:, :, 4)=e4;
e(:, :, 5)=e5;
e(:, :, 6)=e6;
e(:, :, 7)=e7;
e(:, :, 8)=e8;
e(:, :, 9)=e9;
e(:, :, 10)=e10;
e(:, :, 11)=e11;
e(:, :, 12)=e12;
e(:, :, 13)=e13;
e(:, :, 14)=e14;
f=NaN(th,width,files);
f(:, :, 1)=f1;
f(:, :, 2)=f2;
f(:, :, 3)=f3;
f(:, :, 4)=f4;
f(:, :, 5)=f5;
f(:, :, 6)=f6;
f(:, :, 7)=f7;
f(:, :, 8)=f8;
f(:, :, 9)=f9;
f(:, :, 10)=f10;
f(:, :, 11)=f11;
f(:, :, 12)=f12;
f(:, :, 13)=f13;
f(:, :, 14)=f14;
p=[0.00117 -0.01538 -0.03885 0.69762 3.53503 -12.94982];
temp=[-17.5;-15;-12.5;-10;-7.5;-5;-2.5;0];
pos=zeros(8,1);
%pixel position
pixellength=[0.083182 0.082764 0.082346 0.081928 0.08151 0.081092
0.080674...
0.080256 0.079838 0.07942 0.079002 0.078584 0.078166 0.077748
0.07733...

```

```

    0.076912 0.076494 0.076076 0.075658 0.07524 0.074822 0.074404
0.073986...
    0.073568 0.07315 0.072732 0.072314 0.071896 0.071478 0.07106
0.070642...
    0.070224 0.069806 0.069388 0.06897 0.068552 0.068134 0.067716
0.067298...
    0.06688 0.066462 0.066044 0.065626 0.065208 0.06479 0.064372
0.063954...
    0.063536 0.063118 0.0627 0.062282 0.061864 0.061446 0.061028
0.06061...
    0.060192 0.059774 0.059356 0.058938 0.05852 0.058102 0.057684
0.057266...
    0.056848 0.05643 0.056012 0.055594 0.055176 0.054758 0.05434
0.053922...
    0.053504 0.053086 0.052668 0.05225 0.051832 0.051414 0.050996
0.050578...
    0.05016 0.049742 0.049324 0.048906 0.048488 0.04807 0.047652
0.047234...
    0.046816 0.046398 0.04598 0.045562 0.045144 0.044726 0.044308
0.04389...
    0.043472 0.043054 0.042636 0.042218 0.0418 0.041382 0.040964
0.040546...
    0.040128 0.03971 0.039292 0.038874 0.038456 0.038038 0.03762
0.037202...
    0.036784 0.036366 0.035948 0.03553 0.035112 0.034694 0.034276
0.033858...
    0.03344 0.033022 0.032604 0.032186 0.031768 0.03135 0.030932
0.030514...
    0.030096 0.029678 0.02926 0.028842 0.028424 0.028006 0.027588
0.02717...
    0.026752 0.026334 0.025916 0.025498 0.02508 0.024662 0.024244
0.023826...
    0.023408 0.02299 0.022572 0.022154 0.021736 0.021318 0.0209
0.020482...
    0.020064 0.019646 0.019228 0.01881 0.018392 0.017974 0.017556
0.017138...
    0.01672 0.016302 0.015884 0.015466 0.015048 0.01463 0.014212
0.013794...
    0.013376 0.012958 0.01254 0.012122 0.011704 0.011286 0.010868
0.01045...
    0.010032 0.009614 0.009196 0.008778 0.00836 0.007942 0.007524
0.007106...
    0.006688 0.00627 0.005852 0.005434 0.005016 0.004598 0.00418
0.003762...
    0.003344 0.002926 0.002508 0.00209 0.001672 0.001254 0.000836
0.000418 0];
for L=1:8
    Roots=roots(p-[0,0,0,0,0,temp(L)]);
    pos(L)=Roots(5);
end
% Determine position of pixels:
pos1=pixellength-3;
pos2=pixellength-2.5;
pos3=pixellength-2;
pos4=pixellength-1.5;
pos5=pixellength-1;
pos6=pixellength-.5;

```

```

pos7=pixellength-0;
pos8=pixellength+.5;
pos9=pixellength+1;
pos10=pixellength+1.5;
pos11=pixellength+2;
pos12=pixellength+2.5;
pos13=pixellength+3;
pos14=pixellength+3.5;
Pos=NaN(width,files);
Pos(:,1)=pos1-shift-lastshift(1);
Pos(:,2)=pos2-shift-lastshift(2);
Pos(:,3)=pos3-shift-lastshift(3);
Pos(:,4)=pos4-shift-lastshift(4);
Pos(:,5)=pos5-shift-lastshift(5);
Pos(:,6)=pos6-shift-lastshift(6);
Pos(:,7)=pos7-shift-lastshift(7);
Pos(:,8)=pos8-shift-lastshift(8);
Pos(:,9)=pos9-shift-lastshift(9);
Pos(:,10)=pos10-shift-lastshift(10);
Pos(:,11)=pos11-shift-lastshift(11);
Pos(:,12)=pos12-shift-lastshift(12);
Pos(:,13)=pos13-shift-lastshift(13);
Pos(:,14)=pos14-shift-lastshift(14);
% Determine positions of temperatures using polynomial fit of
thermocouple
% data: = 0.00117x5 - 0.01128x4 - 0.07617x3 + 0.57483x2 + 4.43490x -
10.15028
Temp=NaN(width,files);
for h=1:files
    for tz=1:width
        Temp(tz,h)=(0.00117*Pos(tz,h)^5 -0.0112*Pos(tz,h)^4-
0.07617*Pos(tz,h)^3+0.57483*Pos(tz,h)^2+4.43490*Pos(tz,h)-10.15028);
    end
end
%Determine mean temperature of each file:
MeanTemp=NaN(1,files);
for h=1:files
    MeanTemp(h)=mean(Temp(:,h));
end
MeanTempRounded=round(MeanTemp);
% % Force temperatures to 0C for file 13: and 2C for file 14:
% if files>12
%     MeanTemp(13)=0;
% end
% if files>13
%     MeanTemp(14)=2;
% end
A=NaN(th,width,files);
B=NaN(th,width,files);
E=NaN(th,width,files);
F=NaN(th,width,files);

% intervals over which to calculate
for h=1:files
    A(:, :, h)=flipud(a(:, :, h));
    B(:, :, h)=flipud(b(:, :, h));
    E(:, :, h)=flipud(e(:, :, h));

```

```

    F(:,:,h)=flipud(f(:,:,h));
end
C=NaN(th,width,files);
Ratio=NaN(th,width,files);
%Calculating organic and a given ratio at each temperature:
for j=1:th
    for k=1:width
        for h=1:files
            % -20C
            if Temp(k,h)<-17.5
                C(j,k,h)=(A(j,k,h)+16.346)./2.2459;
                if C(j,k,h)>organic20
                    Ratio(j,k,h)=(F(j,k,h)-0.6711)/1.359;
                else
                    if C(j,k,h)>organic10
                        Ratio(j,k,h)=(F(j,k,h)-.6547)/1.3732;
                    else
                        Ratio(j,k,h)=(E(j,k,h)-.7287)/.9144;
                    end
                end
            end
        end
        % -15C
        if Temp(k,h)<-12.5
            if Temp(k,h)>=-17.5
                C(j,k,h)=(A(j,k,h)+16.019)./2.2495;
                if C(j,k,h)>organic20
                    Ratio(j,k,h)=(F(j,k,h)-.6968)/1.289;
                else
                    if C(j,k,h)>organic10
                        Ratio(j,k,h)=(F(j,k,h)-0.6742)/1.3462;
                    else
                        Ratio(j,k,h)=(E(j,k,h)-.7529)/.8683;
                    end
                end
            end
        end
    end
    % -10C
    if Temp(k,h)<-7.5
        if Temp(k,h)>=-12.5
            C(j,k,h)=(A(j,k,h)+15.663)./2.2298;
            if C(j,k,h)>organic20
                Ratio(j,k,h)=(F(j,k,h)-0.7075)/1.28;
            else
                if C(j,k,h)>organic10
                    Ratio(j,k,h)=(F(j,k,h)-0.6934)/1.2944;
                else
                    Ratio(j,k,h)=(E(j,k,h)-.7693)/.8499;
                end
            end
        end
    end
    % -5C
    if Temp(k,h)<-2.5
        if Temp(k,h)>=-7.5
            C(j,k,h)=(A(j,k,h)+15.412)./2.2226;
            if C(j,k,h)>organic20

```



```

end
% Calculate absolute albumin concentration (wt%) after filtering as a %
of
% nominal starting concentration
AlbuminConFiltered=(RatioFiltered.*TrehaloseFiltered);
% TrehalosePercentage=TrehaloseFiltered./(trecon/100);
% Sort Ratio by trehalose concentration:
RatioFiltered_8_10=NaN(th,width,files);
RatioFiltered_10_15=NaN(th,width,files);
RatioFiltered_15_20=NaN(th,width,files);
RatioFiltered_20_25=NaN(th,width,files);
RatioFiltered_25_30=NaN(th,width,files);
RatioFiltered_30_35=NaN(th,width,files);
RatioFiltered_30_100=NaN(th,width,files);
% +/- 5 wt% of nominal concentration
RatioFiltered_nominal=NaN(th,width,files);
for j=1:th
    for k=1:width
        for h=1:files
            % Update to include 30+
            if TrehaloseFiltered(j,k,h)>=30
                if TrehaloseFiltered(j,k,h)<100
                    if RatioFiltered(j,k,h)>0
                        if RatioFiltered(j,k,h)<1
RatioFiltered_30_100(j,k,h)=RatioFiltered(j,k,h);
                        end
                    end
                end
            end
            % 8-10 trehalose
            if TrehaloseFiltered(j,k,h)>=8
                if TrehaloseFiltered(j,k,h)<10
                    if RatioFiltered(j,k,h)>0
                        if RatioFiltered(j,k,h)<1
RatioFiltered_8_10(j,k,h)=RatioFiltered(j,k,h);
                        end
                    end
                end
            end
            % 10-15 trehalose
            if TrehaloseFiltered(j,k,h)>=10
                if TrehaloseFiltered(j,k,h)<15
                    if RatioFiltered(j,k,h)>0
                        if RatioFiltered(j,k,h)<1
RatioFiltered_10_15(j,k,h)=RatioFiltered(j,k,h);
                        end
                    end
                end
            end
            % 15-20 trehalose
            if TrehaloseFiltered(j,k,h)>=15
                if TrehaloseFiltered(j,k,h)<20
                    if RatioFiltered(j,k,h)>0
                        if RatioFiltered(j,k,h)<1
RatioFiltered_15_20(j,k,h)=RatioFiltered(j,k,h);
                        end
                    end
                end
            end
        end
    end
end

```

```

        end
    end
end
% 20-25 trehalose
if TrehaloseFiltered(j,k,h)>=20
    if TrehaloseFiltered(j,k,h)<25
        if RatioFiltered(j,k,h)>0
            if RatioFiltered(j,k,h)<1
                RatioFiltered_20_25(j,k,h)=RatioFiltered(j,k,h);
            end
        end
    end
end
% 25-30 trehalose
if TrehaloseFiltered(j,k,h)>=25
    if TrehaloseFiltered(j,k,h)<30
        if RatioFiltered(j,k,h)>0
            if RatioFiltered(j,k,h)<1
                RatioFiltered_25_30(j,k,h)=RatioFiltered(j,k,h);
            end
        end
    end
end
% 30-35 trehalose
if TrehaloseFiltered(j,k,h)>=30
    if TrehaloseFiltered(j,k,h)<=35
        if RatioFiltered(j,k,h)>0
            if RatioFiltered(j,k,h)<1
                RatioFiltered_30_35(j,k,h)=RatioFiltered(j,k,h);
            end
        end
    end
end
% +/- 5wt% of nominal trehalose concentration
if TrehaloseFiltered(j,k,h)>=treconminus
    if TrehaloseFiltered(j,k,h)<=treconplus
        if RatioFiltered(j,k,h)>0
            if RatioFiltered(j,k,h)<1
                RatioFiltered_nominal(j,k,h)=RatioFiltered(j,k,h);
            end
        end
    end
end
end
end
end
end
% calculate the mean ratio in each trehalose concentration range for
each
% %file
% calculate the mean alb/trehalose
Rm_8_10=NaN(1,files);
Rm_10_15=NaN(1,files);
Rm_15_20=NaN(1,files);
Rm_20_25=NaN(1,files);
Rm_25_30=NaN(1,files);
Rm_30_35=NaN(1,files);

```

```

Rm_30_100=NaN(1,files);
Rm_nominal=NaN(1,files);

Rm2_8_10=NaN(1,files);
Rm2_10_15=NaN(1,files);
Rm2_15_20=NaN(1,files);
Rm2_20_25=NaN(1,files);
Rm2_25_30=NaN(1,files);
Rm2_30_35=NaN(1,files);
Rm2_30_100=NaN(1,files);
Rm2_nominal=NaN(1,files);
% Filter out the ratio by excluding concentration with less than 2%
% frequency:
Rm_8_10filtered=NaN(1,files);
Rm_10_15filtered=NaN(1,files);
Rm_15_20filtered=NaN(1,files);
Rm_20_25filtered=NaN(1,files);
Rm_25_30filtered=NaN(1,files);
Rm_30_35filtered=NaN(1,files);
Rm_30_100filtered=NaN(1,files);
Rm_nominalfiltered=NaN(1,files);

Rm2_8_10filtered=NaN(1,files);
Rm2_10_15filtered=NaN(1,files);
Rm2_15_20filtered=NaN(1,files);
Rm2_20_25filtered=NaN(1,files);
Rm2_25_30filtered=NaN(1,files);
Rm2_30_35filtered=NaN(1,files);
Rm2_30_100filtered=NaN(1,files);
Rm2_nominalfiltered=NaN(1,files);
% standard deviation
R_std_8_10=NaN(1,files);
% count values to determine frequency of each concentration range:
Count_FilteredRatio=NaN(1,files);
Count_8_10=NaN(1,files);
Count_10_15=NaN(1,files);
Count_15_20=NaN(1,files);
Count_20_25=NaN(1,files);
Count_25_30=NaN(1,files);
Count_30_35=NaN(1,files);
Count_30_100=NaN(1,files);
Count_nominal=NaN(1,files);
% absolute albumin concentration/trehalose in each file as % of
nominal:
% determines absolute albumin and trehalose content and then calculates
% ratio, which is susceptible to error in high concentration trehalose
OverallAlbuminRatio=NaN(1,files);
MeanRatio=NaN(1,files);
MeanRatioPercentage=NaN(1,files);
TrehalosePercentage=NaN(1,files);
for h=1:files
    % Calculate the overall albumin/trehalose ratio using absolute
    % concentrations... prone to error at high trehalose
    concentration

```

```

%
OverallAlbuminRatio(1,h)=(nansum(AlbuminConFiltered(:, :, h))/nansum(TrehaloseFiltered(:, :, h)));...

MeanRatio(1,h)=nansum(nansum(RatioFiltered(:, :, h)))/nnz(RatioFiltered(:, :, h)>0);

TrehalosePercentage(1,h)=nansum(nansum(TrehaloseFiltered(:, :, h)))/...
    (nnz(TrehaloseFiltered(:, :, h)>0)*trecon/100);

MeanRatioPercentage(1,h)=nanmean(nanmean(RatioFiltered(:, :, h)))/(ratio
    nominal/100);
    % Averages the average of each column in a file, which doesn't
    % account for the different weight of each column due to NaN
%
    Rm_8_10(1,h)=nanmean(nanmean(RatioFiltered_8_10(:, :, h)));
%
    Rm_10_15(1,h)=nanmean(nanmean(RatioFiltered_10_15(:, :, h)));
%
    Rm_15_20(1,h)=nanmean(nanmean(RatioFiltered_15_20(:, :, h)));
%
    Rm_20_25(1,h)=nanmean(nanmean(RatioFiltered_20_25(:, :, h)));
%
    Rm_25_30(1,h)=nanmean(nanmean(RatioFiltered_25_30(:, :, h)));
%
    Rm_30_35(1,h)=nanmean(nanmean(RatioFiltered_30_35(:, :, h)));
%
    Rm_30_100(1,h)=nanmean(nanmean(RatioFiltered_30_100(:, :, h)));
%
Rm_nominal(1,h)=nanmean(nanmean(RatioFiltered_nominal(:, :, h)));
    % Directly averages the ratio values of all pixels in a given
    % concentration, without weighting due to absolute content
    % result slightly overrepresents low concentration regions

Rm2_8_10(1,h)=nansum(nansum(RatioFiltered_8_10(:, :, h)))/nnz(RatioFilter
    ed_8_10(:, :, h)>0);

Rm2_10_15(1,h)=nansum(nansum(RatioFiltered_10_15(:, :, h)))/nnz(RatioFilt
    ered_10_15(:, :, h)>0);

Rm2_15_20(1,h)=nansum(nansum(RatioFiltered_15_20(:, :, h)))/nnz(RatioFilt
    ered_15_20(:, :, h)>0);

Rm2_20_25(1,h)=nansum(nansum(RatioFiltered_20_25(:, :, h)))/nnz(RatioFilt
    ered_20_25(:, :, h)>0);

Rm2_25_30(1,h)=nansum(nansum(RatioFiltered_25_30(:, :, h)))/nnz(RatioFilt
    ered_25_30(:, :, h)>0);

Rm2_30_35(1,h)=nansum(nansum(RatioFiltered_30_35(:, :, h)))/nnz(RatioFilt
    ered_30_35(:, :, h)>0);

Rm2_30_100(1,h)=nansum(nansum(RatioFiltered_30_100(:, :, h)))/nnz(RatioFi
    ltered_30_100(:, :, h)>0);

Rm2_nominal(1,h)=nansum(nansum(RatioFiltered_nominal(:, :, h)))/nnz(Ratio
    Filtered_nominal(:, :, h)>0);
    % R_std_8_10(1,h)=nanmean(nanmean(RatioFiltered_8_10(:, :, h)));
    % Count the number of pixels with values within a concentration
    for each file

Count_FilteredRatio(1,h)=nnz(RatioFiltered(:, :, h)>0)/pixels*100;
    Count_8_10(1,h)=nnz(RatioFiltered_8_10(:, :, h)>0)/pixels*100;
    Count_10_15(1,h)=nnz(RatioFiltered_10_15(:, :, h)>0)/pixels*100;

```

```

Count_15_20(1,h)=nnz(RatioFiltered_15_20(:, :,h)>0)/pixels*100;
Count_20_25(1,h)=nnz(RatioFiltered_20_25(:, :,h)>0)/pixels*100;
Count_25_30(1,h)=nnz(RatioFiltered_25_30(:, :,h)>0)/pixels*100;
Count_30_35(1,h)=nnz(RatioFiltered_30_35(:, :,h)>0)/pixels*100;

Count_30_100(1,h)=nnz(RatioFiltered_30_100(:, :,h)>0)/pixels*100;

Count_nominal(1,h)=nnz(RatioFiltered_nominal(:, :,h)>0)/pixels*100;

Count=[Count_10_15;Count_15_20;Count_20_25;Count_25_30;Count_30_100];

    if Count_8_10(1,h)>=threshold
%       Rm_8_10filtered(1,h)=Rm_8_10(1,h);
        Rm2_8_10filtered(1,h)=Rm2_8_10(1,h);
    end
    if Count_10_15(1,h)>=threshold
%       Rm_10_15filtered(1,h)=Rm_10_15(1,h);
        Rm2_10_15filtered(1,h)=Rm2_10_15(1,h);
    end
    if Count_15_20(1,h)>=threshold
%       Rm_15_20filtered(1,h)=Rm_15_20(1,h);
        Rm2_15_20filtered(1,h)=Rm2_15_20(1,h);
    end
    if Count_20_25(1,h)>=threshold
%       Rm_20_25filtered(1,h)=Rm_20_25(1,h);
        Rm2_20_25filtered(1,h)=Rm2_20_25(1,h);
    end
    if Count_25_30(1,h)>=threshold
%       Rm_25_30filtered(1,h)=Rm_25_30(1,h);
        Rm2_25_30filtered(1,h)=Rm2_25_30(1,h);
    end
    if Count_30_35(1,h)>=threshold
%       Rm_30_35filtered(1,h)=Rm_30_35(1,h);
        Rm2_30_35filtered(1,h)=Rm2_30_35(1,h);
    end
    if Count_30_100(1,h)>=threshold
%       Rm_30_100filtered(1,h)=Rm_30_100(1,h);
        Rm2_30_100filtered(1,h)=Rm2_30_100(1,h);
    end
    if Count_nominal(1,h)>=threshold
%       Rm_nominalfiltered(1,h)=Rm_nominal(1,h);
        Rm2_nominalfiltered(1,h)=Rm2_nominal(1,h);
    end
end
% OverallAlbuminRatioPCT=OverallAlbuminRatio./(rationominal/100);
% calculate the mean alb/trehalose ratio as percentage of the nominal
value
% RmPCT_30_100=Rm_30_100*(100/rationominal);
% RmPCT_8_10=Rm_8_10*(100/rationominal);
% RmPCT_10_15=Rm_10_15*(100/rationominal);
% RmPCT_15_20=Rm_15_20*(100/rationominal);
% RmPCT_20_25=Rm_20_25*(100/rationominal);
% RmPCT_25_30=Rm_25_30*(100/rationominal);
% RmPCT_30_35=Rm_30_35*(100/rationominal);

% filtered out small ranges

```

```

% RmPCT_30_100filtered=Rm_30_100filtered*(100/rationominal);
% RmPCT_8_10filtered=Rm_8_10filtered*(100/rationominal);
% RmPCT_10_15filtered=Rm_10_15filtered*(100/rationominal);
% RmPCT_15_20filtered=Rm_15_20filtered*(100/rationominal);
% RmPCT_20_25filtered=Rm_20_25filtered*(100/rationominal);
% RmPCT_25_30filtered=Rm_25_30filtered*(100/rationominal);
% RmPCT_30_35filtered=Rm_30_35filtered*(100/rationominal);
% RmPCT_nominalfiltered=Rm_nominalfiltered*(100/rationominal);

RmPCT2_30_100filtered=Rm2_30_100filtered*(100/rationominal);
RmPCT2_8_10filtered=Rm2_8_10filtered*(100/rationominal);
RmPCT2_10_15filtered=Rm2_10_15filtered*(100/rationominal);
RmPCT2_15_20filtered=Rm2_15_20filtered*(100/rationominal);
RmPCT2_20_25filtered=Rm2_20_25filtered*(100/rationominal);
RmPCT2_25_30filtered=Rm2_25_30filtered*(100/rationominal);
RmPCT2_nominalfiltered=Rm2_nominalfiltered*(100/rationominal);

% Normalize the albumin/trehalose ratio with respect to the:
% mean value in each region
RmNorm_8_10=RmPCT2_8_10filtered./(MeanRatioPercentage/100);
RmNorm_10_15=RmPCT2_10_15filtered./(MeanRatioPercentage/100);
RmNorm_15_20=RmPCT2_15_20filtered./(MeanRatioPercentage/100);
RmNorm_20_25=RmPCT2_20_25filtered./(MeanRatioPercentage/100);
RmNorm_25_30=RmPCT2_25_30filtered./(MeanRatioPercentage/100);
RmNorm_30_100=RmPCT2_30_100filtered./(MeanRatioPercentage/100);
RmNorm_nominal=RmPCT2_nominalfiltered./(MeanRatioPercentage/100);
% Combine into matrix, excluding 8-10:
RmPCT=[RmPCT2_10_15filtered;RmPCT2_15_20filtered;RmPCT2_20_25filtered;.
...
RmPCT2_25_30filtered;RmPCT2_30_100filtered];
RmNorm=[RmNorm_10_15;RmNorm_15_20;RmNorm_20_25;RmNorm_25_30;RmNorm_30_1
00];

%number of files for iteration
n=files;
k=width;
% z=k*13+(n-1)*fc;
zz=0.65;
yy=0.1;
xx=zz+yy*6;

% Create titles for plots:
tRatio1=['Albumin/Trehalose Ratio at
',num2str(MeanTempRounded(1)), '°C'];
tRatio2=['Albumin/Trehalose Ratio at
',num2str(MeanTempRounded(2)), '°C'];
tRatio3=['Albumin/Trehalose Ratio at
',num2str(MeanTempRounded(3)), '°C'];
tRatio4=['Albumin/Trehalose Ratio at
',num2str(MeanTempRounded(4)), '°C'];
tRatio5=['Albumin/Trehalose Ratio at
',num2str(MeanTempRounded(5)), '°C'];
tRatio6=['Albumin/Trehalose Ratio at
',num2str(MeanTempRounded(6)), '°C'];
tRatio7=['Albumin/Trehalose Ratio at
',num2str(MeanTempRounded(7)), '°C'];

```

```

tRatio8=['Albumin/Trehalose Ratio at
',num2str(MeanTempRounded(8)), '°C'];
if files>8
    tRatio9=['Albumin/Trehalose Ratio at
',num2str(MeanTempRounded(9)), '°C'];
end
if files>9
    tRatio10=['Albumin/Trehalose Ratio at
',num2str(MeanTempRounded(10)), '°C'];
end
if files>10
    tRatio11=['Albumin/Trehalose Ratio at
',num2str(MeanTempRounded(11)), '°C'];
end
if files>11
    tRatio12=['Albumin/Trehalose Ratio at
',num2str(MeanTempRounded(12)), '°C'];
end
if files>12
    tRatio13=['Albumin/Trehalose Ratio at
',num2str(MeanTempRounded(13)), '°C'];
end
if files>13
    tRatio14=['Albumin/Trehalose Ratio at
',num2str(MeanTempRounded(14)), '°C'];
end

tTre1=['Trehalose at ', num2str(MeanTempRounded(1)), '°C'];
tTre2=['Trehalose at ', num2str(MeanTempRounded(2)), '°C'];
tTre3=['Trehalose at ', num2str(MeanTempRounded(3)), '°C'];
tTre4=['Trehalose at ', num2str(MeanTempRounded(4)), '°C'];
tTre5=['Trehalose at ', num2str(MeanTempRounded(5)), '°C'];
tTre6=['Trehalose at ', num2str(MeanTempRounded(6)), '°C'];
tTre7=['Trehalose at ', num2str(MeanTempRounded(7)), '°C'];
tTre8=['Trehalose at ', num2str(MeanTempRounded(8)), '°C'];
if files>8
    tTre9=['Trehalose at ', num2str(MeanTempRounded(9)), '°C'];
end
if files>9
    tTre10=['Trehalose at ', num2str(MeanTempRounded(10)), '°C'];
end
if files>10
    tTre11=['Trehalose at ', num2str(MeanTempRounded(11)), '°C'];
end
if files>11
    tTre12=['Trehalose at ', num2str(MeanTempRounded(12)), '°C'];
end
if files>12
    tTre13=['Trehalose at ', num2str(MeanTempRounded(13)), '°C'];
end
if files>13
    tTre14=['Trehalose at ', num2str(MeanTempRounded(14)), '°C'];
end

tIce1=['Ice at ', num2str(MeanTempRounded(1)), '°C'];
tIce2=['Ice at ', num2str(MeanTempRounded(2)), '°C'];

```

```

tIce3=['Ice at ',num2str(MeanTempRounded(3)), '°C'];
tIce4=['Ice at ',num2str(MeanTempRounded(4)), '°C'];
tIce5=['Ice at ',num2str(MeanTempRounded(5)), '°C'];
tIce6=['Ice at ',num2str(MeanTempRounded(6)), '°C'];
tIce7=['Ice at ',num2str(MeanTempRounded(7)), '°C'];
tIce8=['Ice at ',num2str(MeanTempRounded(8)), '°C'];
if files>8
    tIce9=['Ice at ',num2str(MeanTempRounded(9)), '°C'];
end
if files>9
    tIce10=['Ice at ',num2str(MeanTempRounded(10)), '°C'];
end
if files>10
    tIce11=['Ice at ',num2str(MeanTempRounded(11)), '°C'];
end
if files>11
    tIce12=['Ice at ',num2str(MeanTempRounded(12)), '°C'];
end
if files>12
    tIce13=['Ice at ',num2str(MeanTempRounded(13)), '°C'];
end
if files>13
    tIce14=['Ice at ',num2str(MeanTempRounded(14)), '°C'];
end

% Create figure 1 for filtered Albumin/Trehalose Ratio

figure1 = figure('Colormap',...
    [0.0416666679084301 0 0;0.08333333358168602 0 0;0.125 0 0;...
    0.166666667163372 0 0;0.20833332836628 0 0;0.25 0
0;0.291666656732559...
    0 0;0.333333343267441 0 0;0.375 0 0;0.416666656732559 0 0;...
    0.458333343267441 0 0;0.5 0 0;0.541666686534882 0 0;...
    0.583333313465118 0 0;0.625 0 0;0.666666686534882 0 0;...
    0.708333313465118 0 0;0.75 0 0;0.791666686534882 0 0;...
    0.833333313465118 0 0;0.875 0 0;0.916666686534882 0 0;...
    0.958333313465118 0 0;1 0 0;1 0.0416666679084301 0;...
    1 0.0833333358168602 0;1 0.125 0;1 0.16666667163372 0;...
    1 0.20833332836628 0;1 0.25 0;1 0.291666656732559 0;...
    1 0.333333343267441 0;1 0.375 0;1 0.416666656732559 0;...
    1 0.458333343267441 0;1 0.5 0;1 0.541666686534882 0;...
    1 0.583333313465118 0;1 0.625 0;1 0.666666686534882 0;...
    1 0.708333313465118 0;1 0.75 0;1 0.791666686534882 0;...
    1 0.833333313465118 0;1 0.875 0;1 0.916666686534882 0;...
    1 0.958333313465118 0;1 1 0;1 1 0.0625;1 1 0.125;1 1 0.1875;...
    1 1 0.25;1 1 0.3125;1 1 0.375;1 1 0.4375;1 1 0.5;1 1 0.5625;...
    1 1 0.625;1 1 0.6875;1 1 0.75;1 1 0.8125;1 1 0.875;1 1 0.9375;...
    1 1 1]), 'Color',[1 1 1], 'Position', fsize);

%ratio 1
axes1 = axes('Parent', figure1, 'YTick', zeros(1,0), 'YDir', 'reverse',...
    'XTick', zeros(1,0),...
    'PlotBoxAspectRatio',[200 10 1],...
    'OuterPosition',[0 zz-yy*(-1+1) 1 0.5],...
    'Layer','top',...
    'DataAspectRatio',[1 1 1],...
    'CLim',[0 plotRatioHi]);

```

```

box(axes1, 'on');
hold(axes1, 'all');
image(RatioFiltered(:, :, 1), 'Parent', axes1, 'CDataMapping', 'scaled');
title({tRatio1}, 'FontWeight', 'bold', ...
      'FontSize', msize, ...
      'FontName', 'Arial');
colorbar('peer', axes1, 'fontsize', 12);
%ratio 2
axes2 = axes('Parent', figure1, 'YTick', zeros(1,0), 'YDir', 'reverse', ...
            'XTick', zeros(1,0), ...
            'PlotBoxAspectRatio', [200 10 1], ...
            'OuterPosition', [0 zz-yy*(-1+2) 1 0.5], ...
            'Layer', 'top', ...
            'DataAspectRatio', [1 1 1], ...
            'CLim', [0 plotRatioHi]);
box(axes2, 'on');
hold(axes2, 'all');
image(RatioFiltered(:, :, 2), 'Parent', axes2, 'CDataMapping', 'scaled');
title({tRatio2}, 'FontWeight', 'bold', ...
      'FontSize', msize, ...
      'FontName', 'Arial');
colorbar('peer', axes2, 'fontsize', 12);
%ratio 3
axes3 = axes('Parent', figure1, 'YTick', zeros(1,0), 'YDir', 'reverse', ...
            'XTick', zeros(1,0), ...
            'PlotBoxAspectRatio', [200 10 1], ...
            'OuterPosition', [0 zz-yy*(-1+3) 1 0.5], ...
            'Layer', 'top', ...
            'DataAspectRatio', [1 1 1], ...
            'CLim', [0 plotRatioHi]);
box(axes3, 'on');
hold(axes3, 'all');
% Create image
image(RatioFiltered(:, :, 3), 'Parent', axes3, 'CDataMapping', 'scaled');
title({tRatio3}, 'FontWeight', 'bold', ...
      'FontSize', msize, ...
      'FontName', 'Arial');
colorbar('peer', axes3, 'fontsize', 12);
%ratio 4
axes4 = axes('Parent', figure1, 'YTick', zeros(1,0), 'YDir', 'reverse', ...
            'XTick', zeros(1,0), ...
            'PlotBoxAspectRatio', [200 10 1], ...
            'OuterPosition', [0 zz-yy*(-1+4) 1 0.5], ...
            'Layer', 'top', ...
            'DataAspectRatio', [1 1 1], ...
            'CLim', [0 plotRatioHi]);
box(axes4, 'on');
hold(axes4, 'all');
image(RatioFiltered(:, :, 4), 'Parent', axes4, 'CDataMapping', 'scaled');
title({tRatio4}, 'FontWeight', 'bold', ...
      'FontSize', msize, ...
      'FontName', 'Arial');
colorbar('peer', axes4, 'fontsize', 12);
%ratio 5
axes5 = axes('Parent', figure1, 'YTick', zeros(1,0), 'YDir', 'reverse', ...
            'XTick', zeros(1,0), ...
            'PlotBoxAspectRatio', [200 10 1], ...

```

```

    'OuterPosition',[0 zz-yy*(-1+5) 1 0.5],...
    'Layer','top',...
    'DataAspectRatio',[1 1 1],...
    'CLim',[0 plotRatioHi]);
box(axes5,'on');
hold(axes5,'all');
image(RatioFiltered(:, :, 5), 'Parent', axes5, 'CDataMapping', 'scaled');
title({tRatio5}, 'FontWeight', 'bold', ...
      'FontSize', msize, ...
      'FontName', 'Arial');
colorbar('peer', axes5, 'fontsize', 12);
%ratio 6
axes6 = axes('Parent', figure1, 'YTick', zeros(1,0), 'YDir', 'reverse', ...
            'XTick', zeros(1,0), ...
            'PlotBoxAspectRatio',[200 10 1], ...
            'OuterPosition',[0 zz-yy*(-1+6) 1 0.5], ...
            'Layer','top', ...
            'DataAspectRatio',[1 1 1], ...
            'CLim',[0 plotRatioHi]);
box(axes6,'on');
hold(axes6,'all');
image(RatioFiltered(:, :, 6), 'Parent', axes6, 'CDataMapping', 'scaled');
title({tRatio6}, 'FontWeight', 'bold', ...
      'FontSize', msize, ...
      'FontName', 'Arial');
colorbar('peer', axes6, 'fontsize', 12);
axes7 = axes('Parent', figure1, 'YTick', zeros(1,0), 'YDir', 'reverse', ...
            'XTick', zeros(1,0), ...
            'PlotBoxAspectRatio',[200 10 1], ...
            'OuterPosition',[0 zz-yy*(-1+7) 1 0.5], ...
            'Layer','top', ...
            'DataAspectRatio',[1 1 1], ...
            'CLim',[0 plotRatioHi]);
box(axes7,'on');
hold(axes7,'all');
image(RatioFiltered(:, :, 7), 'Parent', axes7, 'CDataMapping', 'scaled');
title({tRatio7}, 'FontWeight', 'bold', ...
      'FontSize', msize, ...
      'FontName', 'Arial');
colorbar('peer', axes7, 'fontsize', 12);
saveas(figure1, 'Ratio1.bmp')

% Create ratio figure 2
figure2 = figure('Colormap', ...
    [0.0416666679084301 0 0;0.08333333358168602 0 0;0.125 0 0;...
    0.16666667163372 0 0;0.20833332836628 0 0;0.25 0
0;0.291666656732559...
    0 0;0.333333343267441 0 0;0.375 0 0;0.416666656732559 0 0;...
    0.458333343267441 0 0;0.5 0 0;0.541666686534882 0 0;...
    0.583333313465118 0 0;0.625 0 0;0.666666686534882 0 0;...
    0.708333313465118 0 0;0.75 0 0;0.791666686534882 0 0;...
    0.833333313465118 0 0;0.875 0 0;0.916666686534882 0 0;...
    0.958333313465118 0 0;1 0 0;1 0.0416666679084301 0;...
    1 0.08333333358168602 0;1 0.125 0;1 0.16666667163372 0;...
    1 0.20833332836628 0;1 0.25 0;1 0.291666656732559 0;...
    1 0.333333343267441 0;1 0.375 0;1 0.416666656732559 0;...
    1 0.458333343267441 0;1 0.5 0;1 0.541666686534882 0;...

```

```

1 0.5833333313465118 0;1 0.625 0;1 0.6666666686534882 0;...
1 0.7083333313465118 0;1 0.75 0;1 0.7916666686534882 0;...
1 0.8333333313465118 0;1 0.875 0;1 0.9166666686534882 0;...
1 0.9583333313465118 0;1 1 0;1 1 0.0625;1 1 0.125;1 1 0.1875;...
1 1 0.25;1 1 0.3125;1 1 0.375;1 1 0.4375;1 1 0.5;1 1 0.5625;...
1 1 0.625;1 1 0.6875;1 1 0.75;1 1 0.8125;1 1 0.875;1 1 0.9375;...
1 1 1], 'Color', [1 1 1], 'Position', fsize);
axes8 = axes('Parent', figure2, 'YTick', zeros(1,0), 'YDir', 'reverse', ...
'XTick', zeros(1,0), ...
'PlotBoxAspectRatio', [200 10 1], ...
'OuterPosition', [0 zz-yy*(-1+1) 1 0.5], ...
'Layer', 'top', ...
'DataAspectRatio', [1 1 1], ...
'CLim', [0 plotRatioHi]);
box(axes8, 'on');
hold(axes8, 'all');
image(RatioFiltered(:, :, 8), 'Parent', axes8, 'CDataMapping', 'scaled');
title({tRatio8}, 'FontWeight', 'bold', ...
'FontSize', msize, ...
'FontName', 'Arial');
colorbar('peer', axes8, 'fontsize', 12);
%ratio 9
if files>8
axes9 = axes('Parent', figure2, 'YTick', zeros(1,0), 'YDir', 'reverse', ...
'XTick', zeros(1,0), ...
'PlotBoxAspectRatio', [200 10 1], ...
'OuterPosition', [0 zz-yy*(-1+2) 1 0.5], ...
'Layer', 'top', ...
'DataAspectRatio', [1 1 1], ...
'CLim', [0 plotRatioHi]);
box(axes9, 'on');
hold(axes9, 'all');
image(RatioFiltered(:, :, 9), 'Parent', axes9, 'CDataMapping', 'scaled');
title({tRatio9}, 'FontWeight', 'bold', ...
'FontSize', msize, ...
'FontName', 'Arial');
colorbar('peer', axes9, 'fontsize', 12);
end
%ratio 10
if files>9
axes10 = axes('Parent', figure2, 'YTick', zeros(1,0), 'YDir', 'reverse', ...
'XTick', zeros(1,0), ...
'PlotBoxAspectRatio', [200 10 1], ...
'OuterPosition', [0 zz-yy*(-1+3) 1 0.5], ...
'Layer', 'top', ...
'DataAspectRatio', [1 1 1], ...
'CLim', [0 plotRatioHi]);
box(axes10, 'on');
hold(axes10, 'all');
image(RatioFiltered(:, :, 10), 'Parent', axes10, 'CDataMapping', 'scaled');
title({tRatio10}, 'FontWeight', 'bold', ...
'FontSize', msize, ...
'FontName', 'Arial');
colorbar('peer', axes10, 'fontsize', 12);
end
%ratio 11
if files>10

```

```

axes11 = axes('Parent',figure2,'YTick',zeros(1,0),'YDir','reverse',...
    'XTick',zeros(1,0),...
    'PlotBoxAspectRatio',[200 10 1],...
    'OuterPosition',[0 zz-yy*(-1+4) 1 0.5],...
    'Layer','top',...
    'DataAspectRatio',[1 1 1],...
    'CLim',[0 plotRatioHi]);
box(axes11,'on');
hold(axes11,'all');
image(RatioFiltered(:,:,11),'Parent',axes11,'CDataMapping','scaled');
title({tRatio11},'FontWeight','bold',...
    'FontSize',msize,...
    'FontName','Arial');
colorbar('peer',axes11,'fontsize',12);
end
%ratio 12
if files>11
axes12 = axes('Parent',figure2,'YTick',zeros(1,0),'YDir','reverse',...
    'XTick',zeros(1,0),...
    'PlotBoxAspectRatio',[200 10 1],...
    'OuterPosition',[0 zz-yy*(-1+5) 1 0.5],...
    'Layer','top',...
    'DataAspectRatio',[1 1 1],...
    'CLim',[0 plotRatioHi]);
box(axes12,'on');
hold(axes12,'all');
image(RatioFiltered(:,:,12),'Parent',axes12,'CDataMapping','scaled');
title({tRatio12},'FontWeight','bold',...
    'FontSize',msize,...
    'FontName','Arial');
colorbar('peer',axes12,'fontsize',12);
end
%ratio 13
if files>12
axes13 = axes('Parent',figure2,'YTick',zeros(1,0),'YDir','reverse',...
    'XTick',zeros(1,0),...
    'PlotBoxAspectRatio',[200 10 1],...
    'OuterPosition',[0 zz-yy*(-1+6) 1 0.5],...
    'Layer','top',...
    'DataAspectRatio',[1 1 1],...
    'CLim',[0 plotRatioHi]);
box(axes13,'on');
hold(axes13,'all');
image(RatioFiltered(:,:,13),'Parent',axes13,'CDataMapping','scaled');
title({tRatio13},'FontWeight','bold',...
    'FontSize',msize,...
    'FontName','Arial');
colorbar('peer',axes13,'fontsize',12);
end
%ratio 14
if files>13
axes14 = axes('Parent',figure2,'YTick',zeros(1,0),'YDir','reverse',...
    'XTick',zeros(1,0),...
    'PlotBoxAspectRatio',[200 10 1],...
    'OuterPosition',[0 zz-yy*(-1+7) 1 0.5],...
    'Layer','top',...
    'DataAspectRatio',[1 1 1],...

```

```

    'CLim',[0 plotRatioHi]);
box(axes14,'on');
hold(axes14,'all');
image(RatioFiltered(:,:,14),'Parent',axes14,'CDataMapping','scaled');
title({tRatio14},'FontWeight','bold',...
      'FontSize',msize,...
      'FontName','Arial');
colorbar('peer',axes14,'fontsize',12);
end
saveas(figure2,'Ratio2.bmp')

% Create figure 1 for filtered Trehalose
figure1 = figure('Colormap',...
    [0.0416666679084301 0 0;0.08333333358168602 0 0;0.125 0 0;...
    0.16666667163372 0 0;0.20833332836628 0 0;0.25 0
0;0.291666656732559...
    0 0;0.333333343267441 0 0;0.375 0 0;0.416666656732559 0 0;...
    0.458333343267441 0 0;0.5 0 0;0.541666686534882 0 0;...
    0.583333313465118 0 0;0.625 0 0;0.666666686534882 0 0;...
    0.708333313465118 0 0;0.75 0 0;0.791666686534882 0 0;...
    0.833333313465118 0 0;0.875 0 0;0.916666686534882 0 0;...
    0.958333313465118 0 0;1 0 0;1 0.0416666679084301 0;...
    1 0.08333333358168602 0;1 0.125 0;1 0.16666667163372 0;...
    1 0.20833332836628 0;1 0.25 0;1 0.291666656732559 0;...
    1 0.333333343267441 0;1 0.375 0;1 0.416666656732559 0;...
    1 0.458333343267441 0;1 0.5 0;1 0.541666686534882 0;...
    1 0.583333313465118 0;1 0.625 0;1 0.666666686534882 0;...
    1 0.708333313465118 0;1 0.75 0;1 0.791666686534882 0;...
    1 0.833333313465118 0;1 0.875 0;1 0.916666686534882 0;...
    1 0.958333313465118 0;1 1 0;1 1 0.0625;1 1 0.125;1 1 0.1875;...
    1 1 0.25;1 1 0.3125;1 1 0.375;1 1 0.4375;1 1 0.5;1 1 0.5625;...
    1 1 0.625;1 1 0.6875;1 1 0.75;1 1 0.8125;1 1 0.875;1 1 0.9375;...
    1 1 1],'Color',[1 1 1],'Position',fsize);
%trehalose 1
axes1 = axes('Parent',figure1,'YTick',zeros(1,0),'YDir','reverse',...
    'XTick',zeros(1,0),...
    'PlotBoxAspectRatio',[200 10 1],...
    'OuterPosition',[0 zz-yy*(-1+1) 1 0.5],...
    'Layer','top',...
    'DataAspectRatio',[1 1 1],...
    'CLim',[0 (20+trecon)]);
box(axes1,'on');
hold(axes1,'all');
image(TrehaloseFiltered(:,:,1),'Parent',axes1,'CDataMapping','scaled');
title({tTrel},'FontWeight','bold',...
      'FontSize',msize,...
      'FontName','Arial');
colorbar('peer',axes1,'fontsize',12);
%trehalose 2
axes2 = axes('Parent',figure1,'YTick',zeros(1,0),'YDir','reverse',...
    'XTick',zeros(1,0),...
    'PlotBoxAspectRatio',[200 10 1],...
    'OuterPosition',[0 zz-yy*(-1+2) 1 0.5],...
    'Layer','top',...
    'DataAspectRatio',[1 1 1],...
    'CLim',[0 (20+trecon)]);
box(axes2,'on');

```

```

hold(axes2, 'all');
image(TrehaloseFiltered(:, :, 2), 'Parent', axes2, 'CDataMapping', 'scaled');
title({tTre2}, 'FontWeight', 'bold', ...
      'FontSize', msize, ...
      'FontName', 'Arial');
colorbar('peer', axes2, 'fontsize', 12);
%trehalose 3
axes3 = axes('Parent', figure1, 'YTick', zeros(1,0), 'YDir', 'reverse', ...
            'XTick', zeros(1,0), ...
            'PlotBoxAspectRatio', [200 10 1], ...
            'OuterPosition', [0 zz-yy*(-1+3) 1 0.5], ...
            'Layer', 'top', ...
            'DataAspectRatio', [1 1 1], ...
            'CLim', [0 (20+trecon)]);
box(axes3, 'on');
hold(axes3, 'all');
% Create image
image(TrehaloseFiltered(:, :, 3), 'Parent', axes3, 'CDataMapping', 'scaled');
title({tTre3}, 'FontWeight', 'bold', ...
      'FontSize', msize, ...
      'FontName', 'Arial');
colorbar('peer', axes3, 'fontsize', 12);
%trehalose 4
axes4 = axes('Parent', figure1, 'YTick', zeros(1,0), 'YDir', 'reverse', ...
            'XTick', zeros(1,0), ...
            'PlotBoxAspectRatio', [200 10 1], ...
            'OuterPosition', [0 zz-yy*(-1+4) 1 0.5], ...
            'Layer', 'top', ...
            'DataAspectRatio', [1 1 1], ...
            'CLim', [0 (20+trecon)]);
box(axes4, 'on');
hold(axes4, 'all');
image(TrehaloseFiltered(:, :, 4), 'Parent', axes4, 'CDataMapping', 'scaled');
title({tTre4}, 'FontWeight', 'bold', ...
      'FontSize', msize, ...
      'FontName', 'Arial');
colorbar('peer', axes4, 'fontsize', 12);
%trehalose 5
axes5 = axes('Parent', figure1, 'YTick', zeros(1,0), 'YDir', 'reverse', ...
            'XTick', zeros(1,0), ...
            'PlotBoxAspectRatio', [200 10 1], ...
            'OuterPosition', [0 zz-yy*(-1+5) 1 0.5], ...
            'Layer', 'top', ...
            'DataAspectRatio', [1 1 1], ...
            'CLim', [0 (20+trecon)]);
box(axes5, 'on');
hold(axes5, 'all');
image(TrehaloseFiltered(:, :, 5), 'Parent', axes5, 'CDataMapping', 'scaled');
title({tTre5}, 'FontWeight', 'bold', ...
      'FontSize', msize, ...
      'FontName', 'Arial');
colorbar('peer', axes5, 'fontsize', 12);
%trehalose 6
axes6 = axes('Parent', figure1, 'YTick', zeros(1,0), 'YDir', 'reverse', ...
            'XTick', zeros(1,0), ...
            'PlotBoxAspectRatio', [200 10 1], ...
            'OuterPosition', [0 zz-yy*(-1+6) 1 0.5], ...

```

```

    'Layer','top',...
    'DataAspectRatio',[1 1 1],...
    'CLim',[0 (20+trecon)]);
box(axes6,'on');
hold(axes6,'all');
image(TrehaloseFiltered(:,:,6),'Parent',axes6,'CDataMapping','scaled');
title({tTre6},'FontWeight','bold',...
      'FontSize',msize,...
      'FontName','Arial');
colorbar('peer',axes6,'fontsize',12);
axes7 = axes('Parent',figure1,'YTick',zeros(1,0),'YDir','reverse',...
            'XTick',zeros(1,0),...
            'PlotBoxAspectRatio',[200 10 1],...
            'OuterPosition',[0 zz-yy*(-1+7) 1 0.5],...
            'Layer','top',...
            'DataAspectRatio',[1 1 1],...
            'CLim',[0 (20+trecon)]);
box(axes7,'on');
hold(axes7,'all');
image(TrehaloseFiltered(:,:,7),'Parent',axes7,'CDataMapping','scaled');
title({tTre7},'FontWeight','bold',...
      'FontSize',msize,...
      'FontName','Arial');
colorbar('peer',axes7,'fontsize',12);
saveas(figure1,'Trel.bmp')

% Create trehalose figure 2
figure2 = figure('Colormap',...
    [0.0416666679084301 0 0;0.08333333358168602 0 0;0.125 0 0;...
    0.166666667163372 0 0;0.20833332836628 0 0;0.25 0
0;0.291666656732559...
    0 0;0.333333343267441 0 0;0.375 0 0;0.416666656732559 0 0;...
    0.458333343267441 0 0;0.5 0 0;0.541666686534882 0 0;...
    0.583333313465118 0 0;0.625 0 0;0.666666686534882 0 0;...
    0.708333313465118 0 0;0.75 0 0;0.791666686534882 0 0;...
    0.833333313465118 0 0;0.875 0 0;0.916666686534882 0 0;...
    0.958333313465118 0 0;1 0 0;1 0.0416666679084301 0;...
    1 0.08333333358168602 0;1 0.125 0;1 0.166666667163372 0;...
    1 0.20833332836628 0;1 0.25 0;1 0.291666656732559 0;...
    1 0.333333343267441 0;1 0.375 0;1 0.416666656732559 0;...
    1 0.458333343267441 0;1 0.5 0;1 0.541666686534882 0;...
    1 0.583333313465118 0;1 0.625 0;1 0.666666686534882 0;...
    1 0.708333313465118 0;1 0.75 0;1 0.791666686534882 0;...
    1 0.833333313465118 0;1 0.875 0;1 0.916666686534882 0;...
    1 0.958333313465118 0;1 1 0;1 1 0.0625;1 1 0.125;1 1 0.1875;...
    1 1 0.25;1 1 0.3125;1 1 0.375;1 1 0.4375;1 1 0.5;1 1 0.5625;...
    1 1 0.625;1 1 0.6875;1 1 0.75;1 1 0.8125;1 1 0.875;1 1 0.9375;...
    1 1 1], 'Color',[1 1 1], 'Position',fsize);
axes8 = axes('Parent',figure2,'YTick',zeros(1,0),'YDir','reverse',...
            'XTick',zeros(1,0),...
            'PlotBoxAspectRatio',[200 10 1],...
            'OuterPosition',[0 zz-yy*(-1+1) 1 0.5],...
            'Layer','top',...
            'DataAspectRatio',[1 1 1],...
            'CLim',[0 (20+trecon)]);
box(axes8,'on');
hold(axes8,'all');

```

```

image(TrehaloseFiltered(:,:,8), 'Parent', axes8, 'CDataMapping', 'scaled');
title({tTre8}, 'FontWeight', 'bold', ...
      'FontSize', msize, ...
      'FontName', 'Arial');
colorbar('peer', axes8, 'fontsize', 12);
%trehalose 9
if files>8
axes9 = axes('Parent', figure2, 'YTick', zeros(1,0), 'YDir', 'reverse', ...
            'XTick', zeros(1,0), ...
            'PlotBoxAspectRatio', [200 10 1], ...
            'OuterPosition', [0 zz-yy*(-1+2) 1 0.5], ...
            'Layer', 'top', ...
            'DataAspectRatio', [1 1 1], ...
            'CLim', [0 (20+trecon)]);
box(axes9, 'on');
hold(axes9, 'all');
image(TrehaloseFiltered(:,:,9), 'Parent', axes9, 'CDataMapping', 'scaled');
title({tTre9}, 'FontWeight', 'bold', ...
      'FontSize', msize, ...
      'FontName', 'Arial');
colorbar('peer', axes9, 'fontsize', 12);
end
%trehalose 10
if files>9
axes10 = axes('Parent', figure2, 'YTick', zeros(1,0), 'YDir', 'reverse', ...
             'XTick', zeros(1,0), ...
             'PlotBoxAspectRatio', [200 10 1], ...
             'OuterPosition', [0 zz-yy*(-1+3) 1 0.5], ...
             'Layer', 'top', ...
             'DataAspectRatio', [1 1 1], ...
             'CLim', [0 (20+trecon)]);
box(axes10, 'on');
hold(axes10, 'all');
image(TrehaloseFiltered(:,:,10), 'Parent', axes10, 'CDataMapping', 'scaled'
);
title({tTre10}, 'FontWeight', 'bold', ...
      'FontSize', msize, ...
      'FontName', 'Arial');
colorbar('peer', axes10, 'fontsize', 12);
end
%trehalose 11
if files>10
axes11 = axes('Parent', figure2, 'YTick', zeros(1,0), 'YDir', 'reverse', ...
             'XTick', zeros(1,0), ...
             'PlotBoxAspectRatio', [200 10 1], ...
             'OuterPosition', [0 zz-yy*(-1+4) 1 0.5], ...
             'Layer', 'top', ...
             'DataAspectRatio', [1 1 1], ...
             'CLim', [0 (20+trecon)]);
box(axes11, 'on');
hold(axes11, 'all');
image(TrehaloseFiltered(:,:,11), 'Parent', axes11, 'CDataMapping', 'scaled'
);
title({tTre11}, 'FontWeight', 'bold', ...
      'FontSize', msize, ...
      'FontName', 'Arial');
colorbar('peer', axes11, 'fontsize', 12);

```

```

end
%trehalose 12
if files>11
axes12 = axes('Parent',figure2,'YTick',zeros(1,0),'YDir','reverse',...
    'XTick',zeros(1,0),...
    'PlotBoxAspectRatio',[200 10 1],...
    'OuterPosition',[0 zz-yy*(-1+5) 1 0.5],...
    'Layer','top',...
    'DataAspectRatio',[1 1 1],...
    'CLim',[0 (20+trecon)]);
box(axes12,'on');
hold(axes12,'all');
image(TrehaloseFiltered(:,:,12),'Parent',axes12,'CDataMapping','scaled'
);
title({tTrel2},'FontWeight','bold',...
    'FontSize',msize,...
    'FontName','Arial');
colorbar('peer',axes12,'fontsize',12);
end
%trehalose 13
if files>12
axes13 = axes('Parent',figure2,'YTick',zeros(1,0),'YDir','reverse',...
    'XTick',zeros(1,0),...
    'PlotBoxAspectRatio',[200 10 1],...
    'OuterPosition',[0 zz-yy*(-1+6) 1 0.5],...
    'Layer','top',...
    'DataAspectRatio',[1 1 1],...
    'CLim',[0 (20+trecon)]);
box(axes13,'on');
hold(axes13,'all');
image(TrehaloseFiltered(:,:,13),'Parent',axes13,'CDataMapping','scaled'
);
title({tTrel3},'FontWeight','bold',...
    'FontSize',msize,...
    'FontName','Arial');
colorbar('peer',axes13,'fontsize',12);
end
%trehalose 14
if files>13
axes14 = axes('Parent',figure2,'YTick',zeros(1,0),'YDir','reverse',...
    'XTick',zeros(1,0),...
    'PlotBoxAspectRatio',[200 10 1],...
    'OuterPosition',[0 zz-yy*(-1+7) 1 0.5],...
    'Layer','top',...
    'DataAspectRatio',[1 1 1],...
    'CLim',[0 (20+trecon)]);
box(axes14,'on');
hold(axes14,'all');
image(TrehaloseFiltered(:,:,14),'Parent',axes14,'CDataMapping','scaled'
);
title({tTrel4},'FontWeight','bold',...
    'FontSize',msize,...
    'FontName','Arial');
colorbar('peer',axes14,'fontsize',12);
end
saveas(figure2,'Tre2.bmp')

```

```

% Create figure 1 for Ice
figure1 = figure('Colormap',...
    [0.0416666679084301 0 0;0.08333333358168602 0 0;0.125 0 0;...
    0.16666667163372 0 0;0.20833332836628 0 0;0.25 0
0;0.291666656732559...
    0 0;0.333333343267441 0 0;0.375 0 0;0.416666656732559 0 0;...
    0.458333343267441 0 0;0.5 0 0;0.541666686534882 0 0;...
    0.583333313465118 0 0;0.625 0 0;0.666666686534882 0 0;...
    0.708333313465118 0 0;0.75 0 0;0.791666686534882 0 0;...
    0.833333313465118 0 0;0.875 0 0;0.916666686534882 0 0;...
    0.958333313465118 0 0;1 0 0;1 0.0416666679084301 0;...
    1 0.08333333358168602 0;1 0.125 0;1 0.16666667163372 0;...
    1 0.20833332836628 0;1 0.25 0;1 0.291666656732559 0;...
    1 0.333333343267441 0;1 0.375 0;1 0.416666656732559 0;...
    1 0.458333343267441 0;1 0.5 0;1 0.541666686534882 0;...
    1 0.583333313465118 0;1 0.625 0;1 0.666666686534882 0;...
    1 0.708333313465118 0;1 0.75 0;1 0.791666686534882 0;...
    1 0.833333313465118 0;1 0.875 0;1 0.916666686534882 0;...
    1 0.958333313465118 0;1 1 0;1 1 0.0625;1 1 0.125;1 1 0.1875;...
    1 1 0.25;1 1 0.3125;1 1 0.375;1 1 0.4375;1 1 0.5;1 1 0.5625;...
    1 1 0.625;1 1 0.6875;1 1 0.75;1 1 0.8125;1 1 0.875;1 1 0.9375;...
    1 1 1], 'Color', [1 1 1], 'Position', fsize);

%ice 1
axes1 = axes('Parent', figure1, 'YTick', zeros(1,0), 'YDir', 'reverse', ...
    'XTick', zeros(1,0), ...
    'PlotBoxAspectRatio', [200 10 1], ...
    'OuterPosition', [0 zz-yy*(-1+1) 1 0.5], ...
    'Layer', 'top', ...
    'DataAspectRatio', [1 1 1], ...
    'CLim', [0 (50-trecon)]);
box(axes1, 'on');
hold(axes1, 'all');
image(B(:, :, 1), 'Parent', axes1, 'CDataMapping', 'scaled');
title({tIce1}, 'FontWeight', 'bold', ...
    'FontSize', msize, ...
    'FontName', 'Arial');
colorbar('peer', axes1, 'fontsize', 12);

%ice 2
axes2 = axes('Parent', figure1, 'YTick', zeros(1,0), 'YDir', 'reverse', ...
    'XTick', zeros(1,0), ...
    'PlotBoxAspectRatio', [200 10 1], ...
    'OuterPosition', [0 zz-yy*(-1+2) 1 0.5], ...
    'Layer', 'top', ...
    'DataAspectRatio', [1 1 1], ...
    'CLim', [0 (50-trecon)]);
box(axes2, 'on');
hold(axes2, 'all');
image(B(:, :, 2), 'Parent', axes2, 'CDataMapping', 'scaled');
title({tIce2}, 'FontWeight', 'bold', ...
    'FontSize', msize, ...
    'FontName', 'Arial');
colorbar('peer', axes2, 'fontsize', 12);

%ice 3
axes3 = axes('Parent', figure1, 'YTick', zeros(1,0), 'YDir', 'reverse', ...
    'XTick', zeros(1,0), ...
    'PlotBoxAspectRatio', [200 10 1], ...
    'OuterPosition', [0 zz-yy*(-1+3) 1 0.5], ...

```

```

        'Layer','top',...
        'DataAspectRatio',[1 1 1],...
        'CLim',[0 (50-trecon)]);
box(axes3,'on');
hold(axes3,'all');
% Create image
image(B(:,:,3),'Parent',axes3,'CDataMapping','scaled');
title({tIce3},'FontWeight','bold',...
      'FontSize',msize,...
      'FontName','Arial');
colorbar('peer',axes3,'fontsize',12);
%ice 4
axes4 = axes('Parent',figure1,'YTick',zeros(1,0),'YDir','reverse',...
            'XTick',zeros(1,0),...
            'PlotBoxAspectRatio',[200 10 1],...
            'OuterPosition',[0 zz-yy*(-1+4) 1 0.5],...
            'Layer','top',...
            'DataAspectRatio',[1 1 1],...
            'CLim',[0 (50-trecon)]);
box(axes4,'on');
hold(axes4,'all');
image(B(:,:,4),'Parent',axes4,'CDataMapping','scaled');
title({tIce4},'FontWeight','bold',...
      'FontSize',msize,...
      'FontName','Arial');
colorbar('peer',axes4,'fontsize',12);
%ice 5
axes5 = axes('Parent',figure1,'YTick',zeros(1,0),'YDir','reverse',...
            'XTick',zeros(1,0),...
            'PlotBoxAspectRatio',[200 10 1],...
            'OuterPosition',[0 zz-yy*(-1+5) 1 0.5],...
            'Layer','top',...
            'DataAspectRatio',[1 1 1],...
            'CLim',[0 (50-trecon)]);
box(axes5,'on');
hold(axes5,'all');
image(B(:,:,5),'Parent',axes5,'CDataMapping','scaled');
title({tIce5},'FontWeight','bold',...
      'FontSize',msize,...
      'FontName','Arial');
colorbar('peer',axes5,'fontsize',12);
%ice 6
axes6 = axes('Parent',figure1,'YTick',zeros(1,0),'YDir','reverse',...
            'XTick',zeros(1,0),...
            'PlotBoxAspectRatio',[200 10 1],...
            'OuterPosition',[0 zz-yy*(-1+6) 1 0.5],...
            'Layer','top',...
            'DataAspectRatio',[1 1 1],...
            'CLim',[0 (50-trecon)]);
box(axes6,'on');
hold(axes6,'all');
image(B(:,:,6),'Parent',axes6,'CDataMapping','scaled');
title({tIce6},'FontWeight','bold',...
      'FontSize',msize,...
      'FontName','Arial');
colorbar('peer',axes6,'fontsize',12);
axes7 = axes('Parent',figure1,'YTick',zeros(1,0),'YDir','reverse',...

```

```

    'XTick', zeros(1,0), ...
    'PlotBoxAspectRatio', [200 10 1], ...
    'OuterPosition', [0 zz-yy*(-1+7) 1 0.5], ...
    'Layer', 'top', ...
    'DataAspectRatio', [1 1 1], ...
    'CLim', [0 (50-trecon)]);
box(axes7, 'on');
hold(axes7, 'all');
image(B(:, :, 7), 'Parent', axes7, 'CDataMapping', 'scaled');
title({tIce7}, 'FontWeight', 'bold', ...
      'FontSize', msize, ...
      'FontName', 'Arial');
colorbar('peer', axes7, 'fontsize', 12);
saveas(figure1, 'Icel.bmp')

% Create ice figure 2
figure2 = figure('Colormap', ...
  [0.0416666679084301 0 0; 0.08333333358168602 0 0; 0.125 0 0; ...
  0.166666667163372 0 0; 0.20833332836628 0 0; 0.25 0
0; 0.291666656732559 ...
  0 0; 0.333333343267441 0 0; 0.375 0 0; 0.416666656732559 0 0; ...
  0.458333343267441 0 0; 0.5 0 0; 0.541666686534882 0 0; ...
  0.583333313465118 0 0; 0.625 0 0; 0.666666686534882 0 0; ...
  0.708333313465118 0 0; 0.75 0 0; 0.791666686534882 0 0; ...
  0.833333313465118 0 0; 0.875 0 0; 0.916666686534882 0 0; ...
  0.958333313465118 0 0; 1 0 0; 1 0.0416666679084301 0; ...
  1 0.08333333358168602 0; 1 0.125 0; 1 0.16666667163372 0; ...
  1 0.20833332836628 0; 1 0.25 0; 1 0.291666656732559 0; ...
  1 0.333333343267441 0; 1 0.375 0; 1 0.416666656732559 0; ...
  1 0.458333343267441 0; 1 0.5 0; 1 0.541666686534882 0; ...
  1 0.583333313465118 0; 1 0.625 0; 1 0.666666686534882 0; ...
  1 0.708333313465118 0; 1 0.75 0; 1 0.791666686534882 0; ...
  1 0.833333313465118 0; 1 0.875 0; 1 0.916666686534882 0; ...
  1 0.958333313465118 0; 1 1 0; 1 1 0.0625; 1 1 0.125; 1 1 0.1875; ...
  1 1 0.25; 1 1 0.3125; 1 1 0.375; 1 1 0.4375; 1 1 0.5; 1 1 0.5625; ...
  1 1 0.625; 1 1 0.6875; 1 1 0.75; 1 1 0.8125; 1 1 0.875; 1 1 0.9375; ...
  1 1 1], 'Color', [1 1 1], 'Position', fsize);
axes8 = axes('Parent', figure2, 'YTick', zeros(1,0), 'YDir', 'reverse', ...
  'XTick', zeros(1,0), ...
  'PlotBoxAspectRatio', [200 10 1], ...
  'OuterPosition', [0 zz-yy*(-1+1) 1 0.5], ...
  'Layer', 'top', ...
  'DataAspectRatio', [1 1 1], ...
  'CLim', [0 (50-trecon)]);
box(axes8, 'on');
hold(axes8, 'all');
image(B(:, :, 8), 'Parent', axes8, 'CDataMapping', 'scaled');
title({tIce8}, 'FontWeight', 'bold', ...
      'FontSize', msize, ...
      'FontName', 'Arial');
colorbar('peer', axes8, 'fontsize', 12);
%ice 9
if files>8
axes9 = axes('Parent', figure2, 'YTick', zeros(1,0), 'YDir', 'reverse', ...
  'XTick', zeros(1,0), ...
  'PlotBoxAspectRatio', [200 10 1], ...
  'OuterPosition', [0 zz-yy*(-1+2) 1 0.5], ...

```

```

        'Layer','top',...
        'DataAspectRatio',[1 1 1],...
        'CLim',[0 (50-trecon)]);
box(axes9,'on');
hold(axes9,'all');
image(B(:,:,9),'Parent',axes9,'CDataMapping','scaled');
title({tIce9},'FontWeight','bold',...
      'FontSize',msize,...
      'FontName','Arial');
colorbar('peer',axes9,'fontsize',12);
end
%ice 10
if files>9
axes10 = axes('Parent',figure2,'YTick',zeros(1,0),'YDir','reverse',...
             'XTick',zeros(1,0),...
             'PlotBoxAspectRatio',[200 10 1],...
             'OuterPosition',[0 zz-yy*(-1+3) 1 0.5],...
             'Layer','top',...
             'DataAspectRatio',[1 1 1],...
             'CLim',[0 (50-trecon)]);
box(axes10,'on');
hold(axes10,'all');
image(B(:,:,10),'Parent',axes10,'CDataMapping','scaled');
title({tIce10},'FontWeight','bold',...
      'FontSize',msize,...
      'FontName','Arial');
colorbar('peer',axes10,'fontsize',12);
end
%ice 11
if files>10
axes11 = axes('Parent',figure2,'YTick',zeros(1,0),'YDir','reverse',...
             'XTick',zeros(1,0),...
             'PlotBoxAspectRatio',[200 10 1],...
             'OuterPosition',[0 zz-yy*(-1+4) 1 0.5],...
             'Layer','top',...
             'DataAspectRatio',[1 1 1],...
             'CLim',[0 (50-trecon)]);
box(axes11,'on');
hold(axes11,'all');
image(B(:,:,11),'Parent',axes11,'CDataMapping','scaled');
title({tIce11},'FontWeight','bold',...
      'FontSize',msize,...
      'FontName','Arial');
colorbar('peer',axes11,'fontsize',12);
end
%ice 12
if files>11
axes12 = axes('Parent',figure2,'YTick',zeros(1,0),'YDir','reverse',...
             'XTick',zeros(1,0),...
             'PlotBoxAspectRatio',[200 10 1],...
             'OuterPosition',[0 zz-yy*(-1+5) 1 0.5],...
             'Layer','top',...
             'DataAspectRatio',[1 1 1],...
             'CLim',[0 (50-trecon)]);
box(axes12,'on');
hold(axes12,'all');
image(B(:,:,12),'Parent',axes12,'CDataMapping','scaled');

```

```

title({tIcel2}, 'FontWeight', 'bold', ...
      'FontSize', msize, ...
      'FontName', 'Arial');
colorbar('peer', axes12, 'fontsize', 12);
end
%ice 13
if files>12
axes13 = axes('Parent', figure2, 'YTick', zeros(1,0), 'YDir', 'reverse', ...
             'XTick', zeros(1,0), ...
             'PlotBoxAspectRatio', [200 10 1], ...
             'OuterPosition', [0 zz-yy*(-1+6) 1 0.5], ...
             'Layer', 'top', ...
             'DataAspectRatio', [1 1 1], ...
             'CLim', [0 (50-trecon)]);
box(axes13, 'on');
hold(axes13, 'all');
image(B(:, :, 13), 'Parent', axes13, 'CDataMapping', 'scaled');
title({tIcel3}, 'FontWeight', 'bold', ...
      'FontSize', msize, ...
      'FontName', 'Arial');
colorbar('peer', axes13, 'fontsize', 12);
end
%ice 14
if files>13
axes14 = axes('Parent', figure2, 'YTick', zeros(1,0), 'YDir', 'reverse', ...
             'XTick', zeros(1,0), ...
             'PlotBoxAspectRatio', [200 10 1], ...
             'OuterPosition', [0 zz-yy*(-1+7) 1 0.5], ...
             'Layer', 'top', ...
             'DataAspectRatio', [1 1 1], ...
             'CLim', [0 (50-trecon)]);
box(axes14, 'on');
hold(axes14, 'all');
image(B(:, :, 14), 'Parent', axes14, 'CDataMapping', 'scaled');
title({tIcel4}, 'FontWeight', 'bold', ...
      'FontSize', msize, ...
      'FontName', 'Arial');
colorbar('peer', axes14, 'fontsize', 12);
end
saveas(figure2, 'Ice2.bmp')

% Mean Ratio of Alb/Trehalose as a % of nominal value
% Create figure
figure1 = figure('Position', fsize);
% Create axes
axes1 = axes('Parent', figure1, 'FontSize', xsize, 'FontName', 'Arial');
xlim(axes1, [Tlow Thigh]);
ylim(axes1, [PctLow PctHigh]);
box(axes1, 'on');
hold(axes1, 'all');
% Create plot
plot(MeanTemp, MeanRatioPercentage, 'MarkerSize', 24, 'Marker', '.', ...
     'LineStyle', 'none', ...
     'DisplayName', 'AlbuminPercentage vs. MeanTemp');
xlabel('Temperature [°C]', 'FontSize', xsize, 'FontName', 'Arial');
ylabel('Mean Albumin/Trehalose [% of
nominal]', 'FontSize', ysize, 'FontName', 'Arial');

```

```

title({tAlbTrel,tAlbTre2},'FontSize',tsize,...
      'FontName','Arial');
saveas(figure1,'MeanAlbTre.bmp')

% Total Trehalose Content in control volume percentage of starting
amount
% Create figure
figure1 = figure('Position', fsize);
% Create axes
axes1 = axes('Parent',figure1,'FontSize',xsize,'FontName','Arial');
xlim(axes1,[Tlow Thigh]);
ylim(axes1,[PctLow PctHigh]);
box(axes1,'on');
hold(axes1,'all');
% Create plot
plot(MeanTemp,TrehalosePercentage,'MarkerSize',24,'Marker','.',...
      'LineStyle','none',...
      'DisplayName','AlbuminPercentage vs. MeanTemp');
xlabel('Temperature [°C]','FontSize',xsize,'FontName','Arial');
ylabel('Mean Trehalose Concentration [% of
nominal]','FontSize',ysize,'FontName','Arial');
title({tTreDist1,tTreDist2},'FontSize',tsize,...
      'FontName','Arial');
saveas(figure1,'TrehaloseNominal.bmp')

% Plot the albumin/trehalose ratio for varying concentrations:
figure1 = figure('Color',[1 1 1],'Position', fsize);
% Create axes
axes1 = axes('Parent',figure1,'FontWeight','bold','FontSize',xsize,...
            'FontName','Arial');
% Uncomment the following line to preserve the X-limits of the axes
xlim(axes1,[Tlow Thigh]);
% Uncomment the following line to preserve the Y-limits of the axes
ylim(axes1,[PctLow PctHigh]);
box(axes1,'on');
hold(axes1,'all');
% Create xlabel
xlabel('Temperature [°C]','FontWeight','bold','FontSize',xsize,...
      'FontName','Arial');
% Create ylabel
ylabel({'Normalized Albumin/Trehalose Ratio [%]'},'FontSize',ysize,...
      'FontName','Arial');
% Create title
title({tAlbTrel,tAlbTre2},'FontWeight','bold',...
      'FontSize',tsize,...
      'FontName','Arial');
% Create multiple lines using matrix input to plot
plot1 = plot(MeanTemp,RmPCT2_10_15filtered,...
            MeanTemp,RmPCT2_15_20filtered,...
            MeanTemp,RmPCT2_20_25filtered,...
            MeanTemp,RmPCT2_25_30filtered,...
            MeanTemp,RmPCT2_30_100filtered,...
            MeanTemp,MeanRatioPercentage,...
            'Parent',axes1,'LineStyle','none');
set(plot1(1),'MarkerFaceColor',[1 0 0],'MarkerEdgeColor',[1 0 0],...
     'MarkerSize',11,...

```

```

    'Marker','*','...
    'DisplayName','10-15 wt% Trehalose Equivalent');
set(plot1(2),'MarkerFaceColor',[0 1 1],'MarkerEdgeColor',[0 1 1],...
    'MarkerSize',24,...
    'Marker','.',...
    'DisplayName','15-20 wt% Trehalose Equivalent');
set(plot1(3),'MarkerFaceColor',[0 0 1],'MarkerEdgeColor',[0 0 1],...
    'MarkerSize',8,...
    'Marker','v',...
    'DisplayName','20-25 wt% Trehalose Equivalent');
set(plot1(4),'MarkerFaceColor',[1 0 1],'MarkerEdgeColor',[1 0 1],...
    'MarkerSize',8,...
    'Marker','square',...
    'DisplayName','25-30 wt% Trehalose Equivalent');
set(plot1(5),'MarkerFaceColor',[0 0.498039215803146 0],...
    'MarkerEdgeColor',[0 0.498039215803146 0],...
    'MarkerSize',8,...
    'Marker','diamond',...
    'DisplayName','>30 wt% Trehalose Equivalent');
set(plot1(6),'MarkerFaceColor',[0 1 0],'MarkerEdgeColor',[0 1 0],...
    'MarkerSize',11,...
    'Marker','hexagram',...
    'DisplayName','Mean Solution');
% Create plot
plot(NominalTemp,Nominal,'Parent',axes1,'LineWidth',3,'LineStyle','--
',...
    'DisplayName','Nominal Solution',...
    'Color',[0 0 0]);
% Create legend
legend1 = legend(axes1,'show');
set(legend1,...
    'Position',fposition);
saveas(figure1,'AlbTreNominal.bmp')

% Plot the frequency of each concentration:
figure1 = figure('Color',[1 1 1],'Position', fsize);
% Create axes
axes1 = axes('Parent',figure1,'FontWeight','bold','FontSize',xsize,...
    'FontName','Arial');
% Uncomment the following line to preserve the X-limits of the axes
xlim(axes1,[Tlow Thigh]);
% Uncomment the following line to preserve the Y-limits of the axes
ylim(axes1,[0 trehi]);
box(axes1,'on');
hold(axes1,'all');
% Create xlabel
xlabel('Temperature [°C]','FontWeight','bold','FontSize',xsize,...
    'FontName','Arial');
% Create ylabel
ylabel({'Concentration Frequency [%]'},'FontSize',ysize,...
    'FontName','Arial');
% Create title
title({tTreDist1,tTreDist2},'FontWeight','bold',...
    'FontSize',tsize,...
    'FontName','Arial');
% Create multiple lines using matrix input to plot
plot1 = plot(MeanTemp,Count_10_15,...

```

```

MeanTemp,Count_15_20,...
MeanTemp,Count_20_25,...
MeanTemp,Count_25_30,...
MeanTemp,Count_30_100,...
MeanTemp,Count_nominal,...
'Parent',axes1,'LineStyle','none');
set(plot1(1),'MarkerFaceColor',[1 0 0],'MarkerEdgeColor',[1 0 0],...
'MarkerSize',11,...
'Marker','*',...
'DisplayName','10-15 wt% Trehalose Equivalent');
set(plot1(2),'MarkerFaceColor',[0 1 1],'MarkerEdgeColor',[0 1 1],...
'MarkerSize',24,...
'Marker','.',...
'DisplayName','15-20 wt% Trehalose Equivalent');
set(plot1(3),'MarkerFaceColor',[0 0 1],'MarkerEdgeColor',[0 0 1],...
'MarkerSize',8,...
'Marker','v',...
'DisplayName','20-25 wt% Trehalose Equivalent');
set(plot1(4),'MarkerFaceColor',[1 0 1],'MarkerEdgeColor',[1 0 1],...
'MarkerSize',8,...
'Marker','square',...
'DisplayName','25-30 wt% Trehalose Equivalent');
set(plot1(5),'MarkerFaceColor',[0 0.498039215803146 0],...
'MarkerEdgeColor',[0 0.498039215803146 0],...
'MarkerSize',8,...
'Marker','diamond',...
'DisplayName','>30 wt% Trehalose Equivalent');
set(plot1(6),'MarkerFaceColor',[0 1 0],'MarkerEdgeColor',[0 1 0],...
'MarkerSize',11,...
'Marker','hexagram',...
'DisplayName','Nominal Solution +/- 5 wt%');

% Create legend
legend1 = legend(axes1,'show');
set(legend1,...
'Position',(fposition)+[0 .45 0 0]);
saveas(figure1,'TreFreq.bmp')

% Plot the albumin/trehalose ratio for varying concentrations
normalized
% the mean value:
figure1 = figure('Color',[1 1 1],'Position',fsize);
% Create axes
axes1 = axes('Parent',figure1,'FontWeight','bold','FontSize',xsize,...
'FontName','Arial');
% Uncomment the following line to preserve the X-limits of the axes
xlim(axes1,[Tlow Thigh]);
% Uncomment the following line to preserve the Y-limits of the axes
ylim(axes1,[PctLow PctHigh]);
box(axes1,'on');
hold(axes1,'all');
% Create xlabel
xlabel('Temperature [°C]','FontWeight','bold','FontSize',xsize,...
'FontName','Arial');
% Create ylabel

```

```

ylabel({'Normalized Albumin/Trehalose Ratio [%]'}, 'FontSize', ysize, ...
      'FontName', 'Arial');
% Create title
title({tAlbTrel1, tAlbTrel2}, 'FontWeight', 'bold', ...
      'FontSize', tsize, ...
      'FontName', 'Arial');
% Create multiple lines using matrix input to plot
plot1 = plot(MeanTemp, RmNorm_10_15, ...
            MeanTemp, RmNorm_15_20, ...
            MeanTemp, RmNorm_20_25, ...
            MeanTemp, RmNorm_25_30, ...
            MeanTemp, RmNorm_30_100, ...
            'Parent', axes1, 'LineStyle', 'none');
set(plot1(1), 'MarkerFaceColor', [1 0 0], 'MarkerEdgeColor', [1 0 0], ...
      'MarkerSize', 11, ...
      'Marker', '*', ...
      'DisplayName', '10-15 wt% Trehalose Equivalent');
set(plot1(2), 'MarkerFaceColor', [0 1 1], 'MarkerEdgeColor', [0 1 1], ...
      'MarkerSize', 24, ...
      'Marker', '.', ...
      'DisplayName', '15-20 wt% Trehalose Equivalent');
set(plot1(3), 'MarkerFaceColor', [0 0 1], 'MarkerEdgeColor', [0 0 1], ...
      'MarkerSize', 8, ...
      'Marker', 'v', ...
      'DisplayName', '20-25 wt% Trehalose Equivalent');
set(plot1(4), 'MarkerFaceColor', [1 0 1], 'MarkerEdgeColor', [1 0 1], ...
      'MarkerSize', 8, ...
      'Marker', 'square', ...
      'DisplayName', '25-30 wt% Trehalose Equivalent');
set(plot1(5), 'MarkerFaceColor', [0 0.498039215803146 0], ...
      'MarkerEdgeColor', [0 0.498039215803146 0], ...
      'MarkerSize', 8, ...
      'Marker', 'diamond', ...
      'DisplayName', '>30 wt% Trehalose Equivalent');
% Create plot
plot(NominalTemp, Nominal, 'Parent', axes1, 'LineWidth', 3, 'LineStyle', '--
', ...
      'DisplayName', 'Mean Value', ...
      'Color', [0 0 0]);
% Create legend
legend1 = legend(axes1, 'show');
set(legend1, ...
      'Position', fposition);
saveas(figure1, 'AlbTreNorm.bmp')

% Figures to include Ice, Trehalose Albumin/Trehalose Ratio:

% Create figure 1 for filtered Albumin/Trehalose Ratio
for h=1:files
figure1 = figure('Colormap', ...
                [0.0416666679084301 0 0; 0.08333333358168602 0 0; 0.125 0 0; ...
                0.166666667163372 0 0; 0.20833332836628 0 0; 0.25 0
                0; 0.291666656732559...

```

```

0 0;0.333333343267441 0 0;0.375 0 0;0.416666656732559 0 0;...
0.458333343267441 0 0;0.5 0 0;0.541666686534882 0 0;...
0.583333313465118 0 0;0.625 0 0;0.666666686534882 0 0;...
0.708333313465118 0 0;0.75 0 0;0.791666686534882 0 0;...
0.833333313465118 0 0;0.875 0 0;0.916666686534882 0 0;...
0.958333313465118 0 0;1 0 0;1 0.0416666679084301 0;...
1 0.0833333358168602 0;1 0.125 0;1 0.16666667163372 0;...
1 0.20833332836628 0;1 0.25 0;1 0.291666656732559 0;...
1 0.333333343267441 0;1 0.375 0;1 0.416666656732559 0;...
1 0.458333343267441 0;1 0.5 0;1 0.541666686534882 0;...
1 0.583333313465118 0;1 0.625 0;1 0.666666686534882 0;...
1 0.708333313465118 0;1 0.75 0;1 0.791666686534882 0;...
1 0.833333313465118 0;1 0.875 0;1 0.916666686534882 0;...
1 0.958333313465118 0;1 1 0;1 1 0.0625;1 1 0.125;1 1 0.1875;...
1 1 0.25;1 1 0.3125;1 1 0.375;1 1 0.4375;1 1 0.5;1 1 0.5625;...
1 1 0.625;1 1 0.6875;1 1 0.75;1 1 0.8125;1 1 0.875;1 1 0.9375;...
1 1 1], 'Color',[1 1 1], 'Position',fsize);
% Set title names:
if h==1
    tIce=tIce1;
    tTre=tTre1;
    tRatio=tRatio1;
end
if h==2
    tIce=tIce2;
    tTre=tTre2;
    tRatio=tRatio2;
end
if h==3
    tIce=tIce3;
    tTre=tTre3;
    tRatio=tRatio3;
end
if h==4
    tIce=tIce4;
    tTre=tTre4;
    tRatio=tRatio4;
end
if h==5
    tIce=tIce5;
    tTre=tTre5;
    tRatio=tRatio5;
end
if h==6
    tIce=tIce6;
    tTre=tTre6;
    tRatio=tRatio6;
end
if h==7
    tIce=tIce7;
    tTre=tTre7;
    tRatio=tRatio7;
end
if h==8
    tIce=tIce8;
    tTre=tTre8;
    tRatio=tRatio8;

```

```

end
if h==9
    tIce=tIce9;
    tTre=tTre9;
    tRatio=tRatio9;
end
if h==10
    tIce=tIce10;
    tTre=tTre10;
    tRatio=tRatio10;
end
if h==11
    tIce=tIce11;
    tTre=tTre11;
    tRatio=tRatio11;
end
if h==12
    tIce=tIce12;
    tTre=tTre12;
    tRatio=tRatio12;
end
if h==13
    tIce=tIce13;
    tTre=tTre13;
    tRatio=tRatio13;
end
if h==14
    tIce=tIce14;
    tTre=tTre14;
    tRatio=tRatio14;
end

%ice 1
axes1 = axes('Parent',figure1,'YTick',zeros(1,0),'YDir','reverse',...
    'XTick',zeros(1,0),...
    'PlotBoxAspectRatio',[200 10 1],...
    'OuterPosition',[0 zz-yy*(-1+1) 1 0.5],...
    'Layer','top',...
    'DataAspectRatio',[1 1 1],...
    'CLim',[0 (45-trecon)]);
box(axes1,'on');
hold(axes1,'all');
image(B(:,:,h),'Parent',axes1,'CDataMapping','scaled');
title({tIce},'FontWeight','bold',...
    'FontSize',msize,...
    'FontName','Arial');
f=colorbar('peer',axes1,'fontsize',12,'fontWeight','bold');
xlabel(f,'[a.u.]')

%trehalose 2
axes2 = axes('Parent',figure1,'YTick',zeros(1,0),'YDir','reverse',...
    'XTick',zeros(1,0),...
    'PlotBoxAspectRatio',[200 10 1],...
    'OuterPosition',[0 zz-yy*(-1+2) 1 0.5],...
    'Layer','top',...
    'DataAspectRatio',[1 1 1],...
    'CLim',[0 (20+trecon)]);
box(axes2,'on');

```

```

hold(axes2, 'all');
image(TrehaloseFiltered(:, :, h), 'Parent', axes2, 'CDataMapping', 'scaled');
title({tTre}, 'FontWeight', 'bold', ...
      'FontSize', msize, ...
      'FontName', 'Arial');
f=colorbar('peer', axes2, 'fontsize', 12, 'fontWeight', 'bold');
xlabel(f, '[wt%]')
%ratio 3
axes3 = axes('Parent', figure1, 'YTick', zeros(1,0), 'YDir', 'reverse', ...
            'XTick', zeros(1,0), ...
            'PlotBoxAspectRatio', [200 10 1], ...
            'OuterPosition', [0 zz-yy*(-1+3) 1 0.5], ...
            'Layer', 'top', ...
            'DataAspectRatio', [1 1 1], ...
            'CLim', [0 plotRatioHi]);
box(axes3, 'on');
hold(axes3, 'all');
% Create image
image(RatioFiltered(:, :, h), 'Parent', axes3, 'CDataMapping', 'scaled');
title({tRatio}, 'FontWeight', 'bold', ...
      'FontSize', msize, ...
      'FontName', 'Arial');
f=colorbar('peer', axes3, 'fontsize', 12, 'fontWeight', 'bold');
xlabel(f, '[w/w]')

% namef=AlbTreNorm+num2str(h).bmp;
if h==1
saveas(figure1, 'Summary1.bmp')
end
if h==2
saveas(figure1, 'Summary2.bmp')
end
if h==3
saveas(figure1, 'Summary3.bmp')
end
if h==4
saveas(figure1, 'Summary4.bmp')
end
if h==5
saveas(figure1, 'Summary5.bmp')
end
if h==6
saveas(figure1, 'Summary6.bmp')
end
if h==7
saveas(figure1, 'Summary7.bmp')
end
if h==8
saveas(figure1, 'Summary8.bmp')
end
if h==9
saveas(figure1, 'Summary9.bmp')
end
if h==10
saveas(figure1, 'Summary10.bmp')
end
if h==11

```

```
saveas (figure1, 'Summary11.bmp')
end
if h==12
saveas (figure1, 'Summary12.bmp')
end
if h==13
saveas (figure1, 'Summary13.bmp')
end
if h==14
saveas (figure1, 'Summary14.bmp')
end
end
```